Universidade de Évora - Instituto de Investigação e Formação Avançada
Università degli Studi di Roma "La Sapienza" Aristotle University of Thessaloniki

Mestrado em Ciência dos Materiais Arqueológicos (ARCHMAT)

Dissertação

Estudo de protetivos hidrofóbicos e amigos dos ambiente para proteção e preservação de pedra carbonatada

Forough Armal

Orientador(es) | Pedro Miguel Barrulas
Jose Mirao
Luís Dias

Évora 2022

Universidade de Évora - Instituto de Investigação e Formação Avançada
Università degli Studi di Roma ”La Sapienza” Aristotle University of Thessaloniki

Mestrado em Ciência dos Materiais Arqueológicos (ARCHMAT)

Dissertação

Estudo de protetivos hidrofóbicos e amigos dos ambiente para proteção e preservação de pedra carbonatada

Forough Armal

Orientador(es) | Pedro Miguel Barrulas
Jose Mirao
Luís Dias

Évora 2022

A dissertação foi objeto de apreciação e discussão pública pelo seguinte júri nomeado pelo Diretor do Instituto de Investigação e Formação Avançada:

Presidente | Patrícia Sofia Moita (Universidade de Évora)

Vogais | Donatella Magri (Università degli Studi di Roma "La Sapienza")
Eleni Pavlidou (Aristotle University of Thessaloniki)
Luís Dias (Universidade de Évora)
Panagiotis Spathis (Aristotle University of Thessaloniki)
Pedro Miguel Barrulas (Universidade de Évora) (Orientador)

Évora 2022

Acknowledgments

The accomplishment of this thesis was only possible due to the association and assistance of a group of people that were directly involved in the development of this work. Consequently, the author wishes to express her acknowledgments:

To my supervisors, Pedro Barrulas, Luís Dias, and Jose Mirao for their endless support, degree of exigency, critical analysis, knowledge, technical advice, and generous availability;

To Vera Pires, Carla Lisci, and Fabio Sitzia for their continuous advice, total availability and knowledge that made possible the work, and more importantly for their very good friendships;

To Eco-STONEPROTEC (EXPL/CTA-GEO/0609/2021, funded by Fundação para a Ciência e Tecnologia – FCT) for this opportunity that made possible this work;

To ARCHMAT program and especially to Nick Schiavon for the organization and endless support;

To all my friends and colleagues at Hercules Laboratory, especially those who have helped me in the last six months of my working on the thesis, and their moral support, Dora Boieiro, Sriradha Bhattacharya, Rebecca MacRoberts, and Miriam Pressato;

To all my friends from ARCHMAT, especially those who have been there for me during the writing critical periods, helping me and supporting me, namely, Isabel Valle Herraro, Alejandra Perez Delara, Dorothy Parangao, Zebunnisa Chughtai, and Amira Souliman;

Finally, a special acknowledgment to my family for their belief in me and unconditional love.

Abstrato

O diagnóstico da deterioração e a conservação do património construído em pedra é complexo, exigindo a contribuição de muitas disciplinas para identificar as medidas corretivas e estratégias de gestão adequadas. As questões mais importantes estão relacionadas com a deterioração da pedra e as mudanças cromáticas na estética original da pedra, que têm um impacto direto no seu valor sociocultural. Entre todas as causas de deterioração das pedras, a ação da água é identificada como a principal causa de deterioração das pedras e das alterações cromáticas nos materiais de construção de pedra. Assim, para evitar a penetração de água na matriz de pedra, é necessário um tratamento fundamental. Um revestimento hidrofóbico amigo do ambiente seria a melhor opção para este fim. Atualmente, o desenvolvimento de um material protetor de pedra eficiente, durável e amigo do ambiente é ainda um desafio generalizado.

A tese de mestrado proposta, que faz parte da Eco-STONEPROTEC (EXPL/CTA-GEO/0609/2021, financiada pela Fundação para a Ciência e Tecnologia - FCT), visa abordar a ação da água sobre pedras carbonatadas através do estudo de três revestimentos hidrófobos comerciais diferentes e, especificamente, estudar a sua eficiência, compatibilidade e durabilidade.

Neste estudo, nove pedras carbonatadas diferentes e uma amostra específica de granito foram escolhidas devido às suas variações na natureza física, química e mineralógica. A tarefa deste estudo é a caracterização completa de amostras de pedra selecionadas e estudar a compatibilidade, eficácia e durabilidade de revestimentos hidrofóbicos ecológicos aplicados nessas pedras. Foi realizada uma abordagem multianalítica, como microscopia digital, e colorimetria para avaliar a compatibilidade dos revestimentos hidrofóbicos, acelerando o envelhecimento em câmaras climáticas para avaliar a sua durabilidade, tensiómetro ótico para avaliar a eficácia hidrofóbica, e XRF e XRD para determinar a composição química e mineralógica de amostras de pedra.

De acordo com os resultados obtidos, este trabalho demonstra que o revestimento “CN3”, que é composto de silano/siloxano com aditivos fluorados modificados, é o revestimento hidrofóbico mais eficaz entre todos os revestimentos hidrofóbicos selecionados. Além disso, este revestimento apresenta boa compatibilidade com as amostras de pedra selecionadas. Além disso, os resultados obtidos podem ser os passos pioneiros para o desenvolvimento de revestimentos amigos do ambiente que também são rentáveis

Palavras-chave: deterioração de pedras; proteção do património rochoso; revestimentos hidrofóbicos ecológicos, pedra carbonatada.

Abstract

The decay diagnosis and conservation of stone-built heritage is complex, requiring input across many disciplines to identify appropriate remedial steps and management strategies. The most important issues are related to the stone decay and chromatic changes in the original stone aesthetics, which directly impact their sociocultural value. Among all the causes of stone decay, water action is identified as the major cause of stone decay and chromatic changes in stone building materials. Hence, to prevent the penetrating water into the stone matrix, fundamental treatment is needed. An eco-friendly hydrophobic coating would be the best option for this purpose. Currently, the development of an efficient, durable, and eco-friendly stone protector material is still a widespread challenge.

The proposed Master Thesis, which is part of Eco-STONEPROTEC (EXPL/CTA-GEO/0609/2021, funded by Fundação para a Ciência e Tecnologia – FCT), aims to tackle water action on carbonate stones by studying three different commercial hydrophobic coatings and specifically studying their efficiency, compatibility, and durability.

In this study, nine different carbonate stones and one specific granite sample have been chosen due to their variations in physical, chemical, and mineralogical natures. The task of this study is the full characterization of selected stone samples and study the compatibility, effectiveness, and durability of applied eco-friendly hydrophobic coatings on these stones. A multi-analytical approach was performed such as digital microscopy, and colorimetry to assess the compatibility of the hydrophobic coatings, accelerating ageing in climatic chambers to assess their durability, optical tensiometer to evaluate the hydrophobic effectiveness, and XRF and XRD for determining the chemical and mineralogical composition of stone samples.

According to the obtained results, this work demonstrates that the coating “CN3”, which is composed of silane/siloxane with modified fluorinated additives, is the most effective hydrophobic coating among all the selected hydrophobic coatings. Additionally, this coating shows good compatibility with the selected stone samples. Also, the obtained results can be the pioneer steps for developing eco-friendly coatings which also are cost-effective.

Keywords: stone decay; stone heritage protection; eco-friendly hydrophobic coatings, carbonate stone.

Objectives and aims

Stone material is one of the most challenging subjects when it comes to preservation and conservation. Since stone heritage all over the world is struggling with external environmental circumstances and in most cases, there are fewer options for controlling the environmental conditions, preservation and conservation of stone heritage is becoming a worldwide issue. Therefore, it is urgent to find valuable, durable, practical, and environmentally-friendly solutions that could protect stone-built materials.

Among all the external factors which cause stone decay, water is determined as the most threatening factor. Water is particularly damaging to porous stone materials and determines their limited durability over time, especially if the stone is exposed to external environmental factors. Moreover, water is the main trigger for salt solubility and leads to salt efflorescence, especially in more porous stones.

To prevent the further cause of water actions, the best solution is to prevent water penetration into the stone. To reach this goal applying hydrophobic coatings is one of the best solutions to prevent the future decay and deterioration of stones.

By focusing on ten different samples categorized into limestones, marbles, and granite, corresponding to their different physical, chemical, and mineralogical nature, this study aims to answer the following questions.

- which factors related to the physical, chemical, and mineralogical characterization of stone samples, correlate with the effectivity, compatibility, and durability of hydrophobic coatings?
- Which factors in hydrophobic coatings can make them more effective, compatible, and durable when they are applied on stone materials specifically, carbonate stones?

Answering these questions will shed light on the chemical composition of a coating that better contribute to stone protection and aesthetics maintenance. Consequently, the results of this study would be a pioneering step for developing novel eco-friendly coatings to finally reaching to the destination which would be producing the best hydrophobic coating that considers all the aspects to preserve and conserve the stone heritage while having less functional and aesthetic effects.

Framework and Study Design

Having a short review structural framework of the research helps us to better understand the study. This thesis is structured into 4 chapters, namely Introduction, Materials and Methods, Results and Discussion, and finally the Conclusion. Corresponding references have been inserted at the end of each chapter.

Chapter 1 – Introduction, starts with a short literature review concerning stone decay and deterioration causes. Then, it explains the importance of the subject and why this study needs to focus on this issue. Various numbers of other studies related to this research have been mentioned and discussed in this chapter as well. Also, the general information about the conservation and preservation of stone material is in detailly exposed.

Chapter 2 – Materials and Methodological Approaches, focuses on the approaches and methodologies which have been used in this study which will conclude mainly with analytical and optical techniques. It begins with introducing the materials which have been applied in this study including different lithotypes and specific hydrophobic coatings. Then, it continues by explaining all the techniques and the purposes of using them which are to characterize the samples physically, chemically, and mineralogically and to compare the coatings due to their effectiveness, compatibility, and durability.

Chapter 3 – Results and Discussion, all the obtained data and results of applied techniques are presented and discussed. This chapter is categorized based on two main groups of results, one for the characterization of stones, physically, chemically, and mineralogically, and the other group determines the compatibility, effectiveness, and durability of applied coatings on studied stone samples. Each result has been discussed and it has been tried to correlate and discuss all the obtained results.

Chapter 4 – comprises the conclusions of this master thesis investigation, as well as possible trends for research in the near future on the field of stone materials protection.

TABLE OF CONTENT

List of Figures

List of Tables

CHAPTER 1

1 Introduction

1.1 Stone Decay; description and causes

Anyone who has looked closely at historical stones is probably familiar with stone decay issues. Generally, stone as a construction material is considered one of the most durable and strong materials compared to wood or clay brick. Despite this point of view, stone can deteriorate, and many factors are involved. Before focusing on these factors, it is necessary to understand the stone decay terminology. Finding a common language related to discussing stone decay has always been difficult. And even if unique terms are established to describe specific types of decay, still it can be difficult to regulate the severity or amount of decay. Some researchers and organizations have been working to solve this problem (Price, C., et al., 2011).

The ICOMOS-ISCS (Illustrated Glossary on Stone Deterioration Patterns) helps to define different terms related to the stone community, and distinguish useful definitions such as decay, damage, deterioration, weathering, and degradation. In this order, **decay** defines as *any chemical or physical modification of the intrinsic stone properties leading to a loss of value or the impairment of use*, while **damage** considers a *human perception of the loss of value due to decay.* Additionally, in contrast to **deterioration** which is defined as *a decline in condition, quality, or functional capacity,* **weathering** is *any chemical or mechanical process by which stones exposed to the weather undergo changes in character and deteriorate.* Also, **degradation** is the *process of creating or becoming poorer or lower in quality, value, character, etc.* Hence, it is crucial to use suitable words when it comes to focusing on stone challenges and conditions (Vergès-Belmin, V., 2008).

Due to this current and worldwide issue that seriously threatens the integrity of the world's stone heritage, it is important to categorize and identify these problems based on the initial assessment and the type of stone (Barnoos, V., et al., 2020). In addition to considering the overall goal of the intervention, a proper diagnosis is essential for determining the optimal conservation method to be employed. Therefore, one of the most crucial aspects of stone conservation is knowing the causes of deterioration (Lakhani, R., et al., 2018). The most significant reasons for stone deterioration include air pollution, the presence of soluble salts, biodeterioration, and water action which plays a major role in all the aforementioned causes (Charola, A., 2016).

1.1.1. Air Pollution

The impact of air pollution on stone decay has been a subject matter in the field of stone deterioration. An important component influencing stone weathering in urban environments is the air quality (Alves, C., et al, 2020; Germinario, L., et al., 2017). Building stone deterioration will be affected by changes in air pollution concentration over time (Basu, S., et al, 2020).

It is commonly accepted that the primary pollution-related deterioration processes are gypsum formation and carbonate dissolution (Saba, M., et al, 2018). The most common stone decay feature that happens in stone material, especially limestone is crust weathering (Figure 1.1) (Rodrigues, J., 2015). Additionally, traces of iron oxides and components of the stone substrate like calcite and quartz may be present in crusts, and in certain cases, calcium oxalate from the partial oxidation of organic has also been detected (Comite, V., et al., 2021).

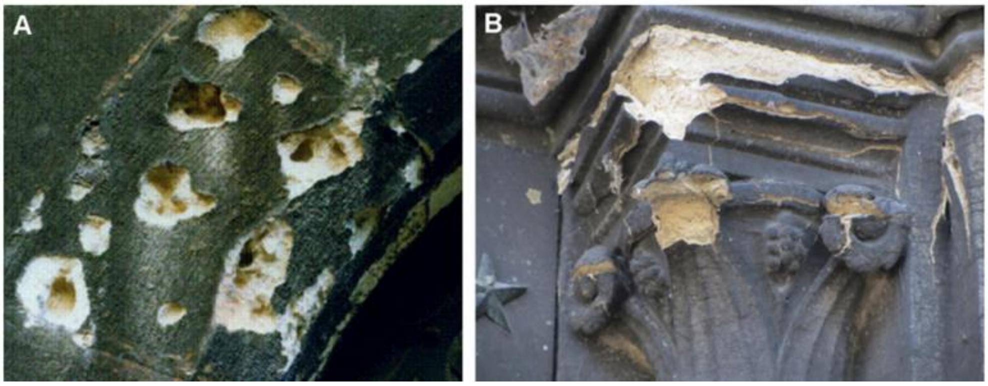

Figure 1.1 Examples of black crusts in limestone substrates (Rodrigues, J., 2015).

It is crucial to differentiate wet deposition, known as acidic rain, from dry deposition to understand air pollution. Wet deposition is typically far less significant than dry deposition, which occurs close to industrial and/or urban regions. Sulphur oxides (SO_2 and SO_3), often known as SOx, are gaseous pollutants that come from a variety of industries. On the other side, vehicle traffic emits nitrogen oxides (NO and NO_2), also known as NOx. These come from fine coal or coal dust furnaces and peat-fired boiler houses, and along with other airborne particles like furnace ashes, aerosols are deposited on the stones' surface, producing a layer. In the case of stone materials, starting from the surface, the corrosion process slowly goes in-depth along the stone, transforming inner layers into new compounds (Saba, M., et al, 2018; Charola, A., 2016).

Wet acid deposition is mostly brought on by sulfuric (H_2SO_4) and nitric (HNO_3) acids. In the first case, it is primarily created in the atmosphere by SO_2 and enters into stone objects during precipitation events, causing gypsum formation at the stone's surface. In the second situation, nitric acid is created when air NO_2 is oxidized, and it combines with calcium carbonate to produce calcium nitrate [$Ca(NO_3)_2$] (Speziale, A., et al., 2020; Saba, M., et al, 2018).

high stone porosity improves water penetration and subsequently carbonate dissolution, while high porosity distribution boost moisture uptake and enhances the deposition of salts and gypsum at stone surface. These stone features have an impact on the level of damage produced by acidic deposition. Therefore, high porous stones like limestones are highly at risk of this deterioration, however lower porosity lithotypes like marble and granite, have the possibility to get affected. Gypsum or other pollution-derived salts, when combined with excessive moisture that causes efflorescence, give the stone a porous outer layer that permits the penetration of chemicals or the formation of thin black crusts (Vidal, F., 2019).

1.1.2. Soluble Salts

The substance that damages the stone the fastest is soluble salts like sodium chloride (NaCl), sodium sulphate (Na2SO4), and sodium or potassium nitrate ($NaNO_3$, KNO_3). In the seaside environment, soluble salts like NaCl can be found suspended in the air. Other soluble salts like Na_2SO_4 and KNO_3 can be found in desert regions and bat guano deposits, respectively (Oguchi, C., et al, 2021).

The presence of moisture is the key factor that influences salt weathering. Since mentioned salts are highly water soluble, they undergo in solution, which allows their transfer and mobility by capillarity along the pore system of the stones (Alves, C., et al., 2021; Lubelli, B., 2018). The trapped water will often evaporate from the stones' surface, allowing salt crystallization and leading to salt efflorescence (Figure 1.2). Repeating this cycle affects the slow growth of salts within the porous material (Lezzerini, M., et al., 2022). Further recrystallizations from hydrate to dehydrate will be caused by variations in relative humidity, and temperature. The hygroscopicity of soluble salts, which can be defined as the capacity of water vapor adsorption like the moisture already present in the air, provides the basis for this matter (Lisci, C., et al., 2022; Morillas, H., et al, 2020).

In addition, the clay which is contained in the stone may absorb the moisture and expand. Thus, this process induces another deterioration mechanism, i.e., expansion-contraction. When only water is present, this mechanism is mainly reversible, but when salts are included, the cycles are no longer reversible, and the expansion gets significantly worse with each successive cycle (Elert, K., et al., 2022)

Figure 1.2 Salt efflorescence (the whitish powder) on granitic stones of a window from a historical structure in the town of Chaves, Portugal (Alves, C., et al., 2021).

1.1.3. Biodeterioration

The injurious effects promoted by the development of microorganisms and plants on the surface of the stones are referred to as biodeterioration (Figure 1.3) (Charola, A., 2016). A combination of physical, chemical, and aesthetic damage to stone material is involved in biodeterioration (Cappitelli, F., et al., 2020). Biocolonization of stone can cause soiling, discoloration, patinas, and fouling, particularly on limestones and marble (Zhang, G., et al., 2019).

Figure 1.3 effects of microorganisms and biodeterioration on limestone (Pinheiro, A., et al., 2019)

Over the time of development of microorganisms on the surface of stone monuments and buildings, colonization of microorganisms occurs (Zhang, G., et al., 2019). Climatic conditions and its changes can promote colonization which leads to more serious problems related to biological growth on the stone surface to convert inorganic CO_2 into biomass, then to deposit and enrich the cellular components on the stone's surface. The microbial population on the surface, which can form a biofilm, modifies the surface properties as soon as the initial immobilization of carbon takes place on the stone's surface (Sesana, E., et al., 2021). The other species may then colonize the stone surface after a biofilm has formed. The formation of lichens, then mosses, liverworts, and ferns may be made possible by the microorganisms in the biofilms, including bacteria, fungi, and algae (Depriest, P., et al., 2017).

Water is the factor that trigger the development of microorganisms as well as sunlight which provides the energy for their photosynthesis (Zhang, G., et al., 2019). While some organisms will be on the surface (epilithic colonization), some of them may penetrate the stone (endolithic colonization). Stones with translucent minerals in their composition, such as calcite, maybe more susceptible to microbial growth, since allows light to reach the interior pass (Charola, A., 2016).

1.1.4. Water Actions

As mentioned in every cause of stone decay, water action plays a key role to make or develop the decay causes. This matter can lead to considering water as the **main cause of stone decay**. Due to its capacity to act as the solvent in acidic rains, transport water-soluble salts by stone capillaries, triggers biological activity at the interfaces between stone and the environment, and in some cases, cause physical deterioration that results in the loss of stone material. These irreversible damages are highly undesired, especially when implies cultural heritage artworks. Additionally, water can be incorporated into stone structures or monuments through precipitation phenomena like rain, snow, hail, fog, and condensation that can be drawn up from the ground by capillary absorption. Furthermore, the importance of the location of a building or monument should not be overlooked. Salts and other potential contaminants, as well as water from different water basins including lakes, rivers, and seas, could be carried by the wind (Morillas, H., et al, 2020; Lee C., et al., 2005).

The damages degree and its frequency, caused by water, in different lithotypes are distinctive as well. Since water can dissolve calcium carbonate, and if its effect is frequent and continuous, carbonate-based stones are the most susceptible to breakdown by water (Benavente, D., et al., 2020). Compact limestones and marbles often have minimal porosities, which limits their capacity to dissolve in water to the surface in direct contact. Porous limestones, on the other hand, are subjected to more harmful action because water is able to penetrate deep into the pores and attack calcium carbonate in deeper layers (Ševčík, R., et al., 2019; Steiger, M., et al., 2011).

Also, it needs to be mentioned that water action can cause unobjectionable mechanical effects on a stone substrate which impacts the integrity of the stone matrix. (Liu, X., et al., 2020). The action of water on stone material is so threatening that needs deeper insights into this field. As mentioned before, carbonate stones fall into a category that extremely suffers from the action of water and requires more focus on preservation and conservation (Hosseini, M., et al., 2018; Ciantia, M., et al., 2015). The fundamental approach to the process of preservation and conservation is to tackle water penetration through stone material and prevent stone deterioration by water actions as aforementioned. This aim can be achieved by using superhydrophobic protective substances (Karapanagiotis, I., et al., 2022).

1.2 Preservation and Conservation of Stone

The first step after diagnosis of the causes of stone decay would be recognizing the suitable treatment (Becerra, J., et al., 2020). Traditionally, the stone would be repaired with mortar, some protective coating would be applied, or the rotten portion of the stone would be removed and replaced with new stone (Price, C., et al., 2011). However, since prevention is better than cure, increasing emphasis on the environment in which the stone finds itself is a better solution. For this purpose, focusing on both preventive and active conservation is fundamental (Morais, M., et al., 2019).

UNESCO gives us a general perspective on conservation and preservation definitions and treatments. It clearly mentions that *in general terms, conservation may be defined as the operations which together are intended to prolong the life of an object by forestalling damage or remedying deterioration. In the domain of cultural property, conservation aims to maintain the physical and cultural characteristics of the object to ensure that its value is not diminished and that it will outlive our limited time span* (Viñas, V., et al., 1988). On the other hand, preservation or preventive deterioration is one type of the actions in the conservation of materials and its aim defines *to obviate damage liable to the caused by an environmental or accidental factor which poses a threat in the immediate surroundings of the object to be conserved. Accordingly, preventive methods and measures are not usually applied directly but are designed to control the microclimatic conditions of the environment with the aim of eradicating harmful agents or elements which may have a temporary or permanent influence on the deterioration of the object* (Viñas, V., et al., 1988).

Hence, preservation and conservation methods must be carried out using the proper tools and materials, considering the degree of decay or degradation of the stone, the exposure circumstances, and the function of the stone element. By using such protective coatings, it is also possible to reduce the amount of repair and maintenance work that needs to be done. It is also cost-effective and time-saving approach for long-term, and enable to preserve the cultural values over time. Therefore, using preservative/conservative approaches has benefited from a sustainability perspective (Karapanagiotis, I., et al., 2022; Lettieri, et al., 2021).

Regarding the characterization of the stone decay, some treatments including cleaning, consolidation, and protective coatings have been applied to prevent the stone material from future deterioration (Tortora, M., et al., 2020).

1.2.1 Cleaning

Cleaning is a challenging problem and a vital part of conservation, and care must be taken to ensure that the treatments don't change the original surfaces (Ortega-Morales, B., et al., 2021). Depends on the type of material that needs to be cleaned and the desired post-cleaning effects, the cleaning technique can be divided into two categories based on the method used: mechanical and chemical (Zhu, G., et al., 2022). Mechanical (brushing and rubbing, washing and steaming, wet and dry abrasives, etc.) and chemical (alkaline treatments, acidic treatments, or organic solvents, etc.) approaches are typically used as the primary cleaning techniques (Bosch-Roig, P., et al., 2015).

The fundamental cleaning methods should take into account the potential harm (and ensuing legal action) that improper or overzealous cleaning may cause, as well as the environmental concerns raised by the use of specific chemicals or excessive water. These strategies ought to have been developed primarily through careful consideration on-site rather than in a laboratory.

Numerous researchers have focused on the techniques for cleaning. As an example, Pozo-Antonio and his associates worked on removing sulphated black crusts from stone materials using mechanical, chemical, and laser cleaning procedures (Pozo-Antonio, J., et al., 2016). Senesi and his research team conducted another study on the removal of black crusts on a limestone using laser cleaning and laser-induced breakdown spectroscopy (Senesi, G., et al., 2016). The results of these studies can prove the emphasis on different cleaning techniques as remedial conservation.

As mentioned in 1.1.1, pollution and dirt present in the air can lead to stone deterioration. Cleaning the surface stones prevents further deterioration, however, a better solution would be to make the surface of the stones self-cleaning. In this case, the minimum intervention related to cleaning would be performed (Colangiuli, D., et. Al., 2019). Hydrophobic and superhydrophobic coatings can be a good option for solving the problem of cleaning by making the surface of stones self-cleaning (Wu, Y., et al., 2022; Hosseini, M., et al, 2018).

1.2.2 Consolidation

Consolidation may be necessary to restore some strength of some parts of the stone that decay causes weakness. Consolidation as treatment should be practically cheap, easy to apply, safe to handle, and completely invisible. Consolidants are typically brushed, sprayed, pipetted, or immersed into the stones' surface and are pulled into the stone by capillarity (Possenti, E., et al., 2019; Scherer, G., et al., 2009).

Since the 19th century, inorganic substances such as silicious consolidants, alkali silicates, calcium, and barium hydroxides, among others, have been used as stone consolidants. The aim of using inorganic consolidants is to produce a decay resistance phase in the porous of deteriorated stones. It can happen by binding stone panicles together through solvent evaporation or chemical reaction with the stone. It is important to consider that the binding agent of the consolidants should be alike the original cement of the stone, thus **chemically compatible**. For instance, calcareous stones such as limestone and marble should be consolidated with substances which result in the formation of calcium or barium carbonate; on the other hand, sandstone should be consolidated with substances which deposit silica as a final product (Borsoi, G., et al., 2016).

Although inorganic consolidants are the most compatible material with deteriorated stones structurally and remain stable over time, they have failed to meet many of the required performances. These failures include inadequate penetration and formation of shallow and hard surface crusts, formation of soluble salts in the consolidation reaction, the growth of precipitated crystals, incapability to improve the mechanical properties of stone, and possible change in the colour of the stone (Menningen, J., et al., 2021).

Alkoxysilanes are a family member of monomeric molecules which can hydrolyze with water to produce either silica or chains of alkylpolysiloxanes. Different types of alkoxysilanes which are often used as stone consolidants are tetraethoxysilane (ethyl silicate or silicic acid ester), triethoxymethylsilane, and trimethoxymethylsilane. Polymerization proceeds by hydrolysis and condensation when the alkoxysilanes are deposited in the stone. Siloxane linkages (-Si-O-Si-) are formed as a strengthening factor at the end of the process (Rodrigues, A., et al., 2021). Even though alkoxysilanes have been commonly applied to sandstone consolidation, they have been applied on marble and limestones, as well. The most noticeable advantage of using alkoxysilanes is the ability to penetrate deeply into porous stones because of their low molecular weight and low viscosity. On the other hand, their dangerous effects on environment, their high cost, their tendency to change the colour of the stone, the possibility of their evaporation from the surface before hydrolysis can take place, and being an irreversible treatment are some of the constraints encountered in their use (Sierra-Fernández, A., et al., 2017).

Synthetic organic polymers are prepared trough polymerization of monomers that are low molecular weight compounds. Two types of synthetic organic polymer application methods have been used to consolidate stones. The first and simpler method is polymerizing the monomeric organic molecules, solubilizing this polymer resin in an organic solvent, and then applying it to the stone. After dryness, the polymer integrates the stone structure. In another method, monomers that are either pure or dissolved in a solvent are polymerized in the pores of the stone after the solution has penetrated the stone (Rodrigues, A., et al., 2022). Besides the advantages of using synthetic organic consolidants which include improving the mechanical properties of disintegrated stone, they have several limitations as well. These weaknesses include their deterioration in the presence of oxygen and light, discoloration of stone, loss of tensile strength, loss of brightness, irreversibility of treatment, and not being environmentally friendly (Xu, F., et. al., 2019).

Since consolidation has several challenges and limitations regards to the compatibility with the stone materials, it is crucial to only take action when it is absolutely necessary.

Therefore, nowadays consolidation treatment has a different approach in the scientific and conservative fields from the past. It has been trying to find a solution to have fewer interventions in the materials as possible (Praticò, Y., et al., 2020).

1.2.3 Surface Coating

In the 1970s and 1980s, many attempts have been made to find one single treatment for both consolidation and protection stones at once (Price, C., et. al., 2011). However, many conservators today recognize the value of both consolidation and protection techniques (Bayer, I. S. 2020). The hydrophobicity was first identified on Lotus leaf surfaces by Neinhaus and Barthlott, and it was subsequently patented as the Lotus effect (Figure 1.4) in 1998 (Parkin, I., et al., 2005).

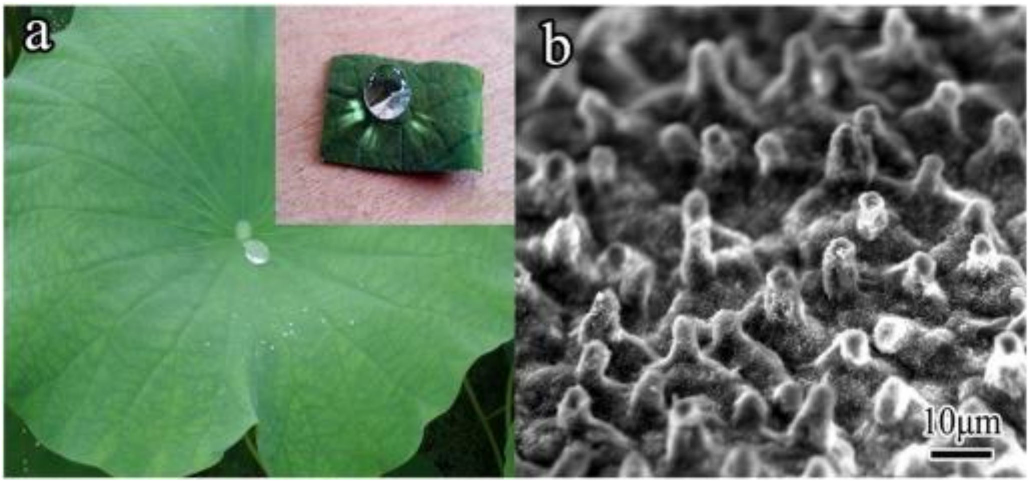

Figure 1.4 (a) Full-scale picture of a lotus leaf with inset to show water droplet on its surface, and (b) microstructure of the surface of a lotus leaf (Wang, T., et. al., 2014)

The reason for the hydrophobicity of the lotus leaf is the hierarchical roughness structure which leads to place air pockets forming inside the grooves underneath the liquid and reduces the contact area between the liquid and the surface (Wang, T., et. al., 2014). Therefore, due to the micro-scale mounds and the nano-scale hair-like structures, hydrophobicity and self-cleaning properties can be explainable. Consequently, roughness of the surface plays a key role in the aspect of hydrophobicity and self-cleaning property of the surface (Chindaprasirt, P., et al., 2020).

The water-repellence strategy has a straightforward justification. Water plays an important role in the stone decays, as previously mentioned. A treatment that tackles water from penetrating should therefore help in reducing deterioration. Developing hydrophobic coatings from irreversible, and toxic compounds to more environmental-friendly and compatible substrates clearly shows the need for cultural heritage community to find a more sustainable solution (Artesani, A., et. al., 2020).

In the past, most of the techniques for creating water repellency rely on the application of organic substances, such as resins, acrylate-based substances, waxes, etc. However, there are some drawbacks related to the use of these compounds, such as high viscosity, colour, and gloss changes leading to a thick, coloured coating (Liu, Q. et al., 2007); formulation based on organic compounds, with insufficient compatibility with the ancient stone and some of them with toxicity upon removal from the substrate (Melo, M.J., et al., 1999); and, eventually, excessive, and thus unsuitable reduction of water vapor permeability, which would result in a detrimental water accumulation inside the stone (Price, C., et al., 2011). Although still, these compounds are somehow preferable in use, they are better to abound since more eco-friendly and sustainable coatings are tested recently (Bayer, I. S. 2020).

The other group of compounds that had been frequently used in the past was solvents basis treatments. The substrate that needs to be protected is coated with the solution containing the polymer (or its monomers), which after solvent dryness it creates the desired film. This process ensures that the protective layer will effectively penetrate the substrate, even into its smallest pores. On the other hand, the use of toxic solvents in protective treatments causes serious issues for the environment where the solvent will evaporate, the operators, and anyone who comes in contact with the treated surfaces (DeBuergo Ballester, M., et. al., 2001).

Starting in the 2010s, the studies took a step forward in the development of protective coatings that were eco-friendly, reversible, and compatible with the substrate (Artesani, A., et. al., 2020). The most important categories for products that repel water include siliconates, silicones, and siloxanes. These products come in a variety of viscosities and can contain an organic solvent, be aqueous solutions, or be water-based emulsions as liquid, cream, and gel (Malaquias, R., et. al., 2022). The Si-O bond is a highly adaptable chemical bond that connects inorganic and organic species as well as serves as a building block for complex 3D oligomers and a wide range of materials and molecules. The siloxane bond is strong in its function as a linkage, chemically resistant to a variety of conditions, and simple to produce, for example, through the reaction of silanes with organic or inorganic hydroxyl groups. In simple words, silanes are extremely small-sized molecules with a strong alkali resistance and the capacity to penetrate deep into less porous material. Siloxane can be used on less porous materials and are alkali resistant, but porous substrates like brick and stone are where they perform best (Glosz, K., et., al. 2020). Water and oil repellency can be achieved by precisely choosing the silane/siloxane product and the concentration of additional nanoparticles (Hosseini, M., et. al., 2018).

The other group of compounds that are considered good water-repellent agents is the fluoropolymers class. When it comes to –CH2 > –CH3 > –CF2 > –CF3, the energy surface decreases, therefore fluorinated and perfluorinated materials have low wettability and are assumed as a logical option to produce hydrophobic materials (Aslanidou, D., et. al., 2018). On the other hand, fluorinated chemicals, including perfluoroalkylsilanes and fluoroacrylic polymers, are dangerous to human health and environment. Main awareness has been focused on the dangerous features of the short and long-chain PFAAs (perfluoroalkyl acids) which have been identified as contaminants of high concern owing to their high persistence, toxicity, bioaccumulation potential, and distribution in the environment (Wang, Z., et. al., 2015).

Another concerning issue refers to eliminating Volatile Organic Compounds (VOCs) from coating formulation to avoid potential negative effects on the environment and the health of users. In order to achieve this environmental goal, coatings have gradually been produced by switching from solvent-based products with high VOCs contents to low- or zero-VOC water-based systems (Artesani, A., et al., 2020).

In this research, eco-friendly hydrophobic coatings with different chemical bases will be discussed in the next chapter. The aim is to study their durability, compatibility, and efficiency to confront external weathering factors and gain insights into the correspondence of their chemical composition with their performance.

BIBLIOGRAPHY

Alves, C., Figueiredo, C., & Sanjurjo-Sánchez, J. (2020). Rock features and alteration of stone materials used for the built environment: a review of recent publications on ageing tests. *Geosciences*, *10*(3), 91.

Artesani, A., Di Turo, F., Zucchelli, M., & Traviglia, A. (2020). Recent advances in protective coatings for cultural heritage–an overview. Coatings, 10(3), 217.

Aslanidou, D., Karapanagiotis, I., & Lampakis, D. (2018). Waterborne superhydrophobic and superoleophobic coatings for the protection of marble and sandstone. Materials, 11(4), 585.

Barnoos, V., Oudbashi, O., & Shekofteh, A. (2020). The deterioration process of limestone in the Anahita Temple of Kangavar (West Iran). *Heritage Science*, *8*(1), 1-19.

Basu, S., Orr, S. A., & Aktas, Y. D. (2020). A geological perspective on climate change and building stone deterioration in London: Implications for urban stone-built heritage research and management. *Atmosphere*, *11*(8), 788.

Bayer, I. S. (2020). Superhydrophobic coatings from ecofriendly materials and processes: a review. *Advanced Materials Interfaces*, *7*(13), 2000095.

Becerra, J., Zaderenko, A. P., Ortiz, R., Karapanagiotis, I., & Ortiz, P. (2020). Comparison of the performance of a novel nanolime doped with ZnO quantum dots with common consolidants for historical carbonate stone buildings. *Applied Clay Science*, *195*, 105732.

Benavente, D., de Jongh, M., & Cañaveras, J. C. (2020). Weathering processes and mechanisms caused by capillary waters and pigeon droppings on porous limestones. *Minerals*, *11*(1), 18.

Borsoi, G., Lubelli, B., van Hees, R., Veiga, R., & Silva, A. S. (2016). Understanding the transport of nanolime consolidants within Maastricht limestone. *Journal of Cultural Heritage*, *18*, 242-249.

Bosch-Roig, P., Lustrato, G., Zanardini, E., & Ranalli, G. (2015). Biocleaning of Cultural Heritage stone surfaces and frescoes: which delivery system can be the most appropriate?. *Annals of microbiology*, *65*(3), 1227-1241.

Cappitelli, F., Cattò, C., & Villa, F. (2020). The control of cultural heritage microbial deterioration. *Microorganisms*, *8*(10), 1542.

Ciantia, M. O., Castellanza, R., Prisco, C. (2015). Experimental study on the water-induced weakening of calcarenites. *Rock Mech Rock Eng*, 48, 441-461.

Charola, A. E. (2016). Stone deterioration characterization for its conservation. *Geonomos*, 24(2), pp 16-20.

Chindaprasirt, P., & Rattanasak, U. (2020). Fabrication of self-cleaning fly ash/polytetrafluoroethylene material for cement mortar spray-coating. Journal of Cleaner Production, 264, 121748.

Colangiuli, D., Lettieri, M., Masieri, M., & Calia, A. (2019). Field study in an urban environment of simultaneous self-cleaning and hydrophobic nanosized TiO2-based coatings on stone for the protection of building surface. *Science of the Total Environment*, *650*, 2919-2930.

Comite, V., Miani, A., Ricca, M., La Russa, M., Pulimeno, M., & Fermo, P. (2021). The impact of atmospheric pollution on outdoor cultural heritage: an analytic methodology for the characterization of the carbonaceous fraction in black crusts present on stone surfaces. *Environmental Research*, *201*, 111565.

DeBuergo Ballester, M. A., & González, R. F. (2001). Basic methodology for the assessment and selection of water-repellent treatments applied on carbonatic materials. Progress in Organic Coatings, 43(4), 258-266.

DePriest, P., Charola, A. (2017). Biological Colonization and 'Ink Strokes' on Buildings. *Conservation of the Exterior of the National Museum of the American Indian Building*, *6*, 39-43.

Elert, K., & Rodriguez-Navarro, C. (2022). Degradation and conservation of clay-containing stone: A review. *Construction and Building Materials*, *330*, 127226.

Germinario, L., Siegesmund, S., Maritan, L., & Mazzoli, C. (2017). Petrophysical and mechanical properties of Euganean trachyte and implications for dimension stone decay and durability performance. *Environmental earth sciences*, *76*(21), 1-21.

Glosz, K., Stolarczyk, A., & Jarosz, T. (2020). Siloxanes—Versatile Materials for Surface Functionalisation and Graft Copolymers. International Journal of Molecular Sciences, 21(17), 6387.

Hosseini, M., & Karapanagiotis, I. (Eds.). (2018). *Advanced materials for the conservation of stone*. Cham, Switzerland: Springer.

Karapanagiotis, I., & Manoudis, P. N. (2022). Superhydrophobic and superamphiphobic materials for the conservation of natural stone: An overview. *Construction and Building Materials*, *320*, 126175.

Lakhani, R., & Sharma, R. K. (2018). Strategies for the restoration of heritage buildings: material issues. *BHAGVAN-A SEARCH*.

Lezzerini, M., Tomei, A., Gallello, G., Aquino, A., & Pagnotta, S. (2022). The Crystallization Effect of Sodium Sulfate on Some Italian Marbles, Calcarenites and Sandstones. *Heritage*, *5*(3), 1449-1461.

Lee C. H., Lee M. S., Suh M., Choi S. W. (2005) Weathering and deterioration of rock properties of the Dabotap pagoda (World Cultural Heritage), Republic of Korea. *Environ Geol*, 47, p. 547–557.

Lettieri, M., Masieri, M., Aquaro, M., Dilorenzo, D., & Frigione, M. (2021). Eco-friendly protective coating to extend the life of artworks and structures made in porous stone materials. *Coatings*, *11*(11), 1270.

Lisci, C., Pires, V., Sitzia, F., & Mirão, J. (2022). Limestones durability study on salt crystallisation: An integrated approach. *Case Studies in Construction Materials*, *17*, e01572.

Lubelli, B., Cnudde, V., Diaz-Goncalves, T., Franzoni, E., van Hees, R. P., Ioannou, I., ... & Viles, H. (2018). Towards a more effective and reliable salt crystallization test for porous building materials: state of the art. *Materials and Structures*, *51*(2), 1-21.

Liu, X., Koestler, R. J., Warscheid, T., Katayama, Y., & Gu, J. D. (2020). Microbial deterioration and sustainable conservation of stone monuments and buildings. *Nature Sustainability*, *3*(12), 991-1004.

Liu, Q. Zhang, B.J. (2007). Syntheses of a novel nanomaterial for the conservation of historic stones inspired by nature. *Materials Letters, 61* (28). pp 4976-4979.

Malaquias, R. H., Bruschi, G. J., & de Senna Brisotto, D. (2022). Performance analysis of gravity chemical blockers in the treatment of rising damp in masonry walls. Revista ALCONPAT, 12(1), 61-75.

Melo, M.J., Bracci, S., Camaiti, M., Chiantore, O., and Piacenti. F. (1999). Photodegradation of acrylic resins used in the conservation of stone. Polymer Degradation and Stability 66: 23-30.

Menningen, J., Sassoni, E., Sobott, R., & Siegesmund, S. (2021). Constraints of the durability of inorganic and organic consolidants for marble. *Environmental Earth Sciences*, *80*(10), 1-18.

Morillas, H., Maguregui, M., Gallego-Cartagena, E., Marcaida, I., Carral, N., & Madariaga, J. M. (2020). The influence of marine environment on the conservation state of Built Heritage: An overview study. *Science of The Total Environment*, *745*, 140899.

Morais, M. J., Masciotta, M. G., Ramos, L. F., Oliveira, D. V., Azenha, M., Pereira, E. N. B., & Monteiro, P. (2019). A proactive approach to the conservation of historic and cultural Heritage: The HeritageCare methodology.

Oguchi, C. T., & Yu, S. (2021). A review of theoretical salt weathering studies for stone heritage. *Progress in Earth and Planetary Science*, *8*(1), 1-23.

Ortega-Morales, B. O., & Gaylarde, C. C. (2021). Bioconservation of historic stone buildings—An updated review. *Applied Sciences*, *11*(12), 5695.

Parkin, I. P., & Palgrave, R. G. (2005). Self-cleaning coatings. Journal of materials chemistry, 15(17), 1689-1695.

Pinheiro, A. C., Mesquita, N., Trovão, J., Soares, F., Tiago, I., Coelho, C., ... & Portugal, A. (2019). Limestone biodeterioration: A review on the Portuguese cultural heritage scenario. *Journal of cultural heritage*, *36*, 275-285.

Possenti, E., Colombo, C., Conti, C., Marinoni, N., Merlini, M., Negrotti, R., ... & Gatta, G. D. (2019). Consolidation of building materials with a phosphate-based treatment: Effects on the microstructure and on the 3D pore network. *Materials Characterization*, *154*, 315-324.

Price, C.A., & Doehne, E. (2011). Stone conservation: an overview of current research. Second ed. *The Getty Conservation Institute, Los Angeles*, pp 1-175.

Rodrigues, A., da Fonseca, B. S., Pinto, A. F., Piçarra, S., & Montemor, M. F. (2022). Synthesis and application of hydroxyapatite nanorods for improving properties of stone consolidants. *Ceramics International*, *48*(10), 14606-14617.

Rodrigues, A., da Fonseca, B. S., Pinto, A. F., Piçarra, S., & Montemor, M. F. (2021). Tailoring alkoxysilanes with poly (ethylene glycol) as potential consolidants for carbonate stones. *Construction and Building Materials*, *289*, 123048.

Rodrigues, J. D. (2015). Defining, mapping and assessing deterioration patterns in stone conservation projects. *Journal of Cultural Heritage*, *16*(3), 267-275.

Saba, M., Quiñones-Bolaños, E. E., & López, A. L. B. (2018). A review of the mathematical models used for simulation of calcareous stone deterioration in historical buildings. *Atmospheric Environment*, *180*, 156-166.

Scherer, G. W., & Wheeler, G. S. (2009). Silicate consolidants for stone. In *Key Engineering Materials* (Vol. 391, pp. 1-25). Trans Tech Publications Ltd.

Sierra-Fernández, A., Gómez Villalba, L. S., Rabanal, M. E., & Fort González, R. (2017). New nanomaterials for applications in conservation and restoration of stony materials: A review.

Sesana, E., Gagnon, A. S., Ciantelli, C., Cassar, J., & Hughes, J. J. (2021). Climate change impacts on cultural heritage: A literature review. *Wiley Interdisciplinary Reviews: Climate Change*, *12*(4), e710.

Ševčík, R., Viani, A., Machová, D., Lanzafame, G., Mancini, L., & Appavou, M. S. (2019). Synthetic calcium carbonate improves the effectiveness of treatments with nanolime to contrast decay in highly porous limestone. *Scientific reports*, *9*(1), 1-13.

Speziale, A., Gonzalez-Sanchez, J. F., Taşcı, B., Pastor, A., Sánchez, L., Fernández-Acevedo, C., & Alvarez, J. I. (2020). Development of multifunctional coatings for protecting stones and lime mortars of the architectural heritage. *International Journal of Architectural Heritage*, *14*(7), 1008-1029.

Steiger, M., Charola, A. E., & Sterflinger, K. (2011). Weathering and deterioration. In *Stone in architecture.* Springer, Berlin, Heidelberg. pp. 227-316.

Tortora, M., Chiarini, M., Spreti, N., & Casieri, C. (2020). 1H-NMR-relaxation and colorimetry for evaluating nanopolymeric dispersions as stone protective coatings. *Journal of Cultural Heritage*, *44*, 204-210.

Vergès-Belmin, V., ed. (2008). Illustrated Glossary on Stone Deterioration Patterns = Glossaire illustré sur les formes d’altération de la pierre. English French ed. Monuments & Sites 15.

Paris: ICOMOS (International Council on Monuments and Sites) and ISCS (International Scientific Committee for Stone). http://international.icomos.org/publications/monuments_and_sites/15/pdf/Monuments_and_Sites_15_ISCS_Glossary_Stone.pdf

Vidal, F., Vicente, R., & Silva, J. M. (2019). Review of environmental and air pollution impacts on built heritage: 10 questions on corrosion and soiling effects for urban intervention. *Journal of Cultural Heritage*, *37*, 273-295.

Wang, Z., Cousins, I. T., Scheringer, M., & Hungerbuehler, K. (2015). Hazard assessment of fluorinated alternatives to long-chain perfluoroalkyl acids (PFAAs) and their precursors: status quo, ongoing challenges and possible solutions. Environment international, 75, 172-179.

Wang, T., Chang, L., Hatton, B., Kong, J., Chen, G., Jia, Y., ... & Wong, C. (2014). Preparation and hydrophobicity of biomorphic ZnO/carbon based on a lotus-leaf template. Materials Science and Engineering: C, 43, 310-316.

Wu, Y., Tan, X., Wang, Y., Tao, F., Yu, M., & Chen, X. (2022). Nonfluorinated, transparent, and antireflective hydrophobic coating with self-cleaning function. *Colloids and Surfaces A: Physicochemical and Engineering Aspects*, *634*, 127919.

Xu, F., Zeng, W., & Li, D. (2019). Recent advance in alkoxysilane-based consolidants for stone. *Progress in organic coatings*, *127*, 45-54.

Zhang, G., Gong, C., Gu, J., Katayama, Y., Someya, T., & Gu, J. D. (2019). Biochemical reactions and mechanisms involved in the biodeterioration of stone world cultural heritage under the tropical climate conditions. *International Biodeterioration & Biodegradation*, *143*, 104723.

Zhu, G., Xu, Z., Jin, Y., Chen, X., Yang, L., Xu, J., ... & Guo, B. (2022). Mechanism and application of laser cleaning: A review. *Optics and Lasers in Engineering*, *157*, 107130.

CHAPTER 2

2 Materials and Methodological Approaches

2.1 Materials

This master thesis was focused on the study and influence of different coatings compositions and their relation for effectiveness, compatibility, and durability on previously selected samples representative of the most important Portuguese lithotypes. The materials used in this research have been categorized into two main groups. The first group is the stone samples and mock-ups which have been selected as case studies. Accordingly, samples from different lithotypes with different physical, chemical, and mineralogical properties were chosen to perform this study in order to have comprehensive data and results, according to their chemical and mineralogical nature. The second group of the studied material is composed of 3 commercial hydrophobic coatings. Therefore, three different hydrophobic coatings with different chemical compositions have been selected.

2.1.1. Stone Specimens

Ten natural stones with high commercial values have been selected to study the effects of the hydrophobic coatings on stones, including five different types of limestone, four various kinds of marble, and one specific type of granite (Table 2.1). The quarry localization of all the studied samples is in Portugal.

The logic behind this selection is as selected stones from different lithotypes have different mineralogical and chemical compositions as well as different physical features such as texture, colour, porosity, roughness, hardness, thermal conductivity, and water vapor permeability which can lead to comprehensive data and results to compare.

In this selection, nine different carbonate stones and one specific granite sample have been chosen. Among all natural stones, granite is one of the hardest and most resistant on the earth. Granite is selected due to its extreme durability, resistance to water, and low open porosity, as well as its different mineralogical and chemical compositions, compared to carbonate stones. The granite sample can be also considered as a non-carbonate benchmark to validate the acquired data and results from all the carbonate samples (Frascá, M., et al., 2006; Pires, V., et al., 2014). Moreover, due to testing the compatibility of the coatings and colour change, it has been tried to select a set of samples with a wide range of colours from dark grey to almost white. The general introduction of samples can be found in table 2.1.

Table 2.1. General Information of the studied stone Samples (Photos are taken by CANON 80D professional camera in Hercules Laboratory, Evora)

Ref N.	***Commercial Name***	***Typology***	***Quarry***	***Macroscopic Appearance***
L1	*Branco Real*	*Limestone*	Arrimal, Porto-de-Mós	
L2	*Rosal Dunas*	*Limestone*	*Codaçal, Serro Ventoso, Porto-de-Mós*	
L3	*Creme Champagne*	*Limestone*	Cruz da Légua, Aljubarrota	
L4	*Moca Creme*	*Limestone*	Relvinha	
L5	*Brecha St. Antonio*	*Limestone*	Santo Antônio, São Bento, Leiria	

M1	*Verde Viana*	*Marble*	Viana do Alentejo	
M2	*BRANCO*	*Marble*	Estremoz	
M3	*Creme JPL*	*Marble*	Estremoz	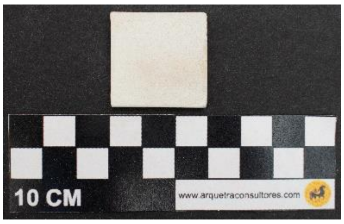
M4	*Rosa JPL*	*Marble*	Estremoz	
G1	*Granito Alpalhão*	*Granite*	Cinza Alpalhao	

2.1.2. Hydrophobic Coatings

As it is already mentioned, three different hydrophobic coatings have been chosen in this research which will be referred to as Coating number 1 (CN1), coating number 2 (CN2), and coating number 3 (CN3). Since all these coatings are commercial the real marketing name and the chemical composition cannot be discussed without preserving the copyrights. Therefore, only the base chemical composition of each coating will be compared.

CN1 is a brownish solution made by modified silane/siloxane micro-nano dispersion in water with particle size from 7 nanometers with free VOC. CN2 is an almost colourless transparent solution produced by modified silicon dioxide (SiO2) nano particles with free VOC. CN3 is a milky solution manufactured by micro-nano emulsion free of Perfluorooctanoic Acid (PFOA) and Perfluorooctanesulfonic Acid (PFOS) and is based on nano silanes, siloxanes, and novel modified C6 fluorinated compounds free of VOC.

The reason for studying and comparing these hydrophobic coatings among each other is although many polymers have been proposed and studied to meet the hydrophobic features, still the sustainability of the treatments, economically and eco-friendly environmentally, is problematic in the 21st century and it is considered when selecting the most appropriate conservation solution (Karapanagiotis, I., et al., 2021). Among all these studied hydrophobic coatings, polysiloxanes, and their precursors, silanes, and silicon dioxide have been frequently used (Lettieri, M., et. al., 2016). Therefore, this study by selecting and comparing these coatings aimed to find out the improvements and challenges of preferred hydrophobic coatings on stone material.

2.2 Methodological approaches

The experimental techniques used in this research have been applied to characterize the stone samples physically, chemically, and mineralogically, and to compare the differences among three applied coatings related to their effectiveness, durability, and compatibility before and after simulating external environmental factors. Hence, all the methodological approaches comprising all the analytical techniques used in this study, are further discussed in detail. Methodological approaches can be categorized into four separate classifications regards to their purpose: full characterization of stone samples, coatings compatibility assays, coatings protective hydrophobic performance, and coatings durability approach. The characterization of stones sample has been sub-categorized into physical, chemical, and mineralogical identification which different techniques have been involved with. Moreover, all the corresponding techniques have been repeated on different states as before and after simulating the external environmental factors. The experimental set-up adopted is presented in figure 2.1.

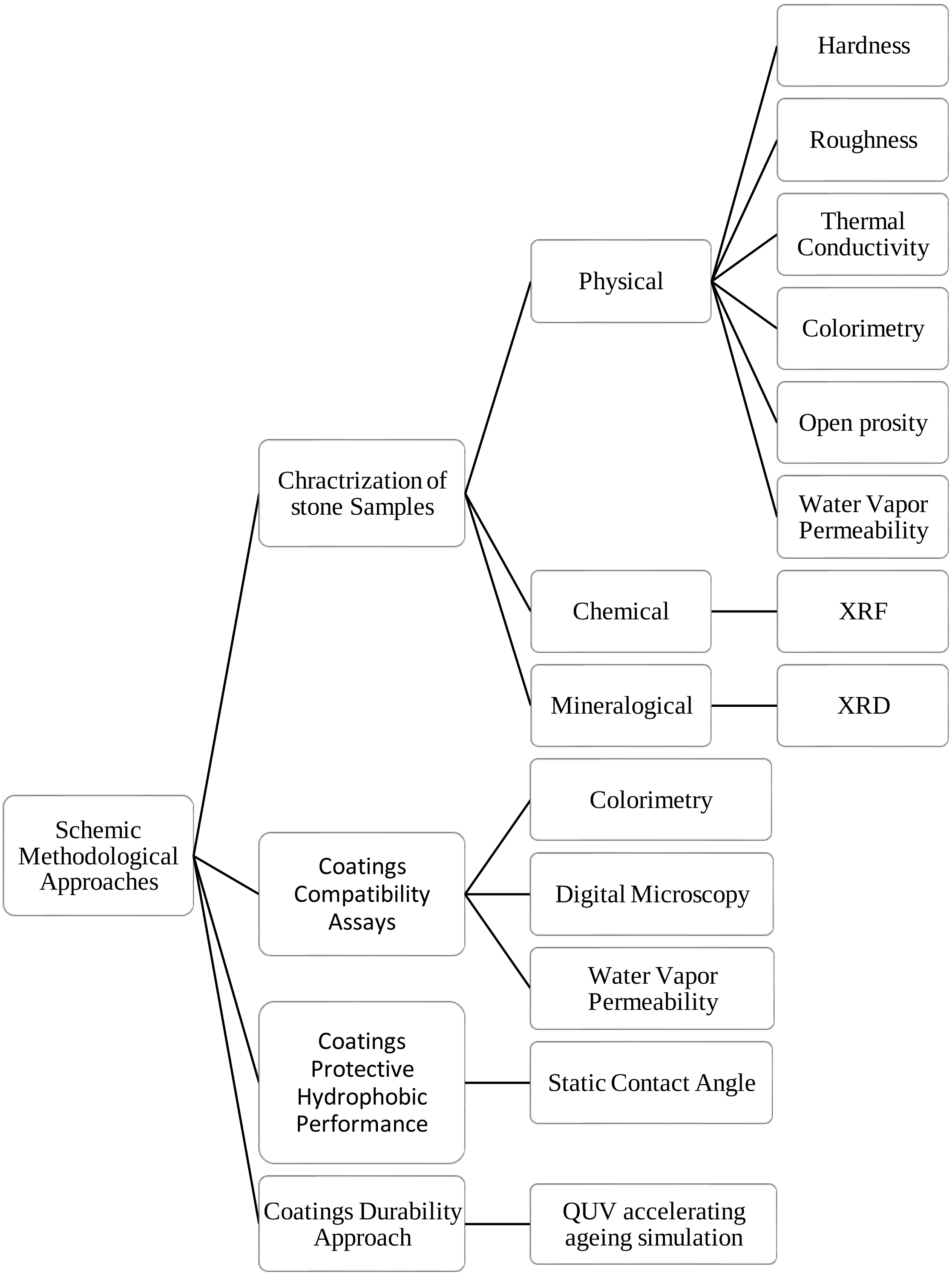

Figure 2.1 The experimental set-up adopted for this study

2.2.1 Sample Preparation

a) stone mock-ups

Generally, for all the techniques applied for stone samples, four different types of mock-ups have been prepared: powder, powder pressed pellets, cut in 30x30x4 mm dimensions, and cut in 50x50x50 mm dimensions. The classification of sample preparation types for applied techniques has been presented in Table 2.2.

Table 2.2. Classification of sample preparation for different techniques

sample preparation types	applied techniques	Examples
powder	• XRD	
powder pressed pellet	• XRF • colorimetry	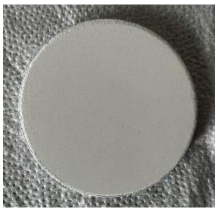
cut in 50x50x50 mm	• hardness • thermal conductivity • open porosity	
cut in 30x30x4 mm	• roughness • colorimetry • water vapor permeability • digital microscopy • static contact angle • ageing simulation	

Samples were powdered with the Planetary Ball Mill PM100 used at 500 rpm for 20 minutes for each sample. Based on the sampling procedure for the XRF technique, which was published in 1997, 10 mg of fine powder has been pressed using a 25-ton Specac's Manual Hydraulic Press to make the pellets (Sampling, I., 1997). The stone specimens were wet cut by a STRUERS cutting saw.

In total, 4 sets of mock-ups have been cut in 30x30x4 mm dimensions: a set as a controlled standard, and three sets corresponding to CN1, CN2, and CN3. All the mock-ups have been washed with distilled water and dried in the oven at 60 degrees.

2.2.1.1 Hydrophobic coatings

The Process of preparing each coating was followed by the application guides provided by their companies. According to the CN1 application guide, it was diluted in distilled water in a ratio of 1:10. Then, it was sprayed on a set of 10 studying stone mock-ups (Figure 2.2.a). The period of time that CN1 needed to be dried was between 4 to 24 hours. The coated samples with CN1 remained at room temperature for 24 hours to be completely dried (Figure 2.2.b).

CN2 application is as same as CN1 which means the ratio of diluted coatings material in distilled water is 1:10. Then, it was sprayed on another set of 10 stone mock-ups. The amount of time that CN2 needed to be dried is between 6 to 24 hours. Therefore, the coated samples were placed at room temperature for 24 hours to be completely dried.

CN3 application guide recommends the range of ratio 1:6 to 1:14 of diluted coatings material in distilled water. The more concentration the greater effects of water repellency. Also, more concentration can cause more colour changes in samples after applying the coating. Therefore, to be getting along with the other coatings concentrations and less colour change, the middle ratio of 1:10 has been considered. Then, the diluted solution was sprayed on the third set of stone mock-ups. Regarding its application guide, 2 or 3 times of spraying on samples depending on their surface´s absorbance are needed. Therefore, another layer of CN3 materials was sprayed on mock-ups while the previous layer was not completely dried. The period that CN3 needed to be dried was between 4 to 24 hours. The coated samples with CN3 remained at room temperature for 24 hours to be completely dried.

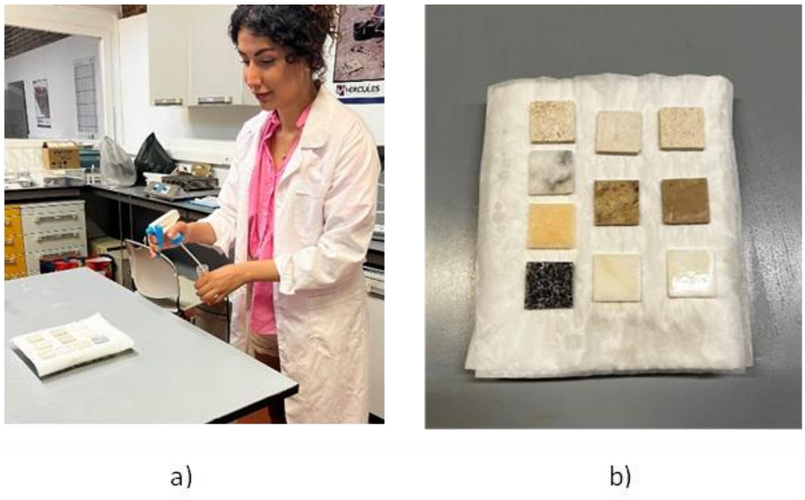
a) b)

Figure 2.2 the process of applying coatings on samples: (a) spraying CN1 on one set of mock-ups; (b) the coated samples with CN1 during the drying process.

2.2.2 Stone Sample Characterization

2.2.2.1 Physical characterization

a) Surface Hardness Testing

Hardness tests have always been important to conclude on specific mechanical characterization of materials, especially stones in a fast, economic, and non-destructive manner (Fort, R., et al., 2013). In this study, the surface hardness test has been done to identify the hardness, one of the physical characterizations of selected stone samples. Hardness has a direct correlation to hydrophobicity (Wang, Y., et. al., 2015). The effectivity of hydrophobic coatings can be directly improved by increasing the material hardness (Zhao, J., et. al., 2022).

In this research, the hardness testing was performed by using an Equotip 550 portable testing device with an impact device D. This testing instrument works with the rebound method. The procedure of operation is like the well-known Schmidt Hammer. It indirectly measures the loss of energy of a so-called impact device D. Leeb, the inventor of this method, defined his hardness value called the Leeb hardness value: HL. Therefore, the results are given as HLD (Wilhelm, K., et al., 2016; Viles, H., et al., 2011).

In this measurement, for each specimen, six different surfaces have been examined. Therefore, six individual measurements were done for each sample, and the average value and standard deviation were calculated. To optimize the testing results the tested surface of the cubical block specimens was polished to reduce the roughness of the material.

b) Surface Roughness Measurement

Material roughness is a physical characteristic of the surface texture that can deeply affect their durability due to its influence on particle retention and adhesion capacity, which may cause their further decay, e.g., particles of organic materials, water drops, and/or atmospheric pollutants that can cause processes of soiling and salt crystallization (black crusts). In general, an increase in material roughness also increases the specific surface; therefore, the material is more exposed to all environmental agents (Vazquez-Calvo, C., et al., 2012). Because of these matters, surface roughness is a key role in the characterization of stone materials.

Since the hydrophobicity improves with increasing the surface roughness (Tang. H., et. al., 2009), in this study surface roughness as a physical characterization, is measured to find out the correlation between the effectivity of the applied hydrophobic coatings and the surface roughness of studied samples.

In this research, the roughness of the specimens´ surfaces has been measured with a Mitutoyo Surftest SJ-210 (calibration standard by ISO1997). The results of this portable, non-destructive device are given as Ra, Rq, and Rz (Figure 2.3) which are the roughness average of the absolute values of the profile heights of the peak heights across the evaluation length, the root mean square of the profile heights over the evaluation length, and the average absolute values of the heights of the five highest-profile peaks and the five deepest valleys within the evaluation length, respectively. (Loo-Morrey, M., 2007).

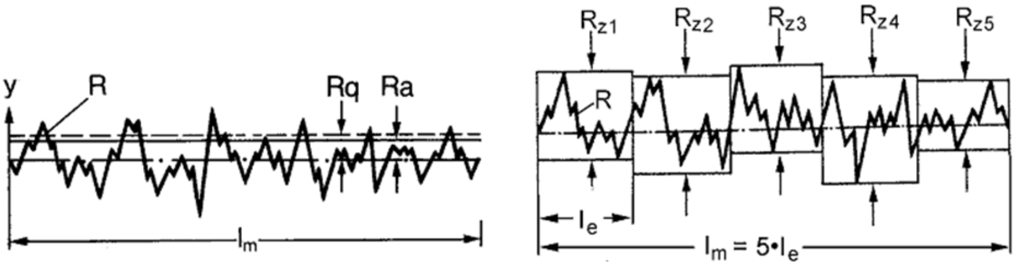

Figure 2.3. Description of Ra, Rq, and Rz values (Loo-Morrey, M., 2007).

In this measurement, six different points of each specimen's surface have been assessed. Therefore, six individual measurements were done for each sample's surface, and the average value and standard deviation has been calculated. Among these parameters, Ra (µm) has been selected as the most appropriate to compare among all the specimens, since it is commonly used for this purpose (Gonçalves, T. 2008; Vázquez, P., 2013).

c) Thermal Conductivity Measurement

A rock's ability to transfer heat through it is determined by its thermal conductivity, which is measured in W/mK by means of watts per meter-Kelvin. It has to do with stationary heat flow, and the higher the value, the easier a rock conducts heat (Amaral, P., et al., 2013). The thermal conductivity of stones changes with their type since they have variable and different mineral constituents (Özkahraman, H., et al., 2003).

Generally, thermal conductivity gives knowledge of the physical and mechanical properties of the material (Popov, Y., et al., 1999). Therefore, in this study, the thermal conductivity values of each stone are compared to have a general perspective of their features for future applications.

In this study, thermal conductivity was measured in ten selected stone samples using an ISOMET 2104 Heat Transfer Analyser (Figure 2.4). The thermal probe used to make the measurements has a range between 2.00 and 6.00 W/mK. The average values and standard deviation for the thermal conductivity of each sample were achieved by placing the probe in three different places on its polished surface.

Figure 2.4. Heat Transfer Analyser ISOMET 2104 with the metal measuring probe on top of the stone sample

d) Colorimetric measurement

One of the most important factors which extremely change in stone when it comes to meeting external environmental factors is its colour. Chromatic change becomes more important when it relates to stone heritage (Sesana, E., et al., 2021). Changes in colour may result from staining by foreign substances or discoloration due to a change in the structure of minerals' structure (Karapanagiotis, I., et al., 2022). Stone colour stability, as well as the colour of natural stones, must be characterized to be able to assess the compatibility of protective coatings that may be applied to it.

In this study, chromatic changes had the main goal of assessing the compatibility of hydrophobic coatings after treatment as well as after artificial ageing simulation (Andreotti, S., et al., 2018). To reach this goal, colorimetric testing has been applied to two different types of samples (Figure 2.5). The first application of a colorimetric measurement is to identify and characterize the colour of the selected stones which has been done on the powder pellets to obtain the bulk colour of each stone. The other measurement assesses the colour difference of each mock-up's surface before and after treatment as well as after ageing process. To limit and reduce the errors corresponding to the heterogeneity of samples' surfaces the center area for each mock-up has been examined during each step (Figure 2.5.b).

The colorimeter which is used in this study is the Datacolor Check II Plus (Figure 2.5.a). The USAV detector has been used on three different points of each sample and the average and standard deviation of the obtained data have been calculated.

In this measurement, the CIELab colour space was automatically used to plot colour measurements. The calculation of colour difference relates to L*a*b parameters in colour space and is based on the Hering Theory (Rivas, T., 2011). He designed a graphic chart that is associated with the three axes of a three-dimensional colour space. L* is the vertical axis representing lightness; 100 represents a complete white sample and 0 is a complete black sample. a* is the axis in the plane normal to L* and represents the redness-greenness quality of the colour. Positive values signify redness and negative values denote greenness. b* is the axis normal to both L* and a* and represents the yellowness-blueness quality of the colour. Positive values indicate yellowness and negative values denote blueness. (Gilchrist, A., et al., 2017).

(a

(b

Figure2.5. The Datacolor Check II Plus (a while processing the colorimetry measurements of stone specimens, (b measurement with LAV aperture.

e) Open Porosity measurement

The porosity of a stone material directly relates to its deformability and deterioration which is different in the various types of stones. Carbonate rocks occur with a wide range of porosities and hence of mechanical character; igneous rocks that have been weakened by weathering processes also have typically high porosities (Franklin, J. A., 1979).

Since the open porosity have a direct correlation with water vapor permeability (Crina, B., et. al., 2013), the open porosity test for each sample has been performed in this study. Water vapor permeability can impact the compatibility of hydrophobic coatings with stone samples (Zuena, M., et. al., 2021) and therefore the role of open porosity can be investigated in studied hydrophobic coatings.

Each stone type's open porosity was assessed by following the test protocol outlined by European Standard EN 1936 (EN 1936, 2006). The test procedure can be summarized as follows:

The samples should if possible be large, to minimize the influence of experimental error. Hence, the mock-ups which have been selected for this measurement are cubical samples with 50x50x50mm dimensions. For each type, six cubes have been cut and examined. The experiments were conducted at 24 ± 1°C room temperature. Throughout testing, the relative humidity was kept at a range of 50 ± 5%. Specimens were dried for 24 hours at 60 ± 5°C in the oven prior to the test, and then they were placed in the desiccator to cool for around 8 hours at room temperature. Each dried specimen was weighed (m_d) before being put into a vacuum vessel, where the pressure was steadily reduced until it reached about 2.0 ± 0.7 kPa (= 15 ± 5 mm Hg). The samples were evacuated half immersed half submerged for 2h to remove trapped air. Demineralized water was then gradually added to the container until all of the specimens were submerged. After then, the pressure was changed to atmospheric, and the specimens were submerged in water for a further 24 hours. Each specimen was weighed after being submerged in water (m_h) and air, and the surface was dried (m_s).
Open porosity, P_0, (percentage) was calculated corresponding to Eq. 1: (Li, Y., et al., 2015)

$$P_0 = \frac{m_s - m_d}{m_s - m_h} \,.\, 100 \qquad \textit{Equation 1}$$

f) Water Vapor Permeability Test

The ability of a porous material to allow water vapor to pass through its pores under the impact of a variation in water vapor concentration is expressed by the water vapor permeability test procedure. This feature is determined by the structure of porous materials and can characterize the material as a physical parameter (Togkalidou, T., et al., 2013).

In this study, water vapor permeability has been performed to determine the breathability and therefore compatibility of hydrophobic coatings on the studied stone samples (Ghezal, I., et. al., 2021).

In order to perform the test, the cup method (ASTM, 2014) is applied for measuring water vapor transmission which leads to water vapor permeance. According to the technical criteria established by the Water Vapour Permeability Coefficients, W_{VP}, was measured in $g.m^{-1}.s^{-1}.Pa^{-1}$ using a straightforward gas-flow method with a constant pressure differential across the specimen. The average of the differences between mass by a time unit (in g/h) of at least three values obtained in steady-state flow is used to estimate the water vapor flux, G_w. W_{VP} is provided in $g.m^{-1}.s^{-1}.Pa^{-1}$ by the Eq.2 :

$$W_{VP} = \frac{G_w.h}{A_s.\Delta P.36*10^5} \qquad \textit{Equation 2}$$

where:

G_w - Water vapor flux;

h – thickness of Specimens;

A_S - Specimens tested area;

ΔP^1 - Vapor pressure inside and outside the container differs.

The following provides a general overview of the experimental design. Before measuring permeability, specimens were first dried for 24 hours at 60 ± 5°C degrees in the oven. After that, they were placed in the desiccator for the same amount of time. Each dry specimen was weighed separately (m_d). The stone specimens were prepared for receiving in special containers. Each container was filled with cotton and 1 cm of distilled water to produce a completely wet environment (Figure 2.6). Following that, each stone specimen cut in 30x30x4mm was set on the container's square opening in size of 25x25mm, and silicone mastic was used to seal off any potential air entries. Each set of a container, water, and stone specimen was weighed (in milligrams), and it was then put within Aralab FitoClima 600 stability test chamber with 20°C temperature and 40% of relative humidity. The test was weighted continually every 24 hours after it started. When the sets acquired a mass difference of 0.1%, the test was concluded.

Figure 2.6. The sets of containers, wet cotton, and the specimens glued to the plastic covers.

2.2.2.2 Chemical Characterization of stone samples

a) X-Ray Florescence Spectroscopy

X-ray fluorescence (XRF) spectroscopy is an analytical technique that can be applied to determine the elemental composition of many kinds of materials (Liritzis, I., et al., 2011). One of the most crucial methods for the examination and quantification of the elements that constitute rocks is XRF, which has a long history of success according to various studies such as (Chubarov, V., et al., 2010), (El-Taher, A., 2012), and (Janssens, K., et al., 2004). Therefore, this study tried to identify the elemental composition of stone samples by using the XRF technique to find out any relation between the elemental composition of stones and the compatibility, effectiveness, and durability of applied coatings.

The energy-dispersive X-ray fluorescence analysis for this investigation was carried out using a portable spectrometer, the Tracer III SD Bruker AXS, running at 40 kV and 11 µA. The device has a silicon drift X-Flash SDD detector with a Peltier cooling system and a spot size of 3 to 4 mm. The device has been used on the powder pellets of each sample. For each pellet, 3 different spectra have been obtained and each spectrum was acquired for 60 seconds. The energy resolution of the spectrometer was 150 eV at 5.9 keV. The instrument's head was not subjected to vacuum. The sample surface was brought into contact with the instrument’s window. Data was collected using S1PXRF® Software, and spectra were analysed using ARTAX® X-ray software. The obtained data were normalized using the RhKα peak.

2.2.2.3 Mineralogical Characterization of stone samples

a) X-Ray Diffraction Analysis

The practical method of X-ray diffraction (XRD) is used to identify crystalline materials. It offers details on the structures, phases, preferred crystal orientations (texture), and other key elements such as grain size, crystallinity, strain, and crystal defects (Bunaciu, A. Et al., 2015).

Proving diffractograms to determine the mineralogical characterization follows Bragg's Law (Eq. 3):

$$n_r\lambda = 2d\sin\vartheta \qquad \text{Equation 3}$$

where:

n_r – reflection order;

λ – wavelength;

d – distance between atomic plans;

θ – Bragg angles (Jauncey, G., 1924).

Since, the hydrophobicity of stone surface could relate to its mineral composition (Andreotti, S., et. al., 2018), in this study, the XRD technique has been used to identify the mineralogical compositions of each stone sample to find out any correlation between the mineralogical composition of samples and the effectiveness of applied coatings. All X-ray diffraction analyses in this thesis were only carried out from a qualitative standpoint in order to compare with other investigations. Due to this, quantitative X-ray diffraction analysis will not receive any special attention.

In this research, 2 mg fine-grained powder was obtained from the stone sample using the Ball Mill PM100. XRD measurements were performed by using up a Bruker-AXS D8 Advance

(Bruker AXS Inc., Madison, WI, USA) diffractometer, with Cu–K_α radiation (λ = 0.15406 nm), operating at 40 kV and 40 mA. Powder diffraction data was gathered in steps of 0.05° with a measuring duration of 1 second in the range of 5–75° (2θ). The obtained XRD patterns were identified with the PDF-ICDD Diffraction Database, using DIFFRAC.SUITE EVA and Highscore Plus software.

2.2.3 Coating Compatibility essays

2.2.3.1 Chromatic changes

The following equations (Eq. 4,5, and 6) can be used to determine differences in the L*, a*, and b* parameters:

$$\Delta L^* = L_t^* - L_0^* \qquad \text{Equation 4}$$

$$\Delta a^* = a_t^* - a_0^* \qquad \text{Equation 5}$$

$$\Delta b^* = b_t^* - L_0^* \qquad \text{Equation 6}$$

where "0" stands for the reference stone specimen's initial colour,

and "t" stands for the altered stone specimens' colour following any accelerated aging test or hydrophobic coatings treatment (Prieto, B., et al., 2010).

Colour differences can be stated as a single numerical value, ΔE* (Eq. 7), which does not specify how the colours differ but rather their magnitude. (Prieto, B., et al., 2010)

$$\Delta E^* = (\Delta L^{*2} + \Delta a^{*2} + \Delta b^{*2})^{1/2} \qquad \text{Equation 7}$$

2.2.3.2 Digital Microscopy

Digital microscopy is an effective technique for visualizing data, including high-resolution photographic and observational data that may help with research on the need of having high-resolution detailed 2D and 3D modeling images (Martín-Viveros, J., et al., 2020).

In this study, an active top light 200X magnification Hirox HRX-01 microscope was used for the observation of the stone specimens. Then, the acquired pictures have used to compare the color change or stain trace on stone samples after coating treatment. Also, the comparison has been repeated after the ageing procedure as well.

2.2.4 Hydrophobic effectiveness

2.2.4.1 Contact Angle Measurement

Water contact angle measurement is a technique that will immediately indicate the wettability of the solid. When a drop of a pure liquid is placed on a planar, solid surface, adhesive forces are created between the liquid and the surface that favor spreading, while cohesive forces inside the liquid work to prevent spreading. The contact angle is determined by the equilibrium between these forces. Young's equation (Eq. 8), which links the contact angle to the surface free energy of a system including solids (S), liquids (L), and vapors (V), states that,

$$\gamma_{SV} - \gamma_{SL} = \gamma_{LV} \cos\vartheta \qquad \textit{Equation 8}$$

where

γ_{SV} is the solid surface free energy,

γ_{LV} is the liquid surface free energy (also known as surface tension),

and γ_{SL} is the solid-liquid interfacial free energy (Young, T., 1805).

The liquid will wet the solid surface if the substrate's surface energy is relatively large but less than the liquid's surface tension, and the resulting contact angle is 0 to 90. In contrast, if the solid surface's surface energy is low, the drop will adhere poorly and wet the surface poorly, increasing the contact angle. For instance, a solid surface is described as hydrophobic when a water drop has a contact angle of greater than 90 (Lamour, G., et al., 2010).

Contact angle measurements can be an extremely helpful technique to measure the effectiveness of hydrophobic treatments on stone. several research as (Facio, D., et al., 2015), (Ferri, L., et al., 2011), and (Manoudis, P., et al., 2014) have focused on the contact angle measurements and how they can determine the wettability of the surfaces. Hence, in this study, static contact angle measurement is extremely practical for comparing the impacts of hydrophobic coatings on different selected stone samples.

The measurement of the static contact angle is required by the UNI10921:2001 norm. The test procedure was done to evaluate the hydrophobicity of the treated stone surface by measuring the static contact angle on stones samples, before, after the treatment, and after the weathering simulation. Measurements were done by using a ramé-hart Model 210 Goniometer/Tensiometer. In this procedure, a pipette was filled with deionized water and a dropper was placed on a sample holder, and the test surface was in a horizontal position (Figure 2.6). To have a good average appraisal, the contact angle of the drop deposited on a stone surface was measured between 3 to 10 seconds for each sample. 12 drops on each sample surface were performed and for each drop 4 measurements have been considered. Obtained values were averaged and the standard deviation was calculated. The obtained images and data were processed with DROPimage software.

Figure 2.6 ramé-hart Model 210 Goniometer/Tensiometer during static contact angle measurement on a sample

2.2.5 Durability assessment

2.2.5.1 QUV accelerating ageing simulation

Several studies such as (Carmona-Quiroga, P., et al., 2017), (Corcione, C., et al., 2017), and (Lisci, C., et al., 2022) have focused on the durability of hydrophobic treatments on the stone when it comes to meeting weather conditions by controlled ageing situations in the laboratory. Therefore, in this study has tried to examine the durability of applied coatings on stone samples by comparing their color, water vapor permeability, and contact angle before and after the ageing simulation.

Samples were put through weathering cycles in the QUV-spray chamber in accordance with ASTM G154-C7 (ASTM G154C7, 2006). This standard includes 15 minutes of spray mode (7 L per 1 min of MilliQ-water) and 3:45 hours of condensations at 50 °C. It also includes 8 hours of UVA radiation of 340 nm at 60 °C (1.55 W/m2 irradiance). A cycle lasts 12 hours. There are 14 days in the test. The samples' color, contact angle, and water vapor permeability were assessed at time 0 (before aging) and at time 14.

BIBLIOGRAPHY

Andreotti, S., Franzoni, E., Esposti, M. D., & Fabbri, P. (2018). Poly (hydroxyalkanoate) s-based hydrophobic coatings for the protection of stone in cultural heritage. Materials, 11(1), 165.

Andriani, G., & Walsh, N. (2003). Fabric, porosity, and water permeability of calcarenites from Apulia (SE Italy) used as building and ornamental stone. *Bulletin of Engineering Geology and the Environment*, *62*(1), 77-84.

Amaral, P. M., Fernandes, J. C., & Rosa, L. G. (2006). A comparison between X-ray diffraction and petrography techniques used to determine the mineralogical composition of granite and comparable hard rocks. In *Materials science forum*. Vol. 514, pp. 1628-1632.

Amaral, P., Correia, A., Lopes, L., Rebola, P., Pinho, A., & Carrilho Lopes, J. (2013). On the use of thermal properties for characterizing dimension stones. Trans Tech Publications Ltd. In *Key Engineering Materials*. Vol. 548, pp. 231-238.

ASTM G154C7 (2006). resistance of a nonmetallic material to simulated sunlight and moisture exposure.

ASTM (2014). ASTM E96/E96M-14: Standard Test Methods for Water Vapor Transmission of Materials. West Conshohocken, Penn. ASTM International.

Benavente, D., Martínez-Verdú, F., Bernabeu, A., Viqueira, V., Fort, R.,García del Cura, M.A., Illueca, C., Ordóñez, S. (2003) Influence of surface roughness on color changes in building stones, Color Research and Application, Vol. 28, 343–351.

Bunaciu, A. A., UdriŞTioiu, E. G., & Aboul-Enein, H. Y. (2015). X-ray diffraction: instrumentation and applications. *Critical reviews in analytical chemistry*, *45*(4), 289-299.

Carmona-Quiroga, P. M., Jacobs, R. M., Martínez-Ramírez, S., & Viles, H. A. (2017). Durability of anti-graffiti coatings on stone: natural vs accelerated weathering. *PLoS One*, *12*(2), e0172347.

Çelik, M. Y., & Ozkan, O. (2022). Geotechnical characterization of low-porous limestones (beige–cream marble, Turkey) and evaluation of durability by salt crystallization experiments. *Bulletin of Engineering Geology and the Environment*, *81*(1), 1-20.

Chubarov, V. M., & Finkel'shtein, A. L. (2010). X-ray fluorescence determination of the FeO/Fe2O 3 tot ratio in rocks. *Journal of Analytical Chemistry*, *65*(6), 620-627.

Cody, R. D., & Thompson, G. L. (1976). Quantitative X-ray powder diffraction analyses of clays using an orienting internal standard and pressed disks of bulk shale samples. *Clays and clay minerals*, *24*(5), 224-231.

Corcione, C. E., De Simone, N., Santarelli, M. L., & Frigione, M. (2017). Protective properties and durability characteristics of experimental and commercial organic coatings for the preservation of porous stone. *Progress in Organic Coatings*, *103*, 193-203.

Crina, B., Blaga, M., Luminita, V., & Mishra, R. (2013). COMFORT PROPERTIES OF FUNCTIONAL WEFT KNITTED SPACER FABRICS. Journal of Textile & Apparel/Tekstil ve Konfeksiyon, 23(3).

El-Taher, A. (2012). Elemental analysis of granite by instrumental neutron activation analysis (INAA) and X-ray fluorescence analysis (XRF). *Applied Radiation and Isotopes*, *70*(1), 350-354.

EN 1936, Natural stone test methods - Determination of real density and apparent density, and of total and open porosity (2006), Brussels: Europeans Committee for Standardization.

Facio, D. S., & Mosquera, M. J. (2013). Simple strategy for producing superhydrophobic nanocomposite coatings in situ on a building substrate. *ACS Applied Materials & Interfaces*, *5*(15), 7517-7526.

Ferri, L., Lottici, P. P., Lorenzi, A., Montenero, A., & Salvioli-Mariani, E. (2011). Study of silica nanoparticles–polysiloxane hydrophobic treatments for stone-based monument protection. *Journal of Cultural Heritage*, *12*(4), 356-363.

Fort, R., de Buergo, M. A., & Perez-Monserrat, E. M. (2013). Non-destructive testing for the assessment of granite decay in heritage structures compared to quarry stone. *International Journal of Rock Mechanics and Mining Sciences*, *61*, 296-305.

Franklin, J. A. (1979). Suggest methods for determining water content, porosity, density, absorption, and related properties and swelling and slake-durability index properties. *Int. J. Rock Mech. Min. Sci. & Geomech. Abstr.*, *16*, 141-156.

Frascá, M. H. B. O., & Yamamoto, J. K. (2006). Ageing tests for dimension stone-experimental studies of granitic rocks from Brazil. In *Proceedings 10th IAEG international congress. The Geological Society of London, IAEG2006 Paper*. No. 224.

Ghezal, I., Moussa, A., Ben Marzoug, I., El-Achari, A., Campagne, C., & Sakli, F. (2022). Investigating Waterproofness and Breathability of a Coated Double-Sided Knitted Fabric. Coatings, 12(10), 1572.

Gilchrist, A., & Nobbs, J. (2017). Colorimetry, theory. *Encyclopedia of spectroscopy and spectrometry*, 328-333.

Gonçalves, T. S., Spohr, A. M., de Souza, R. M., & Macedo de Menezes, L. (2008). Surface roughness of auto polymerized acrylic resin according to different manipulation and polishing methods: an in situ evaluation. *The Angle Orthodontist*, *78*(5), 931-934.

Jauncey, G. E. M. (1924). The scattering of x-rays and Bragg's law. *Proceedings of the national academy of sciences*, *10*(2), 57-60.

Janssens, K., Proost, K., & Falkenberg, G. (2004). Confocal microscopic X-ray fluorescence at the HASYLAB microfocus beamline: characteristics and possibilities. *Spectrochimica Acta Part B: Atomic Spectroscopy*, *59*(10-11), 1637-1645.

Karapanagiotis, I., & Manoudis, P. N. (2022). Superhydrophobic and superamphiphobic materials for the conservation of natural stone: An overview. *Construction and Building Materials*, *320*, 126175.

Lamour, G., Hamraoui, A., Buvailo, A., Xing, Y., Keuleyan, S., Prakash, V., ... & Borguet, E. (2010). Contact angle measurements using a simplified experimental setup. *Journal of chemical education*, *87*(12), 1403-1407.

Lettieri, M., & Masieri, M. (2016). Performances and coating morphology of a siloxane-based hydrophobic product applied in different concentrations on a highly porous stone. *Coatings*, *6*(4), 60.

Li, Y., Dong, W., Li, H., & Li, Z. (2015). Method of vacuum water absorption to determine the porosity of hardened concrete. *International Journal of Structural and Civil Engineering Research*, *4*, 282-286.

Lindawati, L., Mursal, M., & Afdhal, A. (2019). Determination of mineral contents in Meukek marble using XRD and SEM-EDS analysis. In *IOP Conference Series: Materials Science and Engineering*. Vol. 506, No. 1, p. 12-23.

Liritzis, I., & Zacharias, N. (2011). Portable XRF of archaeological artifacts: current research, potentials, and limitations. *X-ray fluorescence spectrometry (XRF) in geoarchaeology*, 109-142.

Lisci, C., Sitzia, F., Pires, V., & Mirão, J. (2022). Building stones durability by UVA radiation, moisture and spray accelerated weathering. *Journal of Building Pathology and Rehabilitation*, *7*(1), 1-14.

Loo-Morrey, M., (2007). A study of the slip characteristic of natural and manmade stone flooring materials. Health and Safety Laboratory (HSE), Buxton. pp.26.

Manoudis, P. N., & Karapanagiotis, I. (2014). Modification of the wettability of polymer surfaces using nanoparticles. *Progress in Organic Coatings*, *77*(2), 331-338.

Martín-Viveros, J. I., & Ollé, A. (2020). Using 3D digital microscopy and SEM-EDX for in-situ residue analysis: a multi-analytical contextual approach on experimental stone tools. *Quaternary International*, *569*, 228-262.

Mosquera, M. J., Rivas, T., Prieto, B., & Silva, B. (2000). Capillary rise in granitic rocks: interpretation of kinetics on the basis of pore structure. *Journal of Colloid and Interface Science*, *222*(1), 41-45.

Özkahraman, H. T., & Işık, E. C. (2003). Determination of thermal conductivity of building stones from P-wave velocity. In *18th International Mining Congress and Exhibition of Turkey-IMCET*: pp. 557-564.

Prieto, B., Sanmartín, P., Silva, B., & Martínez-Verdú, F. (2010). Measuring the color of granite rocks: a proposed procedure. *Color Research & Application*, *35*(5), 368-375.

Popov, Y. A., Pribnow, D. F., Sass, J. H., Williams, C. F., & Burkhardt, H. (1999). Characterization of rock thermal conductivity by high-resolution optical scanning. *Geothermics*, *28*(2), 253-276.

Rivas, T., Prieto, B., & Silva, B. (2001). Permeability to water vapour in granitic rocks. Application to the study of deleterious effects of conservation treatments. *Building and Environment*, *36*(2), 239-246.

Rivas, T., Matías, J. M., Taboada, J., & Ordóñez, C. (2011). Functional experiment design for the analysis of colour changes in granite using new L∗ a∗ b∗ functional colour coordinates. *Journal of Computational and Applied Mathematics*, *235*(16), 4701-4716.

Sampling, I. A. E. A. (1997). storage and sample preparation procedures for X-ray fluorescence analysis of the environmental materials. *International Atomic Energy Agency, Vienna*.

Sesana, E., Gagnon, A. S., Ciantelli, C., Cassar, J., & Hughes, J. J. (2021). Climate change impacts on cultural heritage: A literature review. *Wiley Interdisciplinary Reviews: Climate Change*, *12*(4), e710.

Tang, H., Cao, T., Liang, X., Wang, A., Salley, S. O., McAllister, J., & Ng, K. S. (2009). Influence of silicone surface roughness and hydrophobicity on adhesion and colonization of Staphylococcus epidermidis. Journal of Biomedical Materials Research Part A: An Official Journal of The Society for Biomaterials, The Japanese Society for Biomaterials, and The Australian Society for Biomaterials and the Korean Society for Biomaterials, 88(2), 454-463.

Togkalidou, T., Karoglou, M., Bakolas, A., Giakoumaki, A., & Moropoulou, A. (2013). Correlation of water vapor permeability with microstructure characteristics of building materials using robust chemometrics. *Transport in porous media*, *99*(2), 273-295.

UNI 10921:2001 Protocol, (2001). “Evaluation of the efficacy of water repellent treatments applied on stone materials of cultural and artistic interest”.

Vazquez-Calvo, C., Alvarez de Buergo, M., Fort, R., & Varas-Muriel, M. J. (2012). The measurement of surface roughness to determine the suitability of different methods for stone cleaning. *Journal of Geophysics and Engineering*, *9*(4): 108-117.

Vázquez, P., Luque, A., Alonso, F. J., & Grossi, C. M. (2013). Surface changes on crystalline stones due to salt crystallisation. *Environmental Earth Sciences*, *69*(4), 1237-1248.

Viles, H., Goudie, A., Grab, S., & Lalley, J. (2011). The use of the Schmidt Hammer and Equotip for rock hardness assessment in geomorphology and heritage science: a comparative analysis. *Earth surface processes and landforms*, *36*(3), 320-333.

Wang, Y., Zhou, Q., Li, K., Zhong, Q., & Bui, Q. B. (2015). Preparation of Ni–W–SiO2 nanocomposite coating and evaluation of its hardness and corrosion resistance. Ceramics International, 41(1), 79-84.

Wilhelm, K., Viles, H., & Burke, Ó. (2016). Low impact surface hardness testing (Equotip) on porous surfaces–advances in methodology with implications for rock weathering and stone deterioration research. *Earth Surface Processes and Landforms*, *41*(8), 1027-1038.

Young, T. (1805). III. An essay on the cohesion of fluids. *Philosophical transactions of the royal society of London*, (95), 65-87.

Zhao, J., Gao, X., Chen, S., Lin, H., Li, Z., & Lin, X. (2022). Hydrophobic or superhydrophobic modification of cement-based materials: A systematic review. Composites Part B: Engineering, 110104.

Zuena, M., Ruggiero, L., Della Ventura, G., Bemporad, E., Ricci, M. A., & Sodo, A. (2021). Effectiveness and compatibility of nanoparticle based multifunctional coatings on natural and man-made stones. Coatings, 11(4), 480.

CHAPTER 3

3 Results and Discussion

3.1 Physical Characterization of Stone Samples

In this section, all the obtained results related to the techniques already mentioned will be presented and discussed to give a comprehensive perspective of the studied stone materials. The results of hardness, roughness, thermal conductivity, colorimetry, open porosity, and water vapor permeability of the studied stone samples are presented and discussed in the following.

3.1.1 Hardness

Surface hardness test results for each stone sample are presented in Table 3.1. Each sample with its typology, Hardness Leeb value (HLD), and the corresponding standard deviation of examined points on the surface has been included.

Table 0.1. Hardness surface Test Results of Stone Samples (6 analyses per each sample were performed to obtain the mean value and standard deviation)

Ref N.	Typology	Mean (HLD)	Stdev (HLD)
L1	Limestone	535.5	8.6
L2	Limestone	478.8	20.9
L3	Limestone	696.1	6.6
L4	Limestone	570.6	36.8
L5	Limestone	665.3	15.1
M1	Marble	459.1	53.9
M2	Marble	533.6	47.2
M3	Marble	573.6	33.0
M4	Marble	554.8	30.0
G1	Granite	862.0	25.8

To better compare the surface hardness of stone samples among each other, the data has been plotted on a bar chart, presented in Figure 3.1.

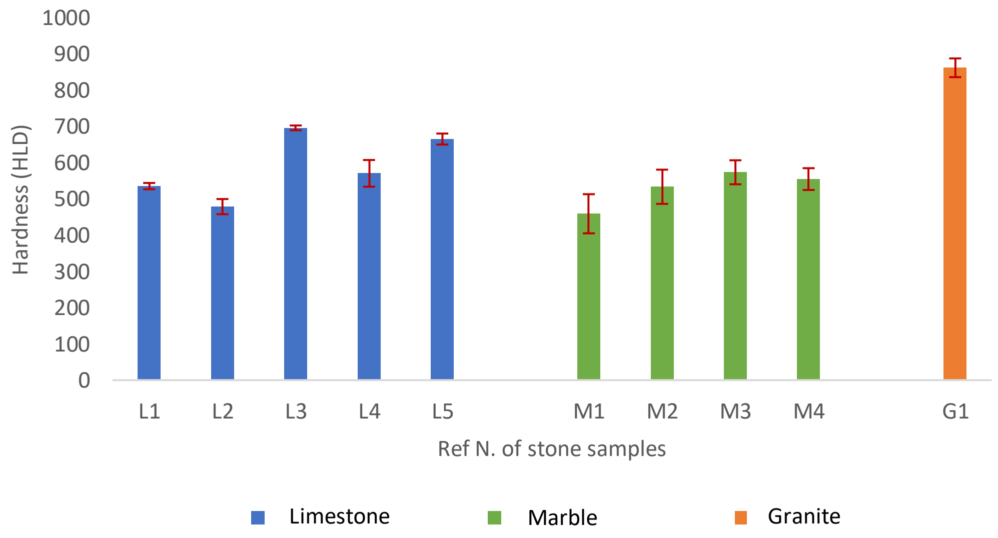

Figure 3.1. Graphic Representation of Surface Hardness of Stone Samples

The results of the surface hardness test show that the surface hardness of all the studied samples ranges from 459.17 ± 53.98 to 862.00 ± 25.89 HLD (Table 3.1). The highest value of surface hardness among all the studied samples belongs to G1. Among marble and limestone samples, M1 and L2 have the lowest rate for surface hardness, respectively (Figure 3.1).

According to Mohs´s hardness scale (Tabor, D., 1954) which determines minerals' resistance to abrasion or scratching, minerals are ranked with the numerical value related to their hardness from 0 to 10 (qualitative ordinal scale). Hence, different materials can have a numerical range of values to compare their hardness (Zeng, X., 2021). When it comes to stone materials, the hardness of composed minerals can determine the hardness of stone (Wahab, G., 2019). Therefore, granite has a rather high degree of hardness, around 7, because of the presence of quartz and other silicate-based minerals. Since marble and limestone are mostly made of calcite, they rate around two on Moh's scale of hardness and because calcite is a major component, the hardness range of marble and limestone is less than granite (Table 3.1).

It is important to take into account that Moh´s scale is just a qualitative ordinal scaling that helps to compare the hardness of different minerals and it did not provide the surface hardness of specific lithotypes. For this reason, the accurate amount of surface hardness is evaluated in this study based on the Hardness Leeb (HLD) scale (Wedekind, W., 2016). However, HLD (Hardness Leeb Degree) is the unit provided by the used equipment for measuring surface hardness, converting this unit to another unit of hardness such as N/mm^2 has not been possible because of the limitation related to the equipment.

3.1.2 Roughness

Surface roughness test results for each stone sample are presented in Table 3.2. The mean value and standard deviation of the *Ra*[1] – Roughness average (µm) parameter of each stone have been included.

Table 0.2. Surface Roughness Test Results of Stone Samples (6 analyses per each sample were performed to obtain the mean value and standard deviation)

Ref N.	**Typology**	***Ra (µm)***	
		Mean	Stdev
L1	Limestone	5.88	1.60
L2	Limestone	3.48	1.18
L3	Limestone	2.50	0.76
L4	Limestone	3.39	0.95
L5	Limestone	2.72	0.32
M1	Marble	3.25	0.58
M2	Marble	2.30	0.24
M3	Marble	4.30	0.13
M4	Marble	4.92	0.86
G1	Granite	4.02	1.10

---

[1] *Ra is the absolute value of the profile height deviations from the mean line, recorded within the evaluation length*

To better compare the roughness of the surfaces of stone samples among each other, the data has been plotted on a bar chart presented in Figure 3.2.

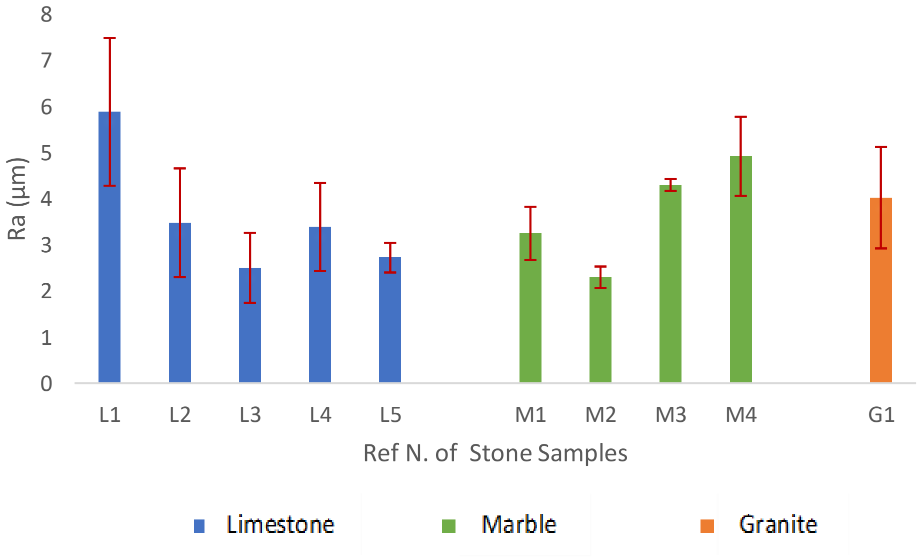

Figure 0.2. Graphic Representation of Surface Roughness of Stone Samples

Based on the results of the surface roughness test, the range of surface roughness of studied samples is from 2.30 ± 0.24 to 5.88 ± 1.60 µm. This range for limestones is from 2.50 ± 0.76 to 5.88 ± 1.60 µm and for marbles is between 2.30 ± 0.24 and 4.92 ± 0.86 µm (Table 3.2). Therefore, the roughest surface among limestones belongs to sample L1, and among marbles belongs to sample M4 (Figure 3.2).

According to Wenzel's theory (Wenzel, R., 1936) enhancement in surface roughness of a hydrophilic surface will increment its capacity to retain water. Therefore, the hydrophobicity of the surfaces directly relates to their roughness. Therefore, the wettability of untreated stone samples of this study does not match perfectly with the results of surface roughness, as will be discussed further.

3.1.3 Thermal Conductivity

Thermal conductivity test results for each stone sample are presented in table 3.3. The mean value and standard deviation of the *λ* $(wm^{-1}k^{-1})$ parameter have been included.

Table 0.3. Thermal Conductivity results of Stone Samples (3 analyses per each sample were performed to obtain the mean value and standard deviation)

Ref N.	Typology	λ $(wm^{-1}k^{-1})$	
		Mean	Stdev
L1	Limestone	2.09	0.00
L2	Limestone	1.95	0.00
L3	Limestone	2.54	0.01
L4	Limestone	2.36	0.01
L5	Limestone	2.35	0.01
M1	Marble	2.46	0.00
M2	Marble	2.33	0.00
M3	Marble	2.53	0.00
M4	Marble	2.57	0.00
G1	Granite	2.46	0.01

To better compare the thermal conductivity of stone samples among each other, the data has been plotted on a bar chart presented in Figure 3.3.

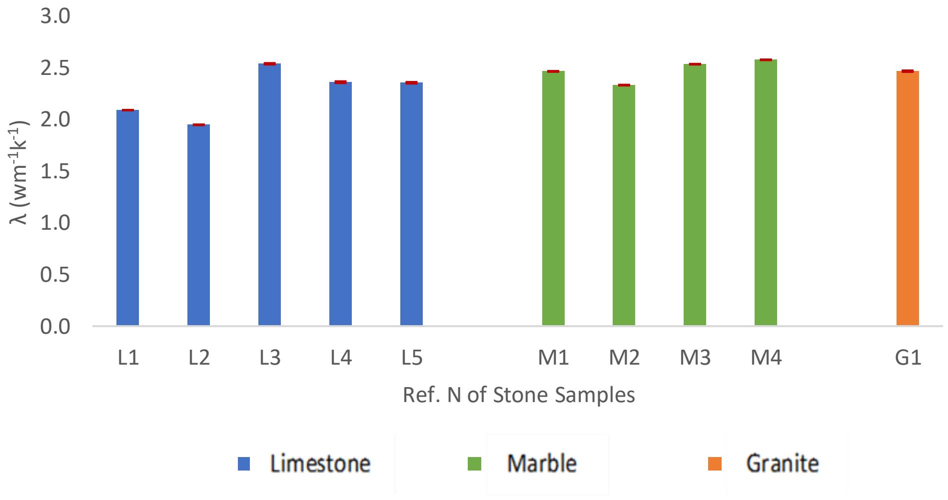

Figure 0.3 Graphic Representation of Thermal Conductivity of Stone Samples

Table 3.3 displays the thermal characteristics of studied samples of dry stones at ambient pressure (1 atm) and temperature (25 ºC). Samples of limestone are found to have thermal conductivities between 1.95 ± 0.00 and 2.54 ± 0.01 $Wm^{-1}K^{-1}$. The thermal conductivity of marble samples is observed in the range of 2.33 ± 0.00 to 2.57 ± 0.00 $Wm^{-1}K^{-1}$. The thermal conductivity of the granite sample is 2.46 ± 0.01 $Wm^{-1}K^{-1}$ (Table 3.3).

Amaral, P and co-authors, categorized rocks for building purposes including limestone, marble, and granite, as quality ranking based on their thermal conductivity. This qualification determines the medium valuation for thermal conductivity ranges from 0.3 to 4 $Wm^{-1}K^{-1}$ (Amaral, P., et al., 2013). Therefore, based on this classification, all the studied samples in this research consider as medium thermal conductivity, and it can be considered that there are no significant differences.

3.1.4 Chromatic Characterization

Colorimetry measurement results for each stone sample are presented in table 3.4. The mean value and standard deviation of three coordinates of the CIELAB space, *L*, a**, and *b**, have been included.

*Table 0.4. a*b*L* parameters of Colorimetry Measurements for Stone Samples (3 analyses per each sample were performed to obtain the mean value and standard deviation)*

Ref N.	**Typology**	***L****		***a****		***b****	
		Mean	Stdev	Mean	Stdev	Mean	Stdev
L1	Limestone	89.98	0.26	1.13	0.02	6.47	0.12
L2	Limestone	92.74	0.20	1.08	0.01	5.18	0.06
L3	Limestone	90.53	0.46	1.05	0.06	5.19	0.13
L4	Limestone	92.25	0.04	1.23	0.00	6.37	0.08
L5	Limestone	89.49	0.32	2.07	0.08	8.69	0.19
M1	Marble	89.29	0.49	-0.39	0.03	-1.45	0.08
M2	Marble	96.45	0.31	0.74	0.24	3.35	0.67
M3	Marble	75.21	0.19	-0.93	0.02	-1.61	0.15
M4	Marble	97.84	0.17	0.52	0.06	1.93	0.25
G1	Granite	81.14	0.06	0.59	0.01	4.02	0.04

The colour space mathematical model can perfectly explain the values of CIE L*a*b* parameters (Delgado-González, M., 2018). In this graph, the horizontal axis (a*) relates to the colour hue from green to red. The -100 value represents pure green while +100 shows pure red. The vertical axis (b*) relates to the colour hue from blue to yellow. The -100 represents pure blue while +100 shows pure yellow. Therefore, each coordinate in the graph determines the specific colour. Moreover, L* column shows the brightness of the related colour. 0 value represents pure black and +100 shows pure white (Figure 3.4).

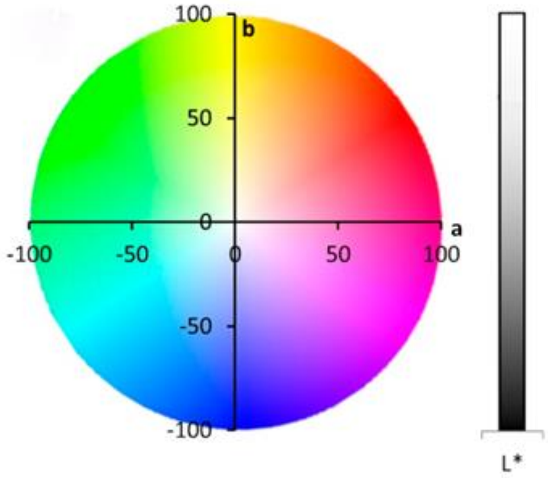

Figure 0.4 *colour space mathematical modelling (Delgado-González, M., 2018).*

The coordinate positions of a*b* parameters of each stone sample have been presented in figure 3.5 which is compared and adapted to figure 3.4. It provides a range of colour hues and coordinates of the stone samples. a* parameter determines a range from -0.93 ± 0.02 to 2.07 ± 0.08 while the b* parameter shows a range from -1.61 ± 0.15 to 8.69 ± 0.19. (Table 3.4).

The colour hue for all the samples in the horizontal and vertical axis is extremely close to 0. It means the colour hue of samples is extremely close to white however the tint of other colours is detectable visually. The most greenish as well as blueish hues belong to M3, and the most reddish and yellowish hues belong to L5 (Figure 3.5).

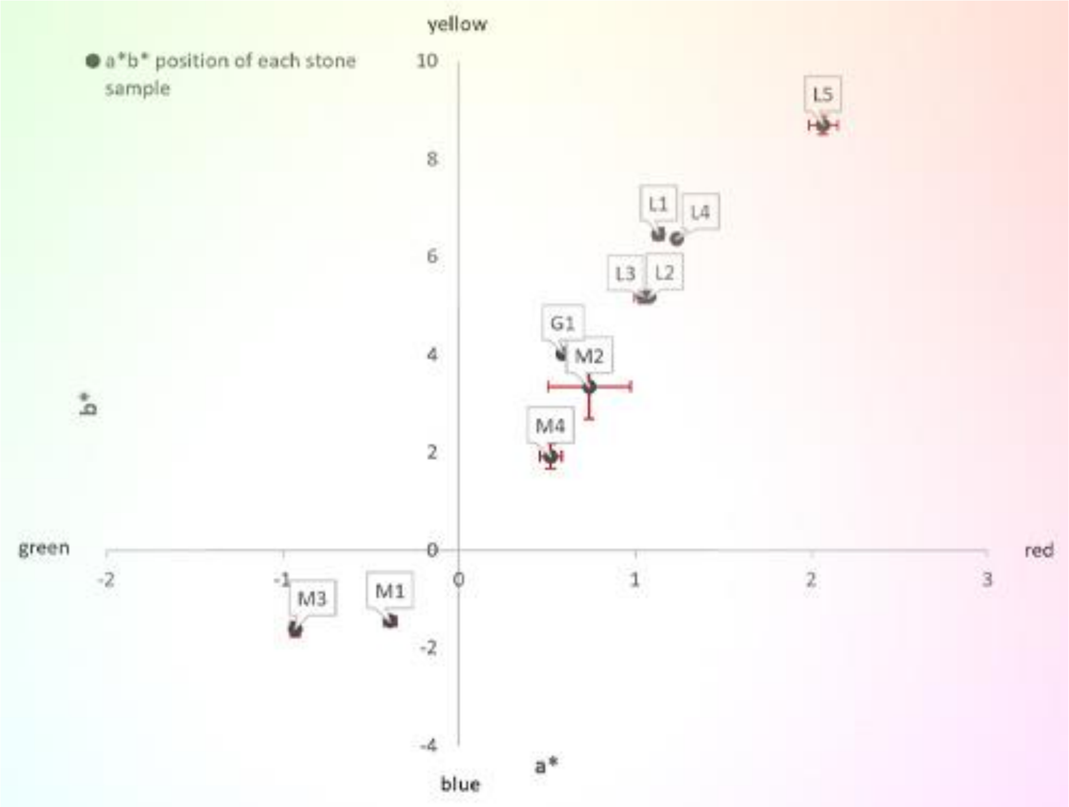

*Figure 0.5. a*b* Position of each stone sample in the colour chart*

L* parameter of each stone sample refers to their brightness is represented in figure 3.6. It shows a range of brightness from 75.21 ± 0.17 to 97.84 ± 0.17 (table 3.4). Therefore, the darkest one belongs to M3 and the brightest one belongs to M4 (figure 3.6).

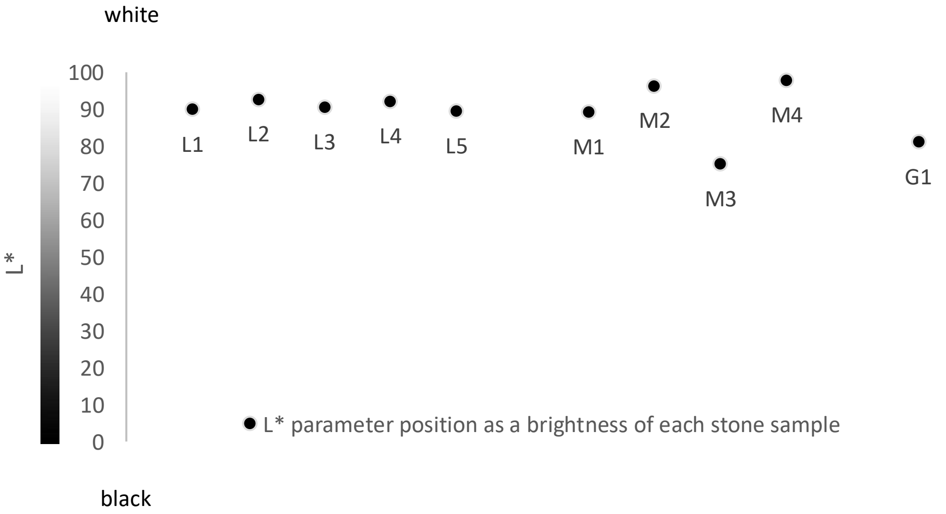

Figure 0.6. the brightness of each stone sample

Finding the exact coordinates of the color of each sample has been done based on the homogenous powder pellets. It has been done for the purpose of recognizing the exact coordinate of the sample´s colours in colour hue chart.

One of the most challenges related to the chromatic characterization of studied stone samples is their heterogeneity. The heterogeneity of the stone samples does not allow a bulk colour characterization. For this matter, homogenous powder pellets have been prepared and analysis for determining the colour of stone samples has been done on these pellets instead of the samples´ surfaces.

On the other hand, studied coatings have been applied on the heterogenous surface of stone samples. The reason is to understand the compatibility and durability of applied coatings on the surface of the stone samples. Therefore, further analysis for determining colour changes has been done on the same point of each surface in every state, before and after treatment as well as after ageing process. Since hydrophobic coatings are applied on the heterogeneous surfaces of each sample, further analysis for colour change has been done on the center of each surface to minimize the errors corresponding to the colour heterogeneity of each stone.

3.1.5 Open porosity

The open porosity of each stone sample is measured and is presented in table 3.6. The mean and standard deviation values are calculated and have been included.

Table 0.5. open porosity [%] values of stone samples (6 analyses per each sample were performed to obtain the mean value and standard deviation)

Ref N.	**Typology**	**Open Porosity (%)**	
		Mean	Stdev
L1	Limestone	13.30	0.20
L2	Limestone	11.33	0.30

L3	Limestone	8.50	0.10
L4	Limestone	0.40	0.01
L5	Limestone	1.21	0.05
M1	Marble	0.20	0.01
M2	Marble	0.50	0.01
M3	Marble	0.21	0.01
M4	Marble	0.34	0.02
G1	Granite	0.66	0.05

To better compare the open porosity of stone samples among each other, the graphic representation has been presented in Figure 3.7.

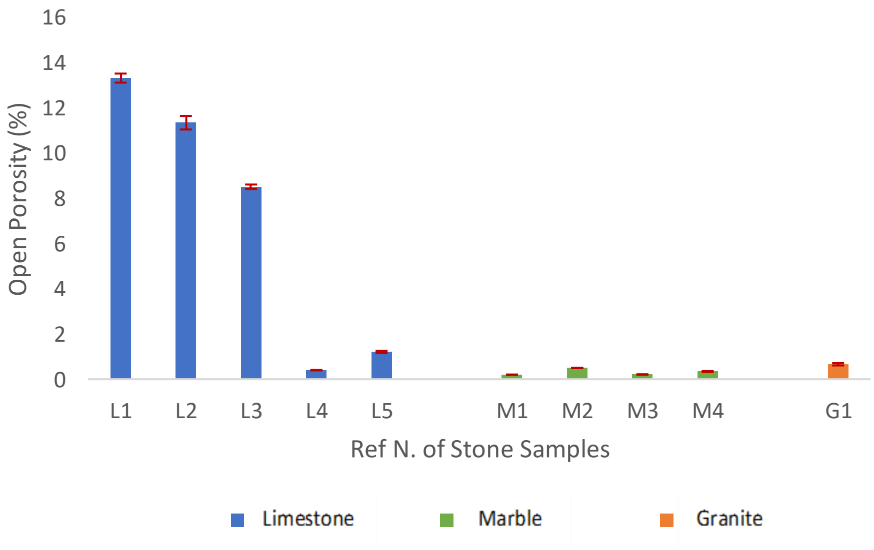

Figure 0.7. *Graphic Representation of open porosity (%) of Stone Samples*

According to table 3.5, the range of open porosity of studied samples is from 0.21 ± 0.01 to 13.30 ± 0.20 %. This range for limestones is from 0.40 ± 0.01 to 13.30 ± 0.20 % and for marbles is between 0.20 ± 0.01 and 0.50 ± 0.01 %. Therefore, the variety of open porosity is highly noticeable among limestones rather than marbles and demonstrates that this study has covered a wide range of different stones regarding this characteristic. The open porosity of granite (G1) is approximately close to marbles and is defined as 0.66 ± 0.05 % (Table 3.5).

Since limestones are generally more porous than marbles and granites, due to the different processes involved in rock s' formation, (McGee, E., 1990) the significant increase in the percentage of open porosity in limestone samples specifically in samples L1, L2, and L3 can be explained (Figure 3.7).

3.1.6 Stone Breathability

Water vapor permeability ($g.m^{-1}.s^{-1}.Pa^{-1}$) test results for each stone sample are presented in table 3.6.

Table 0.6 Water Vapor Permeability Value ($g.m^{-1}.s^{-1}.Pa^{-1}$) for Stone Samples

Ref N.	Typology	W_{VP} ($g.m^{-1}.s^{-1}.Pa^{-1}$)
L1	Limestone	6.03E-12
L2	Limestone	6.31E-12
L3	Limestone	2.95E-12
L4	Limestone	8.93E-12
L5	Limestone	7.70E-12
M1	Marble	2.18E-12
M2	Marble	4.72E-12
M3	Marble	5.11E-12
M4	Marble	3.75E-12
G1	Granite	5.53E-12

One of the limitations of this technique was the extreme amount of time needed to measure the weight loss which happened during the evaporation of water through the surfaces of stones. Therefore, due to the time consumption of this technique and the limited time to perform the expriments, only one test has been performed to have insights into the breathability of the studied stone samples.

Based on the results of the water vapor permeability measurement, the range of W_{VP} (g.m^{-1}.s^{-1}.Pa^{-1}) of studied samples is from 2.18E-12 to 8.93E-12. This range for limestones is from 2.95E-12 to 8.93E-12 and for marbles is between 2.18E-12 and 5.11E-12 g.m^{-1}.s^{-1}.Pa^{-1}. Therefore, the variety of water permeability is highly noticeable among limestones rather than marbles. The water vapor permeability with granite (G1) is defined as 5.53E-12 (Table 3.6).

To better compare the water vapor permeability of stone samples among each other, the graphic representation has been presented in Figure 3.8.

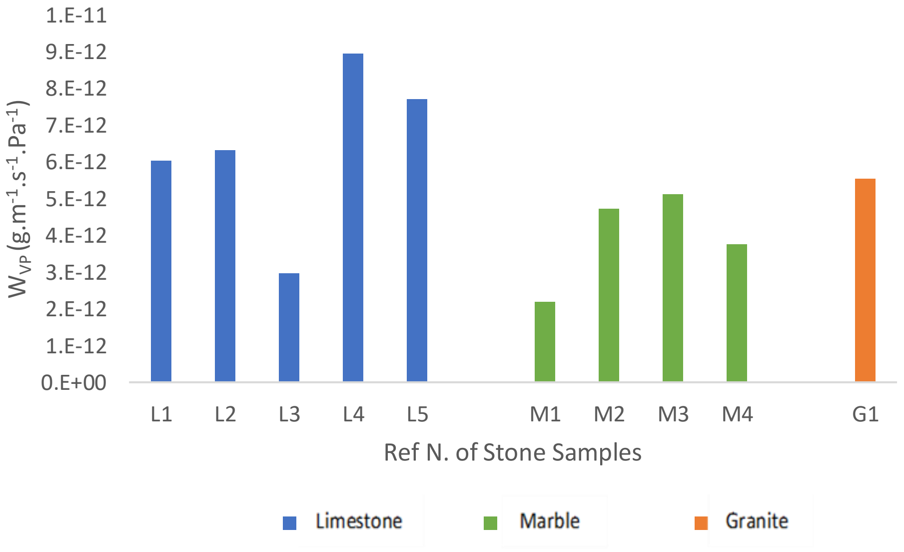

Figure 0.8 *Graphic representation of water vapor permeability value (g.m^{-1}.s^{-1}.Pa^{-1})of Stone Samples*

Differences in permeability were expected in accordance with the typical distinction for porous networks among limestones, marbles, and granites (Zhang, L. 2013). Therefore, the limestones have a higher amount of water vapor permeability rather than other lithotypes, specifically in samples L1, L2, L4, and L5 (Figure 3.8). Sample L3 shows a different behaviour relates to water vapor permeability. The result of open porosity for this sample is approximately high among limestones however the water vapor permeability is the lowest amount (Figure 3.8). As mentioned earlier due to the limitation of having a group of samples to have more solid and representative results, similar tests using more mock-ups have to be performed in the near future.

3.2 Chemical characterization of Stone Samples

Table 3.7 displays the X-ray fluorescence spectrometry results which determined the major elements that are present on the studied stones.

Table 0.7 Elemental XRF Analysis Results (a.u) (3 analyses per each sample were performed)

Ref N.	Typology	Elements (a.u.)											
		Ba	Ca	Fe	K	Mn	P	S	Si	Sr	Ti	Zr	Zn
L1	Limestone	0.01	95.14	0.44	0.34	0.01	0.04	0.05	0.07	0.50	0.03	0.05	-
L2	Limestone	-	95.87	0.32	0.34	0.02	0.04	0.06	0.08	0.39	0.03	0.05	-
L3	Limestone	-	93.01	0.50	0.38	0.04	0.05	0.06	0.11	0.30	0.06	0.05	-
L4	Limestone	-	95.06	0.38	0.34	0.02	0.04	0.06	0.08	0.24	0.03	0.03	-
L5	Limestone	-	58.19	0.83	0.20	0.02	0.02	0.03	0.04	0.31	0.03	0.04	-
M1	Marble	0.01	90.87	0.69	0.37	0.55	0.04	0.04	0.10	0.37	0.03	0.05	-
M2	Marble	-	100.60	0.65	0.41	0.07	0.06	0.06	0.13	0.27	0.06	0.04	-
M3	Marble	-	91.50	0.76	0.38	0.04	0.05	0.05	0.10	0.47	0.04	0.05	-
M4	Marble	0.01	95.00	1.07	0.37	0.06	0.05	0.06	0.10	0.44	0.03	0.05	-
G1	Granite	0.01	1.99	18.13	2.29	0.29	0.00	0.01	1.55	0.71	0.56	0.65	0.09

Generally, limestone and marbles are composed of calcite and/or dolomite (Pecchioni, E., 2019; Shtel'makh, S., 2020). Therefore, among all the elements which have been detected for limestones and marbles, calcium has the highest amount. However, sample L5 is considered as the least amount of calcium.

Considering what is stated by El-Taher, quartz, potassium feldspar, sodium-calcium feldspar, and other common minerals like micas make up most of the coarse grains found in granite (El-Taher, A., 2012). Therefore, XRF granite's analysis reveals that sample G1 is chemically composed of major elements like iron, potassium, calcium, silicon, and traces of other elements including strontium, titanium, and zirconium.

The higher amount of Fe in limestones and marbles relates to samples L5 and M4 respectively. The colorimetry measurements (Figure 3.5) demonstrate that these stones exhibit some reddish hue which can be related to the presence of a high amount of iron-based minerals in these samples.

It is important to consider that the equipment used to characterized the major elements involves some challenges. Due to its limitations, lighter elements, like Na, Al, and Mg, cannot be detected and are not presented in this section. Additionally, some elements including Rh, Pd, Cu, and Ni which have been detected in all spectra are related to the components of the equipment and therefore have not been considered in the presented results.

3.3 Mineralogical Characterization of Stone Samples

Qualitative diffractograms of the limestones, marbles, and granite samples are shown in figures 3.9, 3.10, and 3.11 respectively, which demonstrate the crystalline phases that are present in each stone. A database containing X-ray diffraction patterns of minerals was used to match each diffraction pattern, in reference to d (distance between atomic plans or interatomic distance), obtained for each stone. The peak intensity value is displayed as counts. The mineralogical phases identified in each sample are mentioned in table 3.8. More detailed information about the obtained diffractograms is presented in appendix 1.

According to Houston, E. results from X-ray diffraction on the studied stones allow for the qualitative identification of several minerals. Relative intensity (counts) values can be used as indicators of the rock-forming minerals, but they cannot provide relative proportions of the major minerals present (Houston, E., 1997).

This technique is able to determine that the limestones L1, L2, L3, and L4 are composed of the same minerals, like calcite ($CaCO_3$) and quartz (SiO_2) (Figure 3.9). On the other hand, Sample L5 is composed of dolomite ($CaMg(CO_3)_2$), quartz (SiO_2), and albite ($NaAlSi_3O_8$), and calcite ($CaCO_3$). In sample L5 despite the other studied limestones, calcite is not the main composed mineral. On the other hand, as mentioned before based on the XRF results, L5 has the lowest amount of calcium element (Table 3.7). Since the main mineral for sample L5 is dolomite, it is possible to justify the huge decreased amount of Ca element in this sample based on its mineralogy which is different from the rest of the limestones.

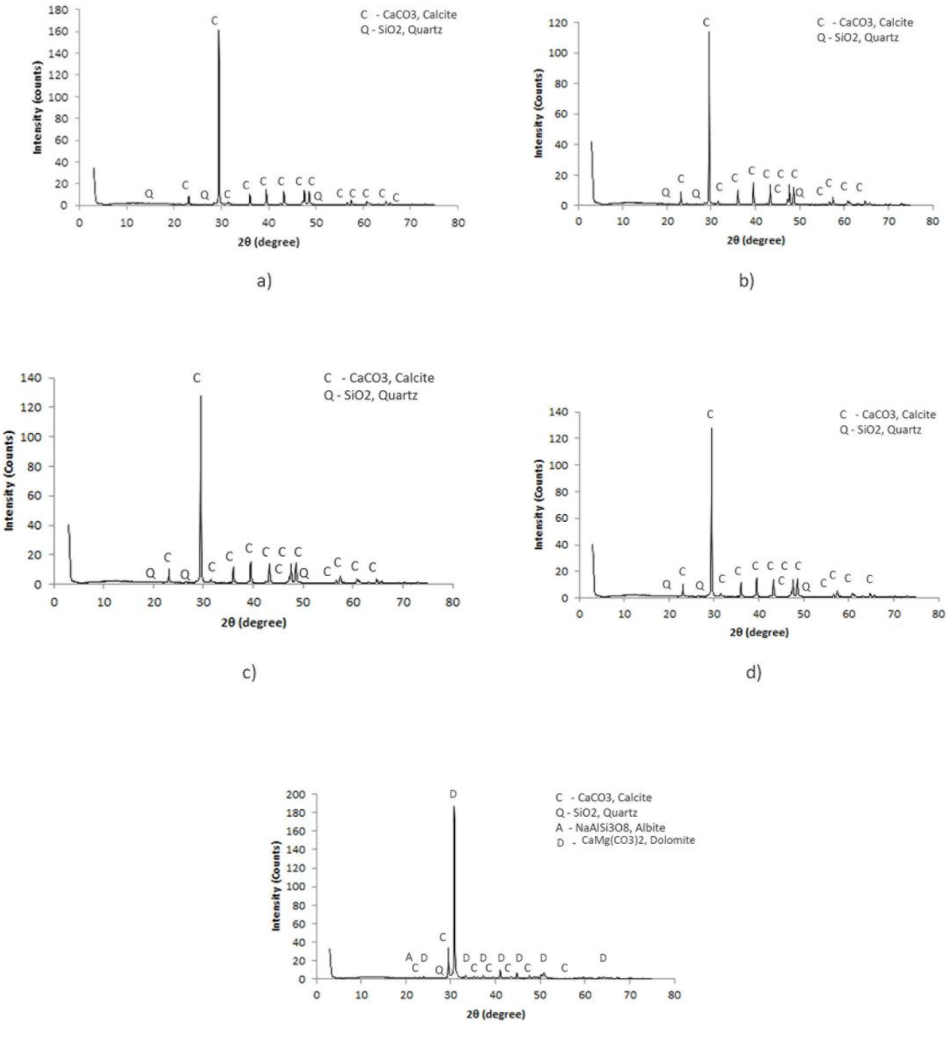

a)

b)

c)

d)

e)

Figure 0.9 Limestones X-ray diffraction patterns. Diffractograms were obtained for a) L1, b) L2, c) L3, d) L4 and e) L5.

According to the diffractograms obtained for the marble samples, it was possible to determine that the main composed mineral for the samples M1, and M2, is calcite, however, it is calcite magnesian in samples M3, and M4. The common mineral is quartz among all the marble samples, however other minerals were identified, including biotite and amphibole in sample M1, phillipsite in sample M2, albite in sample M4, and muscovite in samples M2, M3, and M4 (Figure 3.10).

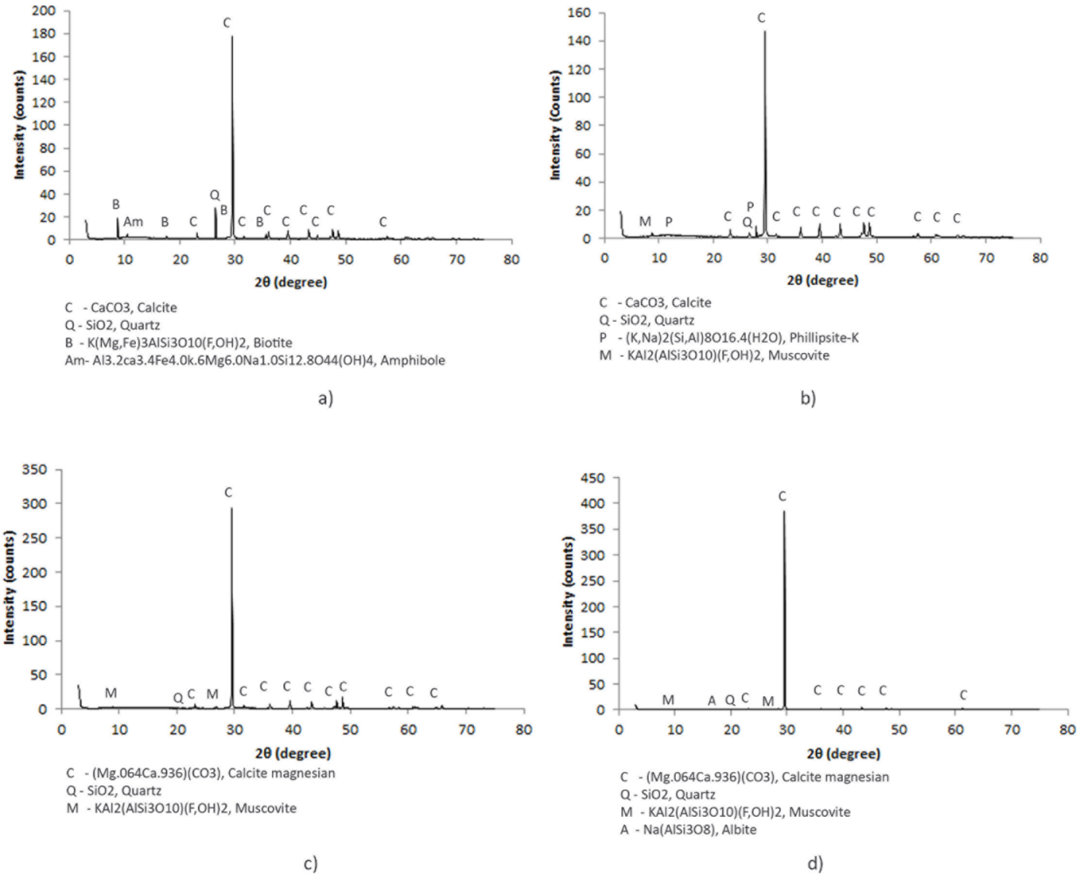

Figure 0.10 *Marbles X-ray diffraction patterns. Diffractograms were obtained for a) M1, b) M2, c) M3, and d) M4.*

G1 diffractograms (Figure 3.11) can be compared with the element contents obtained from XRF analysis (Table 3.7) and it is possible to confirm the high amount of Si element rather than other samples is coincident with the minerals identified. Figure 3.11 shows that identified minerals in sample G1 are quartz, (SiO_2), albite ($Na(AlSi_3O_8)$), Orthoclase ($KAlSi_3O_8$), and Clinochlore ($(Mg.Fe)_6(Si,Al)_4O_{10}(OH)_8$). Therefore, based on the presented minerals, the noticeable amount of Si element (Table 3.7) is complemented with mineralogical identification for this sample.

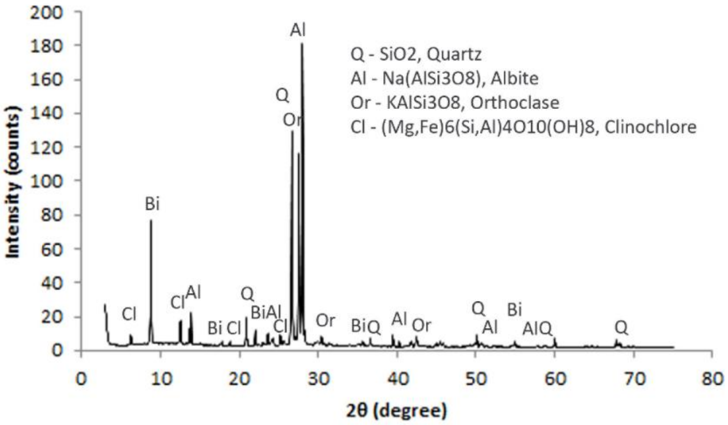

Figure 0.11 *Granite X-ray diffraction patterns*

Table 0.8 The presence of minerals in the studied stone samples; + presence of minerals, - not presence of minerals

Ref N.	**Typology**	**Minerals**										
		Calcite	**Calcite Magnesian**	**Quartz**	**Dolomite**	**Albite**	**Biotite**	**Amphibole**	**Phillipsite**	**Muscovite**	**Clinochlore**	**Orthoclase**
L1	Limestone	+	-	+	-	-	-	-	-	-	-	-
L2	Limestone	+	-	+	-	-	-	-	-	-	-	-
L3	Limestone	+	-	+	-	-	-	-	-	-	-	-
L4	Limestone	+	-	+	-	-	-	-	-	-	-	-
L5	Limestone	+	-	+	+	+	-	-	-	-	-	-
M1	Marble	+	-	+	-	-	+	+	-	-	-	-
M2	Marble	+	-	+	-	-	-	-	+	+	-	-
M3	Marble	-	+	+	-	-	-	-	-	+	-	-
M4	Marble	-	+	+	-	+	-	-	-	+	-	-
G1	Granite	-	-	+	-	+	+	-	-	-	+	+

3.4 Compatibility, Durability, and Effectiveness of The Hydrophobic Coatings

In this section, the results of three main techniques which have been used for purpose of measuring the compatibility, effectiveness, and durability of applied coatings on stone samples are discussed.

3.4.1 Chromatic Change Evaluation

Colour changes are typically the first modifications that are evident to the naked eye before any other investigation. These chromatic alterations can be related to the chemical reaction of stones to the applied hydrophobic coatings, or the weathering resulting from the accelerated ageing process. Therefore, the changes are determined by two different categories, compatibility of the hydrophobic coatings on the stones, and durability of them after ageing process.

3.4.1.1 Compatibility of Hydrophobic Coatings

However, in terms of colour compatibility in the conservation field, must be considered that the colour variations would not be visible to the naked eye after applying any protective treatment (Andreotti, S., et al., 2018). On the other hand, according to the CIE L*a*b system, when ΔE (total difference in colour) is = 1 the colour changes cannot be noticeable by the naked eye, and when ΔE ≥ 5 a significant colour difference is visible (Persia, F., 2010). Therefore, the colour difference of each sample after applying the coating and after using the accelerated ageing chamber has been calculated and the limit acceptance of colour changes would be less than 5. It means each sample with ΔE ≥ 5 is incompatible with the applied treatment. The results of ΔE in each state for each sample are presented in table 3.9.

Table 3.9. ΔE for CN1, CN2, and CN3 applied on studied stone samples before and after ageing process

Ref N.	Typology	ΔE CN1		ΔE CN2		ΔE CN3	
		before ageing	**after ageing**	**before ageing**	**after ageing**	**before ageing**	**after ageing**
L1	Limestone	4.24	3.73	6.63	1.70	5.01	2.14
L2	Limestone	9.82	1.85	5.55	5.45	4.12	1.09
L3	Limestone	2.99	4.31	1.26	2.05	2.85	3.86
L4	Limestone	3.81	2.89	5.54	4.97	2.18	1.07
L5	Limestone	3.55	0.68	7.75	3.63	2.56	1.50
M1	Marble	1.77	2.68	3.05	2.00	1.05	0.48
M2	Marble	1.61	2.98	0.95	0.73	1.11	2.59
M3	Marble	4.46	3.64	2.66	1.25	1.30	3.66
M4	Marble	9.52	3.70	2.85	0.82	2.37	2.74
G1	Granite	7.03	1.34	2.58	7.66	1.11	6.90

For a better comparison, the graphic representation in Figures 3.12 and 3.13 shows all the colour changes on the studied stone samples. The red area shows the colour changes which are visible to the naked eye and therefore the applied coating is not compatible with the related stone sample.

According to table 3.9 and figure 3.12, the difference in colour change in CN1 before and after treatment, is less than 5 except in samples L2, M4, and G1. The colour change for CN2 which is applied on marbles and granite is within the acceptable limit for ΔE. On the other hand, this coating for all the limestones except sample L3 makes an extreme amount of colour changes. Among the three studied coatings, ΔE for CN3 is in the acceptable zone for all the stone samples. However, the colour changes in L1 and L2 are close to the limitation value.

The chromatic changes of stone samples after treatment for each coating could directly relate to their chemical composition. CN1 is silane/siloxane micro-nano based. CN3 is based on nano-silane, siloxane with modified fluorinated compounds. CN2 is based on modified silicon dioxide. Therefore, different lithotypes could react differently to the colour changes after treatments based on their mineralogical and chemical composition as well as the chemical composition of hydrophobic coatings.

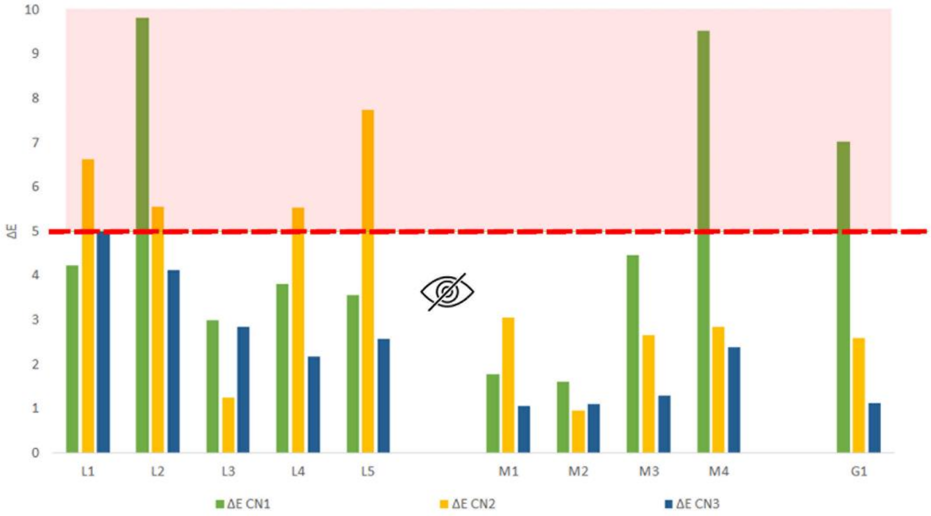

Figure 2.012 *Graphic representation of ΔE for CN1, CN2, and CN3 applied on studied stone samples before and after applying treatment*

Figure 3.13 shows the colour change of stone samples after applying different coatings before and after ageing process. In CN1 the colour change after ageing process is less than 5 in all the samples. Hence, CN1 shows acceptable behaviour in simulation weathering conditions. On the other hand, the colour of samples, L2 and G1 coated with CN2 get changed beyond the limitation after ageing process. Therefore, with this hydrophobic coating, the colour of the marble samples does not change to be visible to the naked eye. Additionally, All the samples coated with CN3 except granite have acceptable colour changes after ageing process.

Comparing figure 3.12 and 3.13 determines that however, samples coated with CN3 are the most compatible in terms of colour changes before and after ageing process, however, compatibility of this coating for sample G1 is challenging after ageing process. Further analysis focused on granite stone samples in terms of colour changes is demanded to help for a better understanding of these challenges.

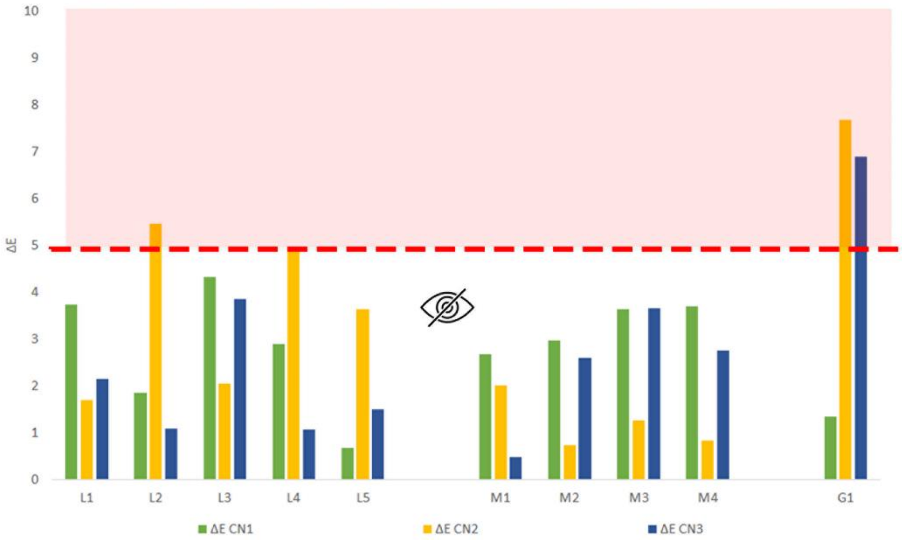

Figure 3.113. *Graphic representation of ΔE for CN1, CN2, and CN3 applied on studied stone samples before and after ageing process*

3.4.1.2 Durability of Hydrophobic Coatings

It is a crucial matter that the colour of stone materials would not change after passing time and facing weathering conditions especially when it comes to stone heritage. It means that the hydrophobic coatings should not only be compatible with the stone samples but also should be durable after facing weathering conditions. For this purpose, the colour difference from aged mock-ups to coated ones has been calculated for each sample. Therefore, for measuring the durability of coatings ΔE after ageing should not be more than 5.

According to Table 3.9. all the values for ΔE after ageing for CN1 are less than 5. It means the colour change after changing compared to after applying coatings for all the samples is not visible to the naked eye. This matter confirms the durability of this coating. CN3 behaves the same except for G1. Colour change for aged mock-ups L2 and G1 coated with CN2 is higher than 5 as well.

For purpose of observing colour changing, every state of each mock-up (11 mock-ups related to each specific stone sample) has been documented through digital pictures (Table 3.10). For better comparison to see the colour changes after applying hydrophobic treatments and the accelerated ageing chamber, all the photos related to each mock-up are gathered in a table. Table 3.10 includes all the pictures that have been taken for sample L2 as an example. More details for other samples are presented in appendix 2.

Since the surfaces of the samples are not homogenous, the colorimeter detector has been placed in the centre of each mock-up. It is due to have a specific area as a standard part among all the mock-ups. Therefore, the colour changes in other parts of the surfaces are not examined. According to table 3.10, yellow stains accrued in sample L2 coated with CN3 coating after ageing process. However, the other mock-up without any treatment behaves the same after ageing process. Hence, the possibility of marking stains in this sample could be not completely related to the applied coating. There is a possibility that L2 coated with CN3 marked a stain after ageing process due to its weakness in the weathering situation generally.

Table 3.110. pictures of every state of sample L2

L2	without any treatments	with applied coatings	after accelerated ageing
initial specimens			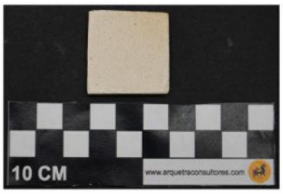
CN1	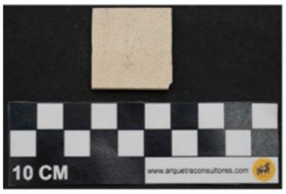	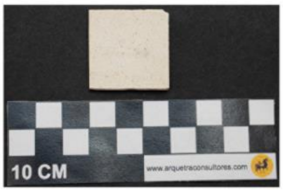	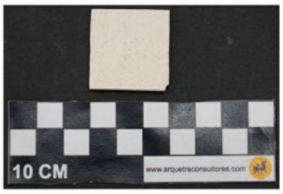
CN2		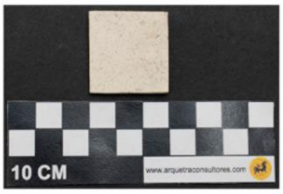	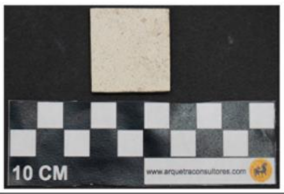
CN3		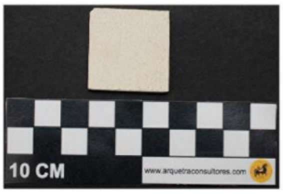	

As a validation of the presented pictures, digital microscopy was used to corroborate the visible colour hue by taking pictures of the samples' surfaces with 80x magnification. It has been tried to take pictures from the stained area of each surface. All the pictures taken by digital microscope for sample L2 in different states are presented in table 3.11. More details about other samples are presented in appendix 3.

Table 3.10 compared to table 3.11, clearly shows the yellow hue on sample L2 coated with CN1 after the accelerated ageing process.

Table 3.111. pictures are taken by digital microscope of every state of sample L2 during the compatibility assessment

L2	without any treatments	with applied coatings	after accelerated ageing
initial specimens			
CN1	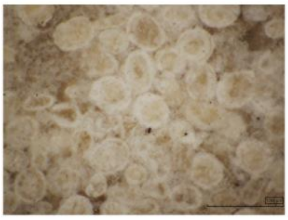		
CN2	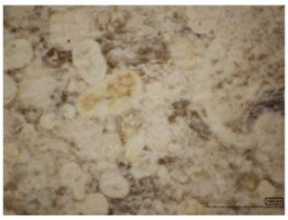		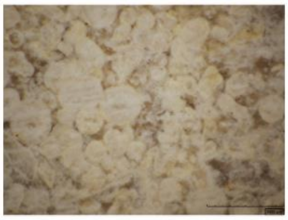
CN3	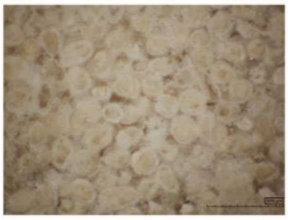		

3.4.2 Hydrophobic Properties

Static contact angles measured on hydrophobized stone samples following studied coatings are shown in table 3.12. It represents the main value and standard deviation of the contact angle of 12 water drops on each surface of the treated and untreated stone samples in different states including before and after ageing process. Since the surfaces of the stone samples are not homogenous and the application of coatings which has been done by hand-spray has some imperfection due to being heterogenous of aerosol, the mean value of the contact angle of 12 drops of water has been considered. To have the comprehensive values, these drops have been spread on four edges of each sample as shown in Figure 3.14.

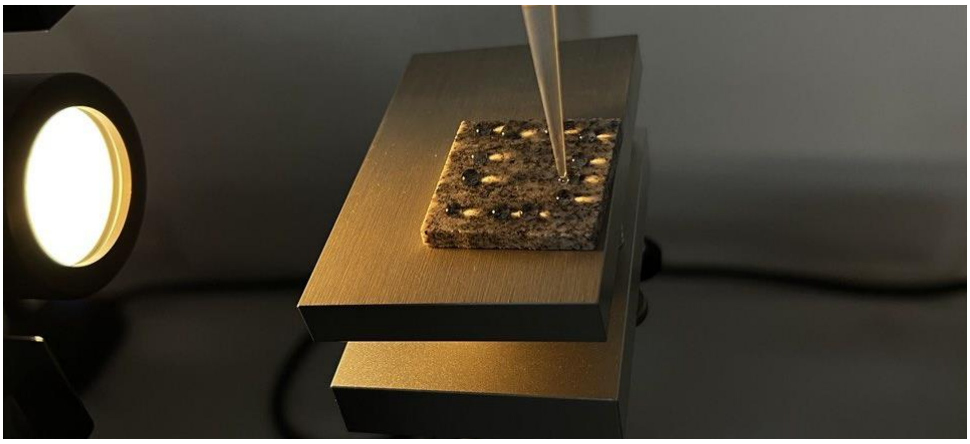

Figure 3.114 *Studying the hydrophobic properties of sample G1 treated with CN3*

Table 3.112 Static contact angle results of applied hydrophobic studied coatings on studied stone samples

Ref N.	**Typology**	**without any treatment**				**CN1**				**CN2**				**CN3**			
		Before ageing		**after ageing**		**before ageing**		**after ageing**		**before ageing**		**after ageing**		**before ageing**		**after ageing**	
		Mean	Stdev	Mean	Stdev	Mean	Stdev	Mean	Stdev	Mean	Stdev	Mean	Stdev	Mean	Stdev	Mean	Stdev
L1	Limestone	58.4	8.0	49.9	10.9	66.2	5.7	57.0	9.8	96.8	13.1	42.3	9.1	120.1	6.5	122.4	6.2
L2	Limestone	47.4	3.1	54.0	11.2	72.9	12.7	70.4	12.9	109.9	24.8	68.4	16.7	131.9	4.4	128.0	3.9
L3	Limestone	65.3	14.8	39.3	12.1	98.1	20.6	99.5	15.7	109.7	11.8	97.8	17.4	124.5	3.8	121.4	7.0
L4	Limestone	56.7	12.8	57.5	8.0	94.8	6.9	90.9	19.7	115.0	9.1	81.9	18.1	120.3	7.0	123.0	5.8
L5	Limestone	52.4	8.4	40.0	9.3	97.9	9.7	88.9	15.5	109.5	12.8	110.9	21.0	108.4	16.2	109.8	11.9
M1	Marble	56.8	12.2	58.4	8.3	100.5	18.7	93.9	11.7	103.2	19.5	104.1	16.2	113.9	6.7	109.5	6.1
M2	Marble	72.2	10.6	38.3	5.6	103.1	18.4	105.9	11.9	105.7	11.6	79.5	14.8	119.3	10.2	114.2	7.9
M3	Marble	64.4	18.2	51.9	9.2	111.1	8.7	112.6	3.5	121.6	12.3	90.9	25.4	120.1	5.4	116.4	9.8
M4	Marble	62.1	10.5	55.4	18.9	113.5	11.7	109.2	9.5	120.4	8.4	124.0	8.8	120.4	11.5	115.2	9.2
G1	Granite	56.0	14.0	57.7	8.5	113.3	5.0	98.1	6.7	124.6	11.0	120.8	12.2	121.6	10.4	110.3	6.3

3.4.2.1 Hydrophobic Effectiveness

As mentioned earlier, according to Wenzel's theory, the contact angle of water drop on an effective hydrophobic coating must be more than 90 degrees (Wenzel, R., 1936), however, this number can be 150 degrees for superhydrophobic surfaces (Malavasi, I., et al., 2015). Therefore, if the contact angle of the water drop on the stone surface reaches 90 degrees or more, the surface considers a hydrophobic surface.

The graphic representation of the contact angle results of coated mock-ups with different coatings and untreated samples (standards) before ageing process is shown in Figure 3.15. The green area presents the hydrophobicity of the studied samples.

According to Figure 3.15 and Table 3.12, the contact angle of CN3 for all the stone samples before ageing state exists in the green area which means all the mock-ups coated with CN3 have effective hydrophobicity. Stone samples coated with CN2 were effectively made hydrophobic after applying the related coating, however, due to the standard deviation in samples L1, L2, and M1 this coating may not fulfil the required expectations. Among all the applied coatings, CN1 has the least hydrophobic effectiveness in all the studied samples.

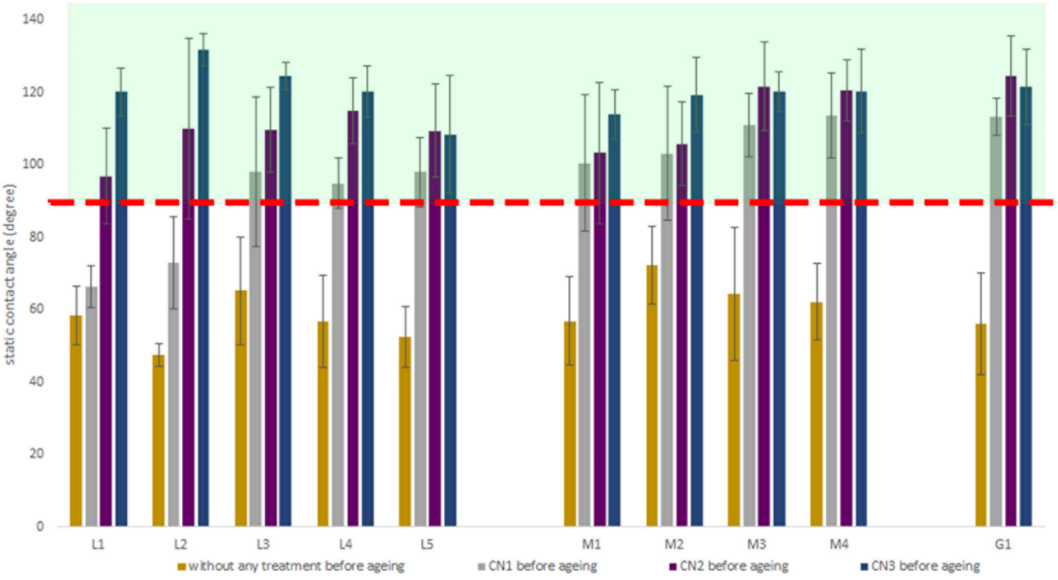

Figure 3.115 *graphic representation of static contact angle results of applied hydrophobic studied coatings on studied stone samples before ageing process*

The graphic representation of the contact angle results of coated mock-ups with different coatings and untreated samples (standards) after ageing process is shown in Figure 3.16. The green area presents the hydrophobicity of the studied samples.

According to Figure 3.16 and compared to Figure 3.15, the contact angle of CN3 for all the stone samples after ageing process still exists in the green area which means all the mock-ups coated with CN3 have effective hydrophobicity even after ageing process, which demonstrate its resistance. Coating CN2, after being submitted to the ageing process contrasted with before ageing which shows an acceptable hydrophobicity in most of the samples, could not fulfil the expected hydrophobicity. However, this coating for sample G1 still shows an acceptable contact angle value. Aged marbles and granite coated with CN1 exist in the green area of hydrophobicity, which means contact angle of water drops higher than 90 degrees, although due to the standard deviation for samples M1, and G1 this coating may not fulfil the required expectations.

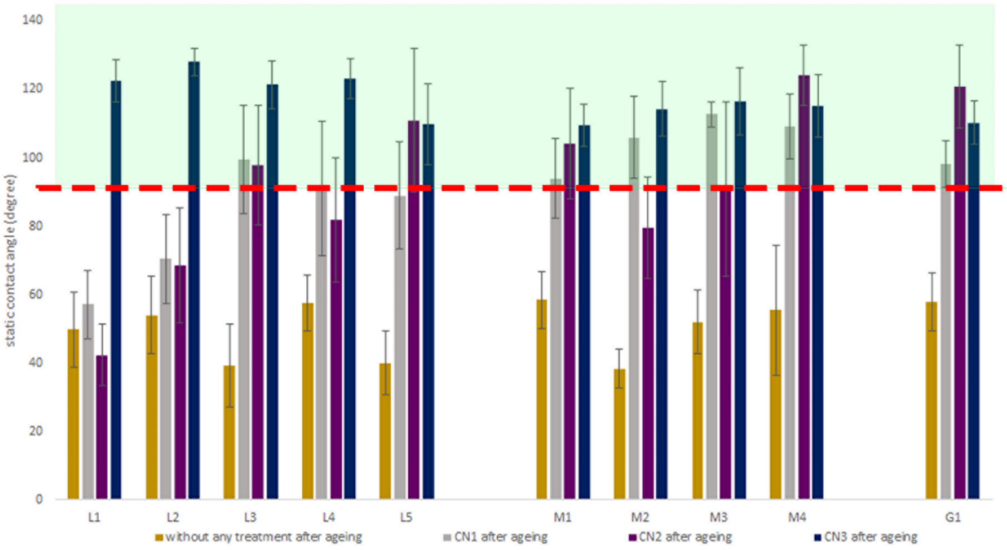

Figure 3.116 *graphic representation of static contact angle results of applied hydrophobic studied coatings on studied stone samples after ageing process*

The enhancements (%) in contact angles of each sample after applying different coatings are presented in figure 3.17. This percentage has been calculated based on the increased contact angle value after applying coatings compared to untreated mock-ups (standards).

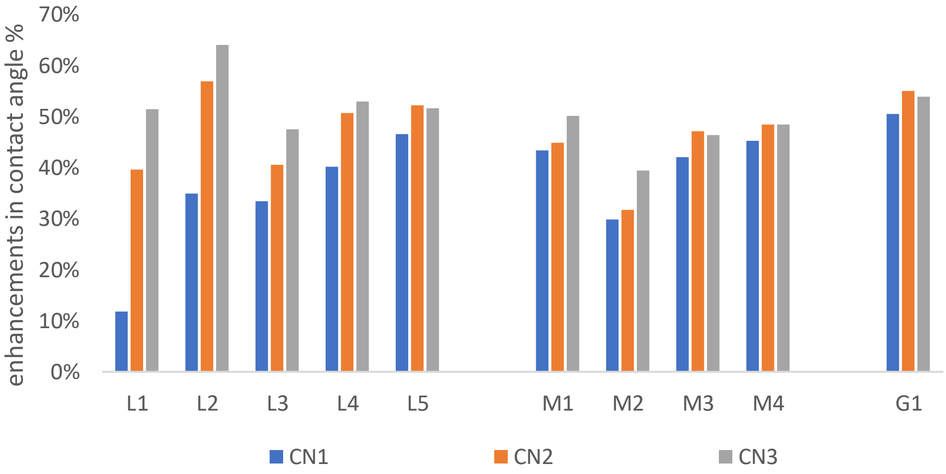

Figure 3.117. *enhancements % in hydrophobicity of studied stone samples for each applied coating*

According to figure 3.17, CN1 has the least improvements in hydrophobicity on the surfaces of stone samples compared to other coatings. The difference is more noticeable among limestones. However, in sample G1, the differences in improvements among all applied coatings are low.

Although CN1 and CN3 both have the silane-siloxane base composition, the noticeable difference in their compatibility with stone samples could be related to modified fluorinated compounds (C6 chemistry) additives in CN3. This chemical composition, due to its ultralow surface energy, achieves a well-performed coating functionality (Bayer, I., 2020). Therefore, this reason can explain the decent effectiveness of CN3 among all the coatings.

3.4.2.2 Hydrophobic Durability

The durability of hydrophobic coatings can be affected by natural or artificial weathering (Corcione, C., et al., 2017). Therefore, the comparison of contact angle value after ageing process with coated samples can give an insight due to the durability of applied coatings. Measurements of the contact angle are taken before and after ageing process to evaluate the eventual loss of hydrophobicity. The reduction percentage of hydrophobicity of studied stone samples coated with studied hydrophobic coatings is presented in Figure 3.18.

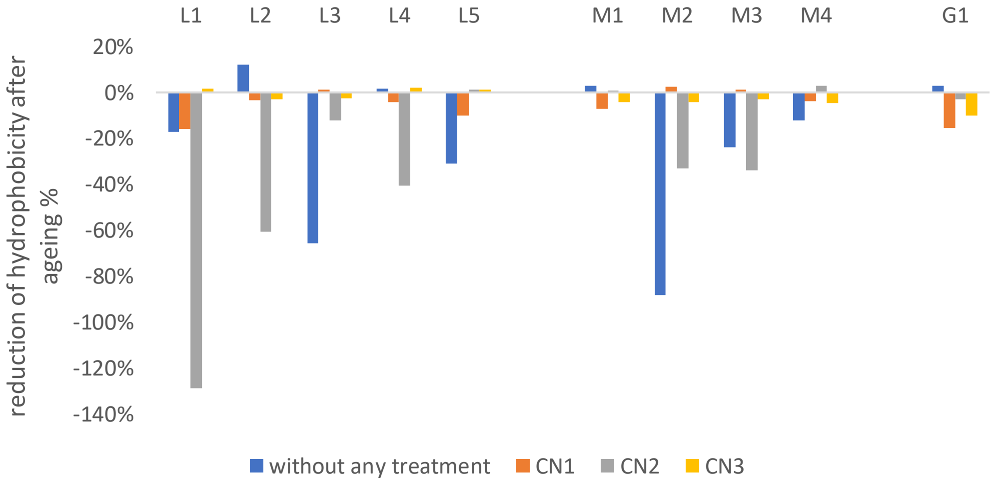

Figure 3.118 *reduction % of hydrophobicity of studied stone samples after ageing process*

The accelerated ageing process can directly affect the durability of the applied coatings through simulation of the weathering conditions (Chen, K., et al., 2015). Therefore, the less percentage of reduction of hydrophobicity of applied coatings after ageing could mean the coatings are durable when it comes to weathering conditions.

According to figure 3.17, the hydrophobicity of mock-ups L3, L5, M2, and M3 without any treatments has decreased significantly. It may be more noticeable in these samples because of their chemical and mineralogical compositions, open porosity, and/or hardness.

Among the applied coatings, the durability of CN2 has the highest reduction percentage in all the studied limestones except sample L5. According to the mineralogical compositions of studied limestones, dolomite is the main mineral for sample L5 in contrast with others which consist mostly of calcite. This difference in mineralogical compositions could be the reason for the different behaviour of this sample in terms of hydrophobic durability.

Among all the applied hydrophobic coatings, CN2 shows the lowest durability especially related to the mock-ups L1, L2, L4, M2, and M3. Additionally, CN3 shows the most durability, although, the durability observed on sample G1 sharply decreased compared to other samples. According to the chemical composition of the studied coatings, CN3 and CN1 are silane/siloxane-based, however, the chemical composition of CN2 is based on silicon dioxide. This chemical composition difference can be able to explain the strong decrease in the durability of CN2.

3.4.3 Water vapor permeability measurements

Due to the limitations for water vapor permeability which are already mentioned and according to the results of chromatic changes and static contact angle, CN3 is chosen as the optimal choice for the hydrophobic coating to measure its water vapor permeability. Since, the other studied coatings, CN1 and CN2, did not fulfil the required expectations related to colour change and hydrophobicity, and also because the water vapor permeability test is a time-consuming technique, this measurement has been done only for stone samples coated with CN3.

3.4.3.1 Compatibility of Hydrophobic Coatings

Water vapor permeability test results for each stone sample before and after treatment and the percentage of their change are presented in table 3.13.

Table 3.113 water vapor permeability value of each stone sample before and after treatment with their change %

Ref N.	Typology	before treatment	after treatment	changes
		(g/m.s.Pa)	(g/m.s.Pa)	%
L1	Limestone	6.03E-12	5.10E-12	-15%
L2	Limestone	6.31E-12	5.93E-12	-6%
L3	Limestone	2.95E-12	1.71E-12	-42%
L4	Limestone	8.93E-12	4.59E-12	-49%

L5	Limestone	7.70E-12	4.04E-12	-48%
M1	Marble	2.18E-12	1.19E-12	-46%
M2	Marble	4.72E-12	3.90E-12	-17%
M3	Marble	5.11E-12	3.65E-12	-29%
M4	Marble	3.75E-12	2.16E-12	-42%
G1	Granite	5.53E-12	3.52E-12	-36%

According to table 3.13, the water vapor permeability value of all the stone samples decreased however the variation of reduction is different among them. Samples L1, L2, and M2 consider in a lower reduction range while samples L3, L4, L5, M1, and M4 have a higher percentage of reduction of water vapor permeability after CN3 application.

To better compare the changes in water vapor permeability for stone samples before and after treatment, the graphic representation is presented in Figure 3.19.

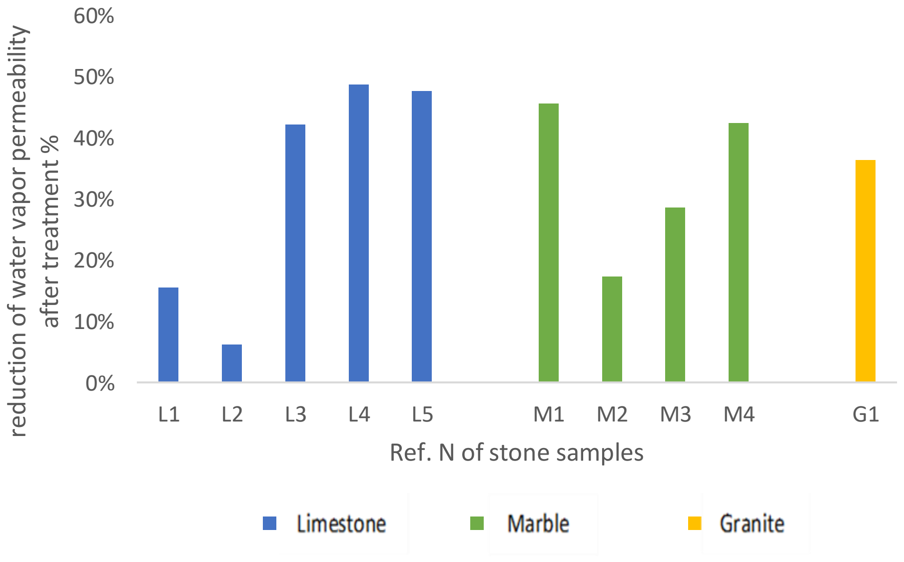

Figure 3.119. *graphic representation of water vapor permeability reduction % after treatment*

Change in water vapor permeability is one of the significant parameters to evaluate the harmless and compatibility of hydrophobic coatings after application (Lettieri, M., et al., 2021). This feature is of utmost importance because if following the application of a coating, the permeability of water vapor significantly decreased, at the interface between the treated and untreated stone sections, water may condense, creating mechanical stress that could start the decaying process (Scheerer, S., et al., 2009). In the other words, the compatible hydrophobic coating should let the surface of the stone *breathe*.

The differences in the reduction of water vapor permeability depend on several indicators. Firstly, the sampling process for this experiment was different. Although the treated and untreated mock-ups derived from one specific stone sample, they have minor differences in their characteristics. Secondly, as mentioned earlier, since the experiment has been done just for one mock-up instead of having a mean value of a group of them, the errors of experiments could be higher. Lastly, due to technical matters, the humidity chamber used for keeping the containers during the test was not the same before and after treatment. Therefore, all the factors could cause variation in the values of the water vapor permeability.

Several researchers mentioned the enhancement of water vapor permeability in stone samples after applying nano F (fluorinate-based) treatments irrespective of the porosity of the stones (Lettieri, M., et. al., 2021; Petronella, F., et. al., 2018; Kronlund, D., et. al., 2015). According to their investigations, it was hypothesized that the treated samples would have less condensation of water molecules on the hydrophobic pore walls. As a result, the permeability of the treated value increased compared to untreated samples. Although the results in table 3.13 do not indicate the enhancement of water vapor permeability in any studied samples, the less reduction percentage of water vapor permeability in samples L1, and L2 which have the most open porosity among studied samples, could relate to this phenomenon. Further tests due to measuring the open porosity of treated stone samples are preferable to investigate better the correlation of open porosity and water vapor permeability after treatment in the future.

On the other hand, the water vapor permeability should not strongly be decreased after treatment. it means protective coatings prevent the breathability of stone sample surfaces

(Castelvetro, V., et. al., 2002). Among all the samples, L4, and L5, show the highest water vapor permeability reduction.

3.4.3.2 Durability of Hydrophobic Coatings

Water vapor permeability test results for each stone sample before and after ageing and the percentage of their change are presented in table 3.14.

Table 3.114 water vapor permeability value of each stone sample after treatment and ageing process with their change %

Ref N.	Typology	after treatment	after ageing	change
		(g/m.s.Pa)	(g/m.s.Pa)	%
L1	Limestone	5.10E-12	4.80E-12	-6%
L2	Limestone	5.93E-12	5.15E-12	-13%
L3	Limestone	1.71E-12	3.39E-12	98%
L4	Limestone	4.59E-12	3.36E-12	-27%
L5	Limestone	4.04E-12	3.52E-12	-13%
M1	Marble	1.19E-12	2.92E-12	145%
M2	Marble	3.90E-12	3.04E-12	-22%
M3	Marble	3.65E-12	3.61E-12	-1%
M4	Marble	2.16E-12	3.35E-12	55%
G1	Granite	3.52E-12	1.97E-12	-44%

The variation of the changes after treatment and ageing process among all the samples is different from after treatment. According to table 3.14, the water vapor permeability decreased in all the samples except L3, M1, and M4, however, the reduction for sample M3 is so low that it can be considered as with no changes.

Weathering conditions can decrease the permeability of water vapor in normal situations however more reduction means less durability of applied treatment (Roncon, R., et. al., 2021).

However, positive changes can determine the breathability of the surfaces in corresponding samples (Castelvetro, V., et. al., 2002). The reason could be because of the enhancement of open porosity in stones after artificial ageing (Lettieri, M., et. al., 2021). Therefore, the positive changes could not totally be related to the lack of durability of the applied coatings. Further tests due to measuring the open porosity of treated stone samples are preferable to investigate better the correlation of open porosity and water vapor permeability after ageing in the future.

BIBLIOGRAPHY

Amaral, P., Correia, A., Lopes, L., Rebola, P., Pinho, A., & Carrilho Lopes, J. (2013). On the use of thermal properties for characterizing dimension stones. In *Key Engineering Materials* (Vol. 548, pp. 231-238). Trans Tech Publications Ltd.

Andreotti, S., Franzoni, E., Esposti, M. D., & Fabbri, P. (2018). Poly (hydroxyalkanoates) s-based hydrophobic coatings for the protection of stone in cultural heritage. *Materials*, *11*(1), 165.

Bayer, I. S. (2020). Superhydrophobic coatings from ecofriendly materials and processes: a review. *Advanced Materials Interfaces*, *7*(13), 2000095.

Castelvetro, V., Aglietto, M., Ciardelli, F., Chiantore, O., Lazzari, M., & Toniolo, L. (2002). Structure control, coating properties, and durability of fluorinated acrylic-based polymers. Journal of Coatings Technology, 74(928), 57-66.

Chen, K., Zhou, S., Yang, S., & Wu, L. (2015). Fabrication of all-water-based self-repairing superhydrophobic coatings based on UV-responsive microcapsules. *Advanced Functional Materials*, *25*(7), 1035-1041.

Corcione, C. E., De Simone, N., Santarelli, M. L., & Frigione, M. (2017). Protective properties and durability characteristics of experimental and commercial organic coatings for the preservation of porous stone. *Progress in Organic Coatings*, *103*, 193-203.

Delgado-González, M. J., Carmona-Jiménez, Y., Rodríguez-Dodero, M. C., & García-Moreno, M. V. (2018). Color space mathematical modeling using Microsoft excel.

El-Taher, A. (2012). Elemental analysis of granite by instrumental neutron activation analysis (INAA) and X-ray fluorescence analysis (XRF). *Applied Radiation and Isotopes*, *70*(1), 350-354.

Houston, E. C., & Smith, J. V. (1997). Assessment of rock quality variability due to smectitic alteration in basalt using X-ray diffraction analysis. *Engineering Geology*, *46*(1), 19-32.

Kronlund, D., Bergbreiter, A., Meierjohann, A., Kronberg, L., Lindén, M., Grosso, D., & Smått, J. H. (2015). Hydrophobization of marble pore surfaces using a total immersion treatment method–product selection and optimization of concentration and treatment time. *Progress in Organic Coatings*, *85*, 159-167.

Lettieri, M., Masieri, M., Aquaro, M., Dilorenzo, D., & Frigione, M. (2021). Eco-Friendly Protective Coating to Extend the Life of Art-Works and Structures Made in Porous Stone Materials. Coatings 2021, 11, 1270.

Malavasi, I., Bernagozzi, I., Antonini, C., & Marengo, M. (2015). Assessing durability of superhydrophobic surfaces. *Surface Innovations*, *3*(1), 49-60.

McGee, E. S. (1990). *Deterioration of Building Stones in Washington, DC: A Field Trip Guide*. Department of the Interior, US Geological Survey.

Persia, F., (2010). Study of Ageing Effects on Treated Marbles by Colorimetry and Laser Induced Fluorescence. International Congress on Science and technology for the Safeguarding of cultural heritage in the Mediterranean basin, Cairo. 239-334.

Petronella, F., Pagliarulo, A., Truppi, A., Lettieri, M., Masieri, M., Calia, A., ... & Comparelli, R. (2018). TiO2 nanocrystal based coatings for the protection of architectural stone: the effect of solvents in the spray-coating application for a self-cleaning surfaces. Coatings, 8(10), 356.

Roncon, R., Borsoi, G., Parracha, J. L., Flores-Colen, I., Veiga, R., & Nunes, L. (2021). Impact of water-repellent products on the moisture transport properties and mould susceptibility of External Thermal Insulation Composite Systems. Coatings, 11(5), 554.

Scheerer, S., Ortega-Morales, O., & Gaylarde, C. (2009). Microbial deterioration of stone monuments—an updated overview. *Advances in applied microbiology*, *66*, 97-139.

Shtel'makh, S. I. (2020). Determination of F, S (total), and Cl in the Calcite Rich Limestone and Marbles by WD-XRF Spectrometry. *Journal of Geological Resource and Engineering*, *8*(5), 137-44.

Tabor, D. (1954). Mohs's hardness scale-a physical interpretation. *Proceedings of the Physical Society. Section B*, *67*(3), 249.

Wahab, G. M., Gouda, M., & Ibrahim, G. (2019). Study of physical and mechanical properties for some of Eastern Desert dimension marble and granite utilized in building decoration. *Ain Shams Engineering Journal*, *10*(4), 907-915.

Wedekind, W., Pötzl, C., Doncel, R. L., Platz, T. V., & Siegesmund, S. (2016). Surface hardness testing for the evaluation of consolidation of porous stones. *SCIENCE AND ART: A FUTURE FOR STONE*, 491.

Wenzel, R. N. (1936). Resistance of solid surfaces to wetting by water. *Industrial & Engineering Chemistry*, *28*(8), 988-994.

Zhang, L. (2013). Aspects of rock permeability. *Frontiers of structural and civil engineering*, *7*(2), 102-116.

Zeng, X., Xiao, Y., Ji, X., & Wang, G. (2021). Mineral identification based on deep learning that combines image and Mohs hardness. *Minerals*, *11*(5), 506.

Chapter 4

4 Conclusion

4.1 Conclusion

In this study, three different nano-particle coatings with different chemical composition introduced as CN1 with silane/siloxane, CN2 with silicon dioxide, and CN3 with silane/siloxane and modified fluorinated additives have been compared by applying them to ten different stone samples including limestone, marble, and granite. Stone samples have been fully characterized due to their physical, chemical, and mineralogical nature to understand how different properties of these samples can correlate with the effectiveness, durability, and compatibility of the applied coatings. Additionally, chromatic changes, wettability, and breathability of treated and untreated stone samples have been compared before and after treatment as well as the artificial ageing process.

The study aimed to answer two main questions. Firstly, which factors related to the physical, chemical, and mineralogical characterization of stone samples, correlate with the effectivity, compatibility, and durability of hydrophobic coatings? Corresponding to this question, according to the mineralogical compositions of studied limestones, dolomite is the main mineral for sample L5 in contrast with others which consist mostly of calcite. This difference in mineralogical compositions could be the reason for the different behaviour of this sample in terms of the hydrophobic durability of applied CN2. Additionally, the result of open porosity and water vapor permeability clearly shows a relation with the compatibility and durability of applied coatings. The less reduction percentage of water vapor permeability in samples L1, and L2 which have the most open porosity among studied samples, could relate to increasing in their water vapor permeability after CN3 treatment.

Secondly, next question is which factors in hydrophobic coatings can make them more effective, compatible, and durable when they are applied on stone materials specifically, carbonate stones? According to the obtained results of chromatic changes, CN3 is the most compatible coating in terms of colour changes before and after ageing process, however, compatibility of this coating for sample G1 is challenging after ageing process. Moreover, this coating clearly has the most hydrophobic effectivity among all the applied protective coatings. Since the CN1 has the least compatibility and effectiveness, Comparing the chemical composition of these coatings reveals that although CN1 and CN3 both have the silane-siloxane base composition, the noticeable difference in their compatibility with stone samples could be related to modified fluorinated compounds (C6 chemistry) additives in CN3. However, the durability of this coating still has some challenges. According to the results obtained from water vapor permeability, some anomalies happened related to samples L4, M1, and M3 due to the enhancement of water vapor permeability after ageing. Compared to other research, The reason could be because of the enhancement of open porosity in stones after artificial ageing. Therefore, these anomalies could not complete due to the lack of durability of the applied coatings and still there is a need for further investigations.

Overall, the results of this study are a pioneering step for developing novel eco-friendly hydrophobic coatings carried out under Eco-STONEPROTEC project (EXPL/CTA-GEO/0609/2021) aims, to finally reaching to the destination which would be producing the competitive, effective, and sustainable hydrophobic coatings that considers all the aspects to preserve and conserve the stone heritage.

Appendices

Appendix 1: XRD diffractograms

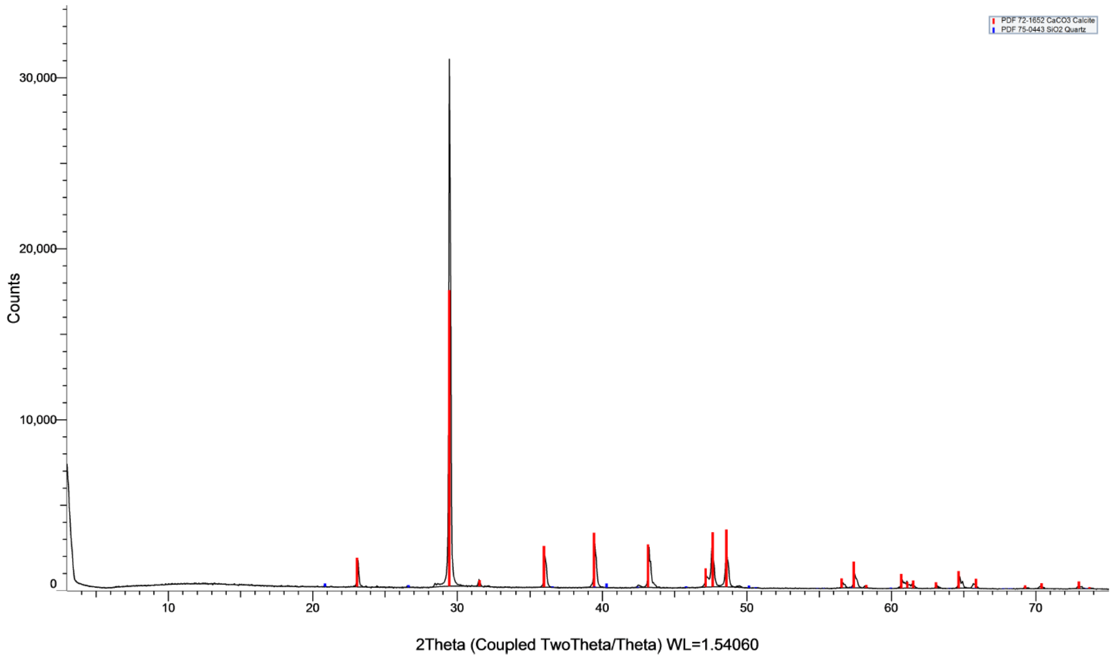

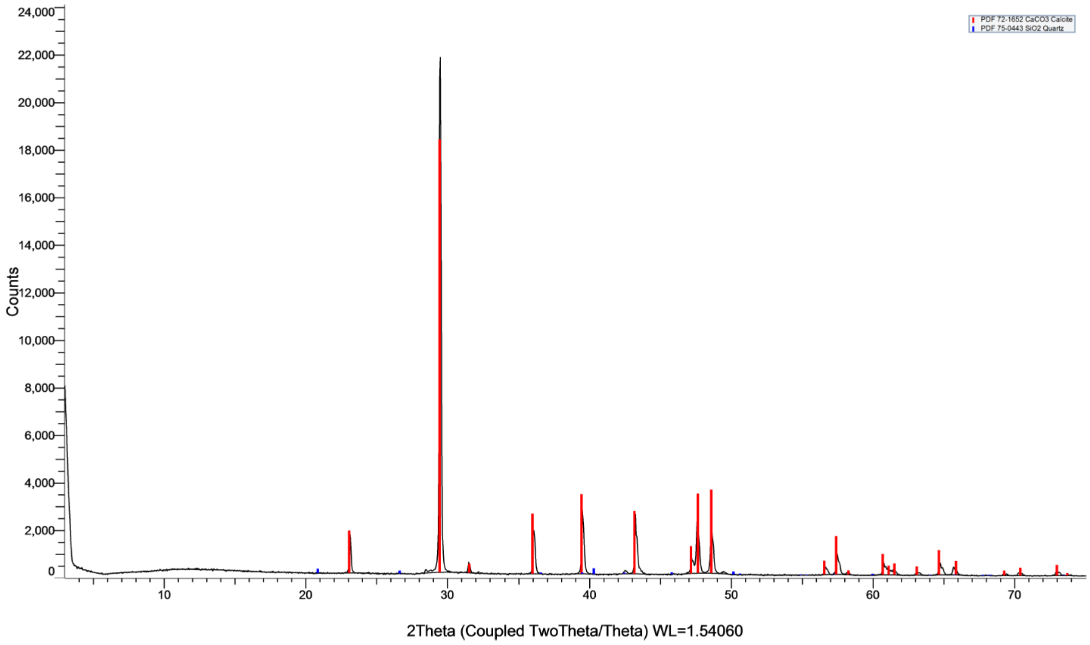
PDF 72-1652 CaCO3 Calcite
PDF 75-0443 SiO2 Quartz
Counts
24,000
22,000
20,000
18,000
16,000
14,000
12,000
10,000
8,000
6,000
4,000
2,000
0
10
20
30
40
50
60
70
2Theta (Coupled TwoTheta/Theta) WL=1.54060

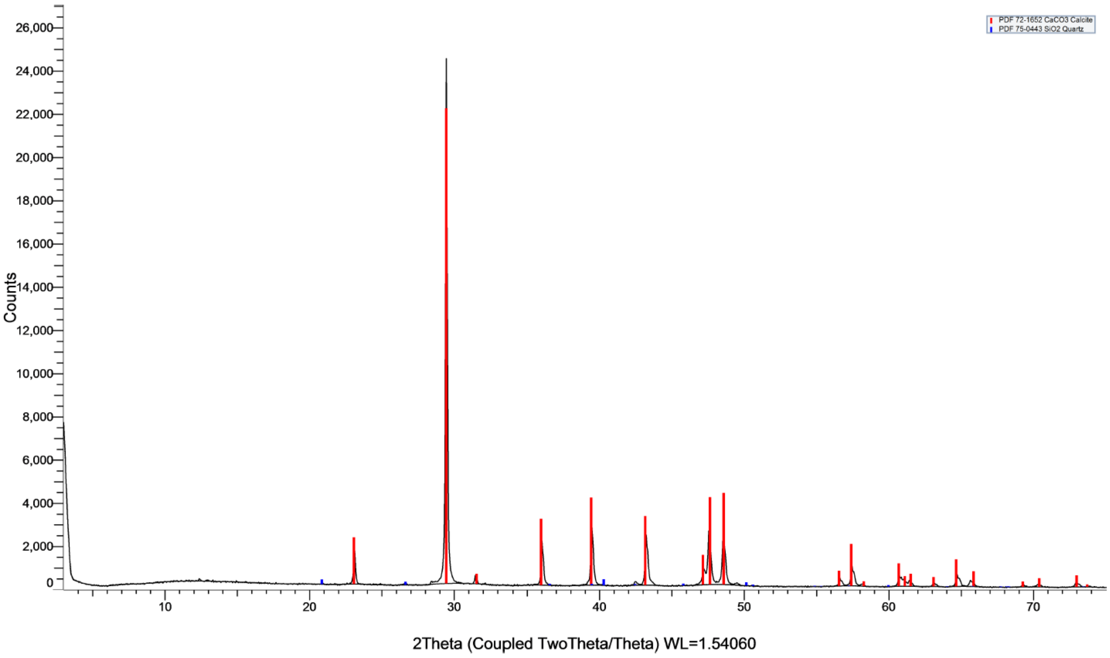
PDF 72-1652 CaCO3 Calcite
PDF 75-0443 SiO2 Quartz
Counts
26,000
24,000
22,000
20,000
18,000
16,000
14,000
12,000
10,000
8,000
6,000
4,000
2,000
0
10
20
30
40
50
60
70
2Theta (Coupled TwoTheta/Theta) WL=1.54060

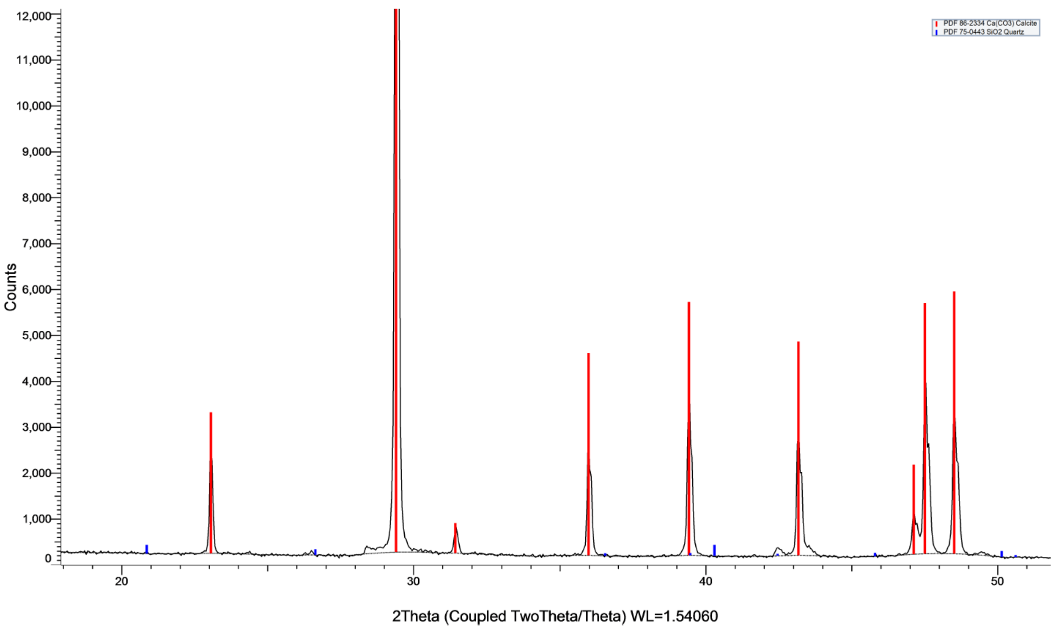
PDF 86-2334 Ca(CO3) Calcite
PDF 75-0443 SiO2 Quartz
Counts
12,000
11,000
10,000
9,000
8,000
7,000
6,000
5,000
4,000
3,000
2,000
1,000
0
20
30
40
50
2Theta (Coupled TwoTheta/Theta) WL=1.54060

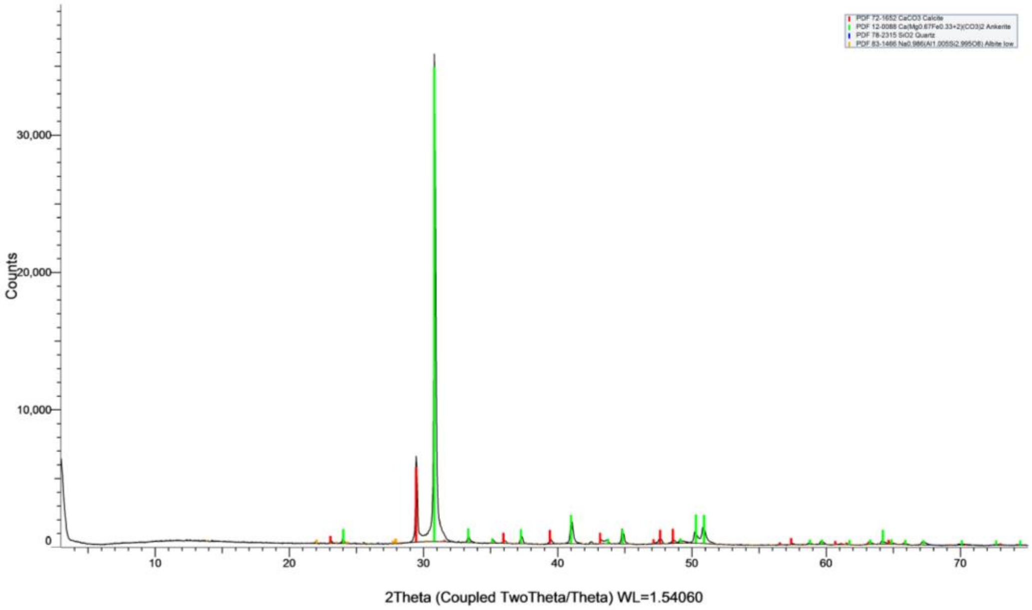
PDF 72-1652 CaCO3 Calcite
PDF 12-0088 Ca(Mg0.67Fe0.33+2)(CO3)2 Ankerite
PDF 78-2315 SiO2 Quartz
PDF 83-1466 Na0.986(Al1.005Si2.995O8) Albite low
Counts
30,000
20,000
10,000
0
10
20
30
40
50
60
70
2Theta (Coupled TwoTheta/Theta) WL=1.54060

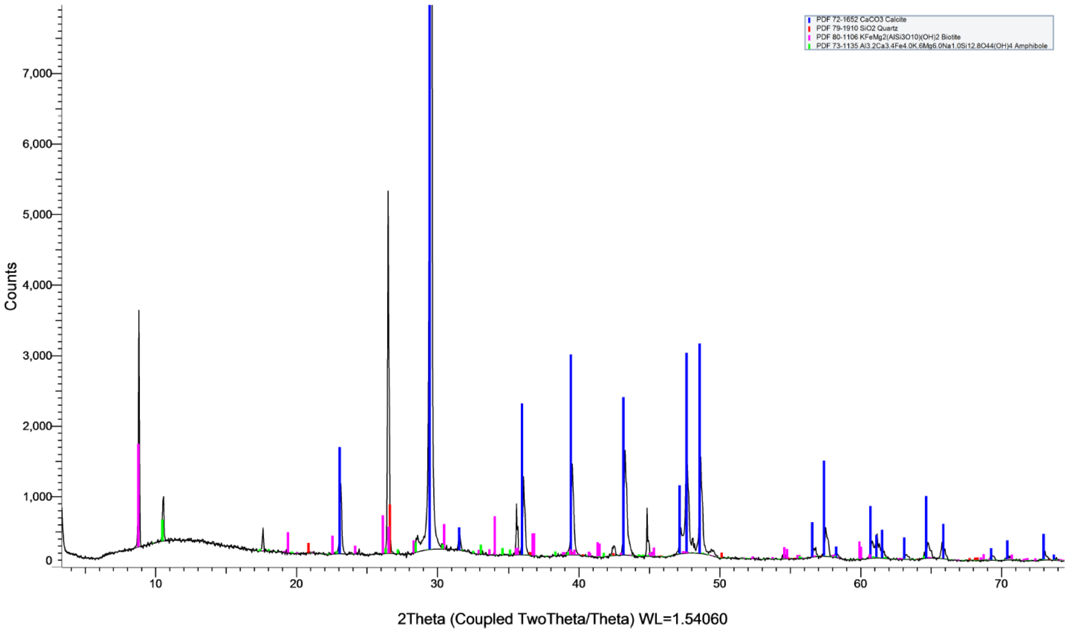

PDF 72-1652 CaCO3 Calcite
PDF 79-1910 SiO2 Quartz
PDF 80-1106 KFeMg2(AlSi3O10)(OH)2 Biotite
PDF 73-1135 Al3.2Ca3.4Fe4.0K.6Mg6.0Na1.0Si12.8O44(OH)4 Amphibole
Counts
7,000
6,000
5,000
4,000
3,000
2,000
1,000
0
10
20
30
40
50
60
70
2Theta (Coupled TwoTheta/Theta) WL=1.54060

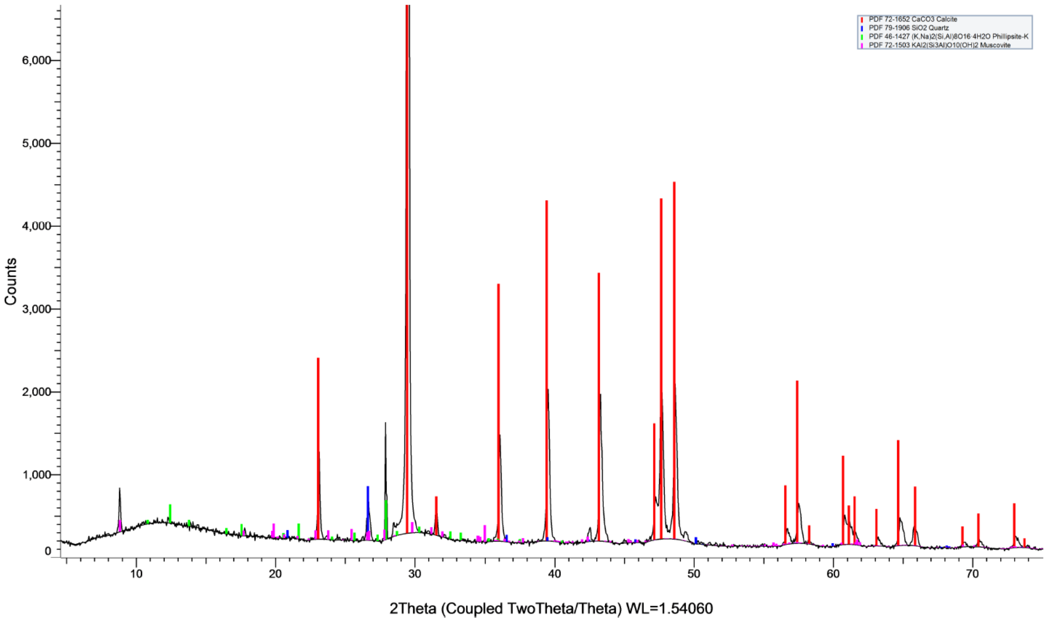

PDF 72-1652 CaCO3 Calcite
PDF 79-1906 SiO2 Quartz
PDF 46-1427 (K,Na)2(Si,Al)8O16·4H2O Phillipsite-K
PDF 72-1503 KAl2(Si3Al)O10(OH)2 Muscovite
Counts
6,000
5,000
4,000
3,000
2,000
1,000
0
10
20
30
40
50
60
70
2Theta (Coupled TwoTheta/Theta) WL=1.54060

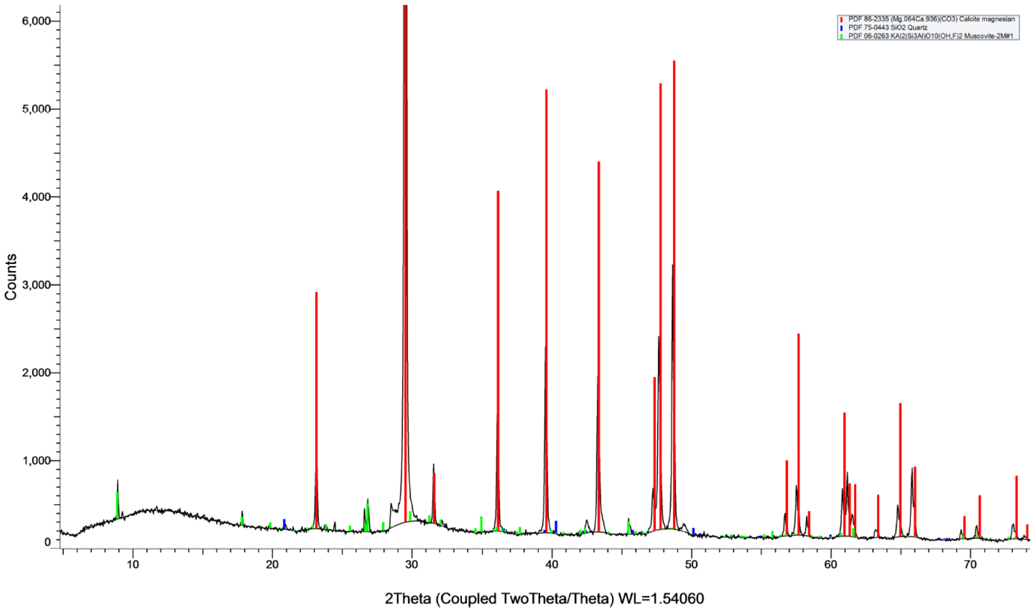

Figure 8. sample M3 XRD diffractogram

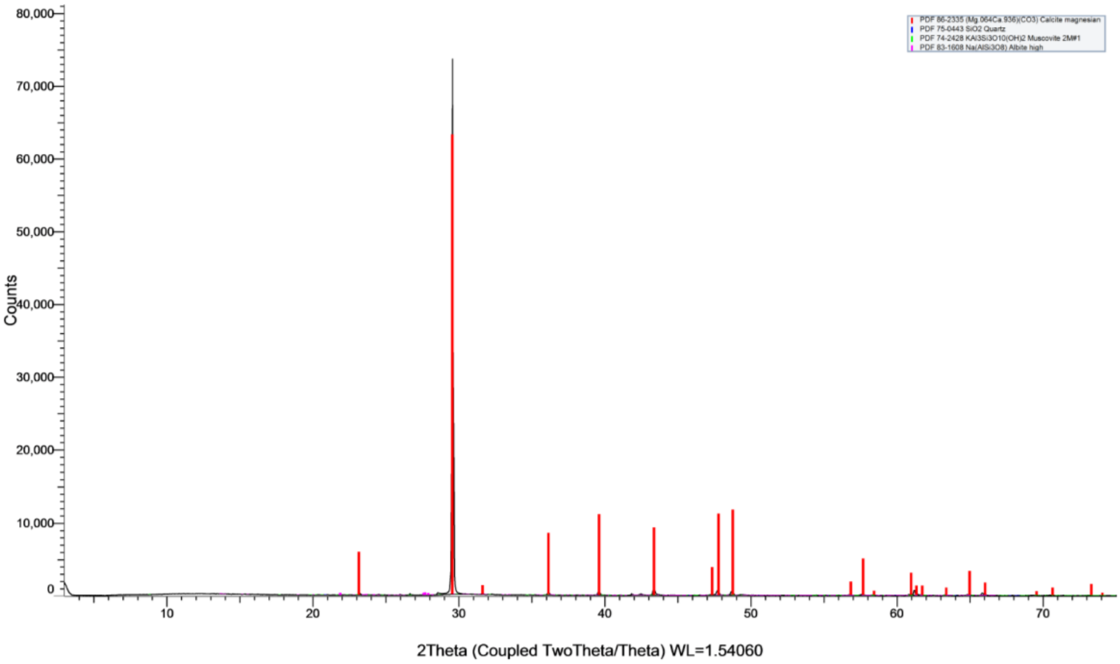

Figure 9. sample M4 XRD diffractogram

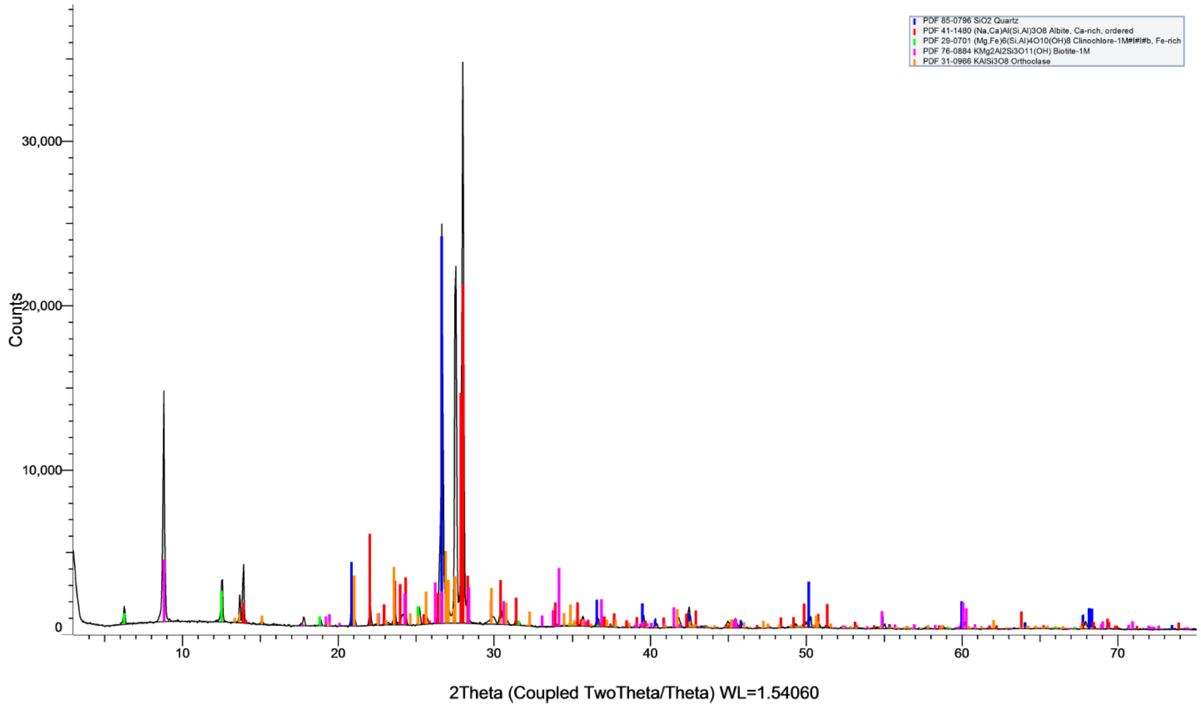

Figure 10. sample G1 XRD diffractogram

Appendix 2: photos of samples in different states taken by CANON 80

L1	without any treatments	with applied coatings	after accelerated ageing
initial specimens	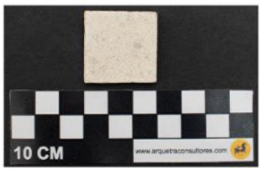		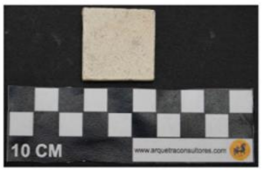
CN1	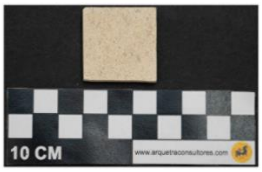	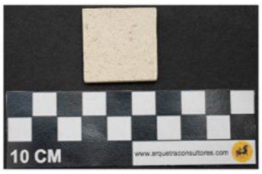	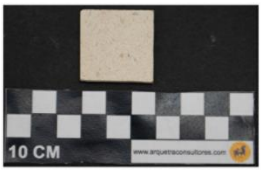
CN2			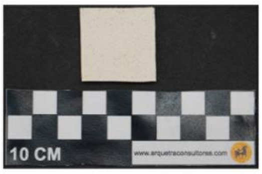
CN3		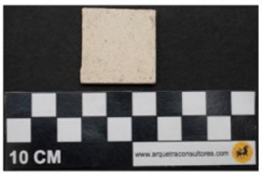	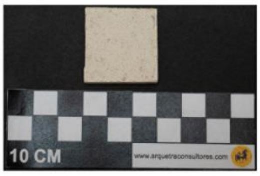

L2	without any treatments	with applied coatings	after accelerated ageing
initial specimens			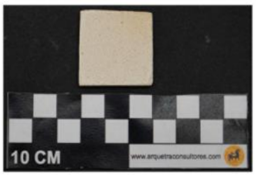
CN1	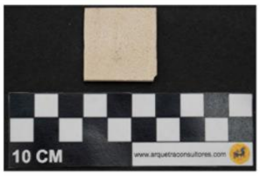	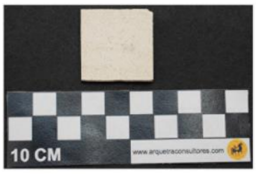	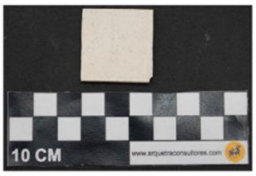
CN2		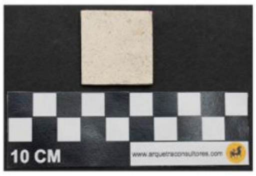	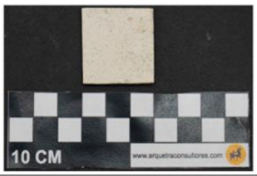
CN3			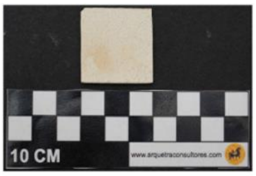

L3	without any treatments	with applied coatings	after accelerated ageing
initial specimens			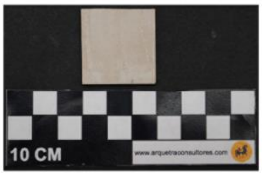
CN1			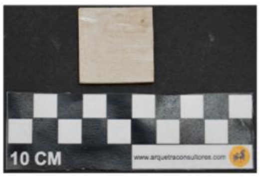
CN2		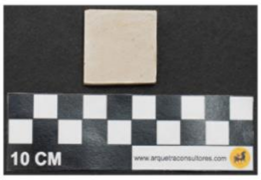	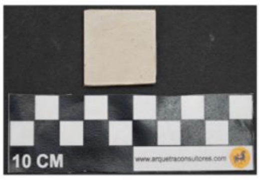
CN3		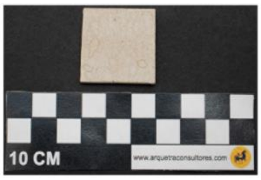	

L4	without any treatments	with applied coatings	after accelerated ageing
initial specimens			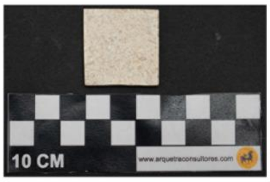
CN1	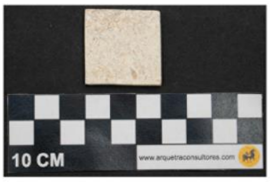	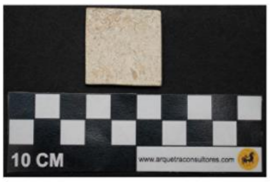	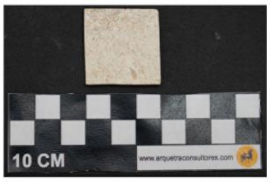
CN2		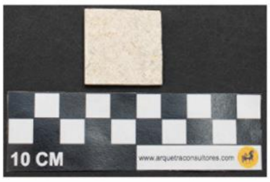	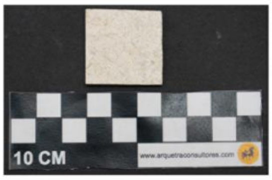
CN3		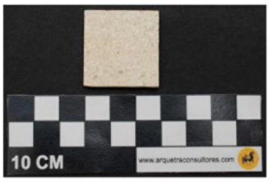	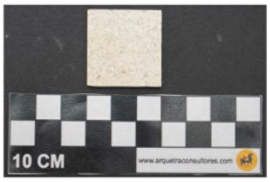

L5	without any treatments	with applied coatings	after accelerated ageing
initial specimens	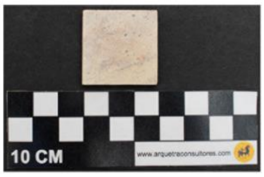		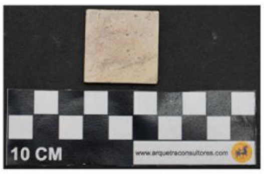
CN1		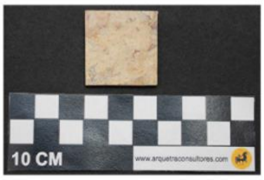	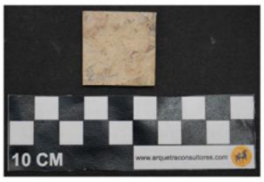
CN2		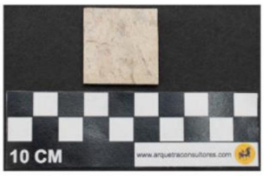	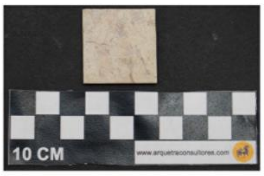
CN3		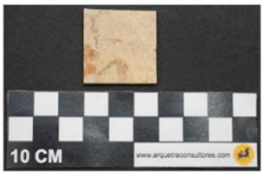	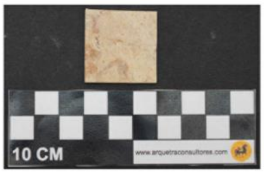

M1	without any treatments	with applied coatings	after accelerated ageing
initial specimens			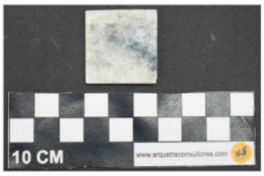
CN1		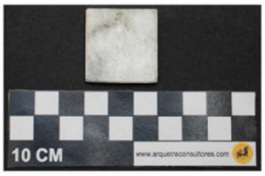	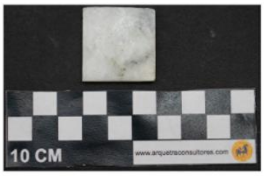
CN2			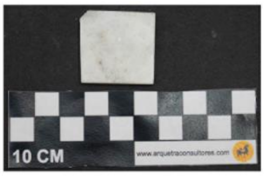
CN3			

M2	without any treatments	with applied coatings	after accelerated ageing
initial specimens			
CN1			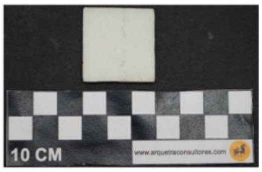
CN2			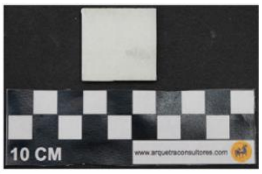
CN3			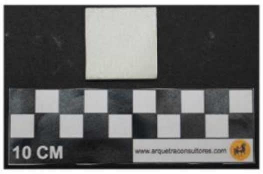

M3	without any treatments	with applied coatings	after accelerated ageing
initial specimens			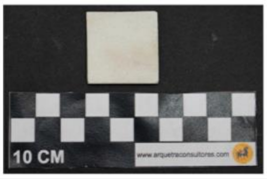
CN1	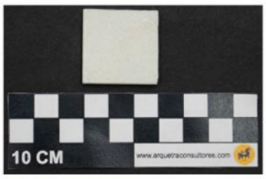		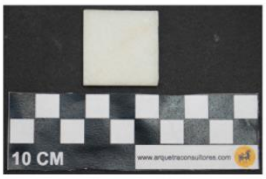
CN2			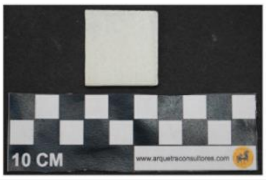
CN3		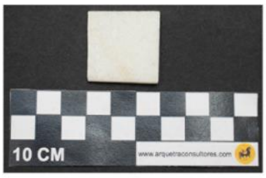	

M4	without any treatments	with applied coatings	after accelerated ageing
initial specimens	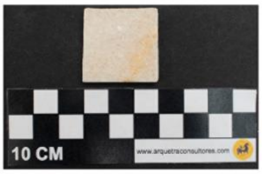		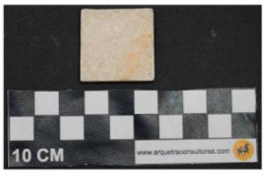
CN1		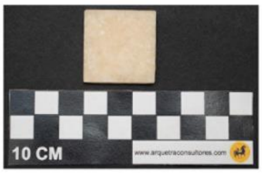	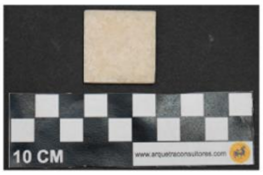
CN2	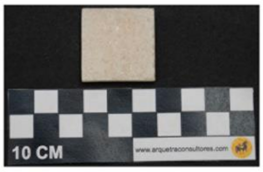		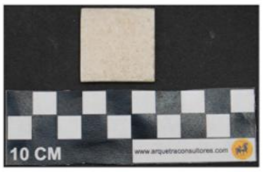
CN3			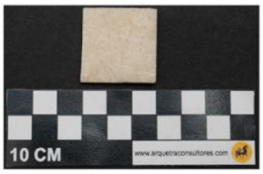

G1	without any treatments	with applied coatings	after accelerated ageing
initial specimens			
CN1	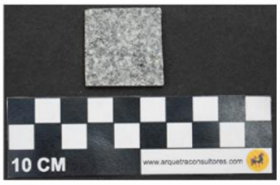	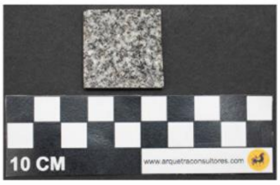	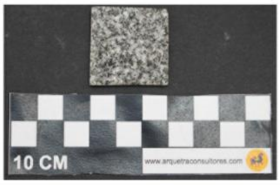
CN2	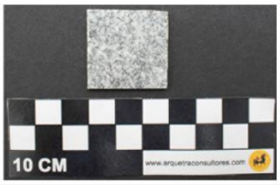	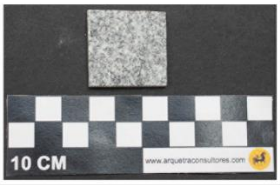	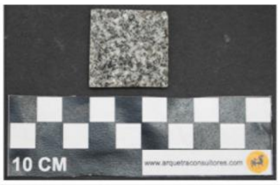
CN3	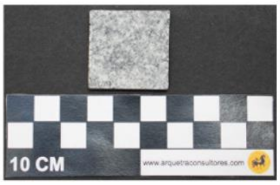	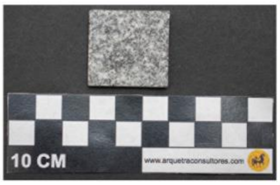	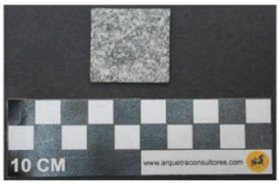

Appendix 3: Digital Microscopy photos of stone samples in different states

L1	without any treatments	with applied coatings	after accelerated ageing
initial specimens			
CN1		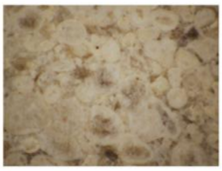	
CN2			
CN3			

L2	without any treatments	with applied coatings	after accelerated ageing
initial specimens			
CN1			
CN2		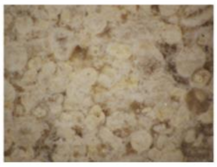	
CN3